DESIGN OF UNIDIRECTIONAL ANTENNAS USING RING ABOVE SQUARE REFLECTOR FOR WIRELESS COMMUNICATIONS

SOUPHANNA VONGSACK

A THESIS SUBMITTED IN FULFILLMENT
OF THE REQUIREMENT FOR THE DEGREE OF
DOCTOR OF ENGINEERING IN ELECTRICAL ENGINEERING
FACULTY OF ENGINEERING
KING MONGKUT'S INSTITUTE OF TECHNOLOGY LADKRABANG
2015

KMITL-2015-NT-D-018-015

DESIGN OF UNIDIRECTIONAL ANTENNAS USING RING ABOVE SQUARE REFLECTOR FOR WIRELESS COMMUNICATIONS

SOUPHANNA VONGSACK

A THESIS SUBMITTED IN FULLFILLMENT
OF THE REQUIREMENT FOR THE DEGREE OF
DOCTOR OF ENGINEERING IN ELECTRICAL ENGINEERING
FACULTY OF ENGINEERING
KING MONGKUT'S INSTITUTE OF TECHNOLOGY LADKRABANG
2015
KMITL-2015-EN-D-018-015

หัวข้อวิทยานิพนธ์	การออกแบบสายอากาศทิศทางเดียวรูปวงแหวนเหนือแผ่นสะท้อนสี่เหลี่ยมจัตุรัสสำหรับการสื่อสารไร้สาย
นักศึกษา	นางสาวสุพันนา วงสัก
รหัสนักศึกษา	52601001
ปริญญา	วิศวกรรมศาสตรดุษฎีบัณฑิต
สาขาวิชา	วิศวกรรมไฟฟ้า
พ.ศ.	2558
อาจารย์ที่ปรึกษาวิทยานิพนธ์	รศ. ดร. ชูวงค์ พงศ์เจริญพาณิชย์

บทคัดย่อ

วิทยานิพนธ์ฉบับนี้นำเสนอสายอากาศที่มีแบบรูปการแพร่กระจายคลื่นทิศทางเดียวสำหรับระบบโครงข่ายท้องถิ่นไร้สายและระบบสื่อสารไวแมกซ์ โดยใช้สายอากาศวงแหวนสี่เหลี่ยมที่ป้อนด้วยโมโนโพลแผ่นวงกลมวางเหนือแผ่นสะท้อนสี่เหลี่ยมจัตุรัส ที่มีแบบรูปการแพร่กระจายคลื่นทิศทางเดียวเพื่อให้ครอบคลุมตลอดช่วงกว้างแถบความถี่ที่ใช้งานตั้งแต่ 2.300 กิกะเฮิรตซ์ ถึง 5.825 กิกะเฮิรตซ์ เพื่อประยุกต์ใช้งานสำหรับให้บริการระบบไวแมกซ์ ซึ่งขนาดของสายอากาศวงแหวนสี่เหลี่ยมโมโนโพลแผ่นวงกลม และค่าตัวแปรต่างๆนั้นได้ทำการจำลองโดยใช้โปรแกรม CST Microwave Studio จากนั้นได้ทำการสร้างสายอากาศต้นแบบและนำไปทดสอบเพื่อเปรียบเทียบกับผลการจำลองทางทฤษฎี ซึ่งพบว่า ผลทั้งสองมีความสอดคล้องกัน ผลการทดสอบได้แสดงค่าการสูญเสียย้อนกลับ $|S_{11}|$ ต่ำกว่า -10 dB ที่มีแบบรูปการแพร่กระจายคลื่นทิศทางเดียวที่ครอบคลุมตลอดย่านความถี่ไวแมกซ์ และมีค่าอัตราการขยายของสายอากาศต่ำสุดและสูงสุดอยู่ที่ 3.70 dBi และ 8.70 dBi ตามลำดับ พร้อมกับแบบรูปการแพร่กระจายคลื่นทิศทางเดียวตลอดย่านความถี่

นอกจากนี้ในส่วนหนึ่งของวิทยานิพนธ์ฉบับนี้ยังออกแบบสายอากาศที่มีแบบรูปการแพร่กระจายคลื่นทิศทางเดียว สำหรับสองย่านความถี่สำหรับโครงข่ายท้องถิ่นไร้สาย (Wireless LAN) ตามมาตรฐาน IEEE 802.11a ที่ครอบคลุมย่านความถี่ 2.400-2.484 กิกะเฮิรตซ์ และ 5.150-5.825 กิกะเฮิรตซ์ ที่มีความถี่กลาง 2.450 กิกะเฮิรตซ์ และ 5.500 กิกะเฮิรตซ์ เหมาะสำหรับกับการประยุกต์ใช้งานการสื่อสารไร้สายแบบจุดต่อจุด โดยได้นำเสนอสายอากาศวงแหวนสี่เหลี่ยมที่ป้อนด้วยร่องตัวยู-โมโนโพลแผ่นวงกลมวางเหนือแผ่นสะท้อนทรงสี่เหลี่ยมจัตุรัสที่สามารถกำจัดความถี่ (Band-rejected) 3.600-4.870 กิกะเฮิรตซ์ ร่องตัวยู-โมโนโพลแผ่นวงกลมประพฤติตัวเสมือนวงจรไฟฟ้าที่ยอมให้กำลังของคลื่นที่ความถี่ใดความถี่หนึ่งหรือช่วงความถี่ใดความถี่หนึ่งเท่านั้นผ่านไปได้ จากนั้นทำการสร้างสายอากาศต้นแบบแล้วนำไปทดสอบและเปรียบเทียบผลที่ได้จากการจำลองทางทฤษฎี ซึ่งพบว่าผลทั้งสองมีความสอดคล้องกัน ซึ่งผลจากจำลองทางทฤษฎีค่า $|S_{11}|$ ต่ำกว่า -10 dB สอดคล้องกับผลการทดสอบ ที่มีอัตราการขยายของสายอากาศ 7.31 dBi ที่ความถี่ 2.450 กิกะ

เฮิรตซ์ และ 4.14 dBi ที่ความถี่ 5.500 กิกะเฮิรตซ์ ตามลำดับ พร้อมสามารถกำจัดความถี่ได้ 29.78% จากคุณสมบัติที่กล่าวมาข้างต้นเห็นได้ชัดเจนว่าสายอากาศนี้เหมาะสำหรับ ให้บริการในช่วงโครงข่ายท้องถิ่นไร้สาย

และนอกเหนือจากนี้ วิทยานิพนธ์ฉบับนี้ยังได้นำเสนอสายอากาศสองโพรบตั้งฉากกระตุ้นวงแหวนวงกลมวางเหนือแผ่นสะท้อนสี่เหลี่ยมจัตุรัส ที่มีแบบรูปการแพร่กระจายคลื่นทิศทางเดียวสำหรับไดเวอร์ซีตี้เชิงการโพลาไรซ์ ไอโซเลเตอร์เชิงเส้นได้ถูกนำเสนอเพื่อปรับปรุงค่าการแยกระหว่างโพรบทั้งสอง (Isolation) สายอากาศนี้ได้นำเสนอสำหรับกับการประยุกต์ใช้งานการสื่อสารไร้สายแบบจุดต่อจุดระหว่างอาคารตามมาตรฐาน IEEE 802.11a ที่ครอบคลุมย่านความถี่ 5.150 กิกะเฮิรตซ์ ถึง 5.825 กิกะเฮิรตซ์ นอกจากนั้นการออกแบบสายอากาศนี้เพื่อให้มีขนาดเล็ก และ เหมาะสำหรับการผลิตจำนวนมากๆ วัสดุที่นำมาใช้ในการออกแบบสายอากาศไม่มีค่าการสูญเสียไดอิเล็กตริก และมีความสามารถในการจัดการพลังงานสูง สายอากาศต้นแบบได้ทำการออกแบบและนำไปทดสอบเพื่อเปรียบเทียบกับผลการจำลองทางทฤษฎี ซึ่งพบว่า ผลทั้งสองมีความสอดคล้องกัน และจากผลการทดสอบที่ความถี่กลาง เห็นว่าความกว้างลำคลื่นครึ่งกำลัง (Half-power beamwidth) ในทั้งสองระนาบเท่ากับ 65 องศา และ 75 องศา อัตราส่วนลำคลื่นด้านหน้าต่อด้านหลังเท่ากับ 31 dB และค่าอัตราการขยายเท่ากับ 7.42 dBi ในขณะที่ค่าสัมประสิทธิ์การสูญเสียย้อนกลับ $|S_{11}|$ และ $|S_{21}|$ เท่ากับ -23.09 dB และ -33.99 dB ตามลำดับ และช่วงกว้างแถบความที่เท่ากับ 23.64%

จากผลที่ได้รับดังที่กล่าวมาข้างบนนั้น พบว่าสายอากาศทิศทางเดียวรูปวงแหวนวางเหนือแผ่นสะท้อนสี่เหลี่ยมจัตุรัสเหมาะสำหรับระบบสื่อสารไวแมกซ์ และระบบโครงข่ายท้องถิ่นไร้สาย

Thesis Title	Design of Unidirectional Antennas Using Ring above Square Reflector for Wireless Communications
Student	Miss Souphanna Vongsack
Student ID.	52601001
Degree	Doctoral of Engineering
Program	Electrical Engineering
Year	2015
Thesis Advisor	Assoc. Prof. Dr. Chuwong Phongcharoenpanich

ABSTRACT

This thesis concerns about a unidirectional ring antenna for WLAN and WiMAX systems by using circular disc monopole (CDM) excited rectangular ring mounted in front of a square reflector. The proposed antenna is designed to cover the frequency range of 2.300 GHz to 5.825 GHz and thereby is suitable for WiMAX applications. Multiple parametric studies were carried out using the CST Microwave Studio simulation program. A prototype antenna was fabricated and experimented. The measurements were taken and compared with the simulation results, which indicates good agreement between both results. The prototype antenna produces an impedance bandwidth ($|S_{11}|$ < -10 dB) that covers the WiMAX frequency range and a constant unidirectional radiation pattern (θ = 0° and ϕ = 90°). The minimum and maximum gains are 3.70 dBi and 8.70 dBi, respectively. The proposed antenna is of compact size and has good unidirectional radiation performance. Thus, it is very suitable for a multitude of WiMAX applications.

Moreover, this part of thesis proposes a unidirectional antenna for the dual-band point-to-point communication of Wireless Local Area Network (WLAN) system

according to the IEEE 802.11a/b standard in which the allocated frequency band ranges from 2.400 GHz to 2.484 GHz and 5.150 GHz to 5.825 GHz. This thesis proposes a rectangular ring antenna excited by U-shaped slot CDM excited rectangular ring antenna, which are placed above a square reflector with 3.600 GHz to 4.870 GHz rejection band. The U-shaped slot in the CDM, band-rejected filtering property in the WiMAX band is achieved. The prototype antenna was fabricated and measured to verify the simulated results. From the results it is found that the simulated $|S_{11}|$ good agree with measured $|S_{11}|$ with the antenna gain is 7.31 dBi at 2.45 GHz and 4.14 dBi at 5.50 GHz, respectively. The obtained band-rejected is 29.78%. From apparent characteristics, it can be confirmed that this antenna is a potential candidate for dual-band unidirectional beam of WLAN applications.

In addition, this thesis presents a circular ring antenna fed by two perpendicular probes, both of which are placed above the square reflector. The antenna is employed to radiate unidirectional beam for polarization diversity reception. A linear isolator is added to improve the isolation between the two probes. The antenna is proposed for the point-to-point communication of WLAN system according to the IEEE 802.11a standard in which the allocated frequency band ranges from 5.150 GHz to 5.825 GHz. The proposed antenna is compact and suitable for mass production. Without the dielectric material, the antenna is free of dielectric loss and capable of high power handling. The prototype antenna was fabricated and measured to verify the theoretical predictions. At the center frequency, the unidirectional pattern with the measured half-power beamwidths in two principal planes of 65 and 75 degrees is achieved. The front-to-back ratio is 31 dB, and the antenna gain is 7.42 dBi. The $|S_{11}|$ and $|S_{21}|$ are respectively -23.09 dB and -33.99 dB while the obtained bandwidth is 23.64%. Based on the aforementioned characteristics, the antenna is a potential candidate for polarization diversity of WLAN applications.

ACKNOWLEDGEMENTS

This dissertation would not have been possible without the help, guidance, support and great patience of my principle supervisor and kind people around me, to only some of whom it is possible to give particular mention here. The followings are devoted to all those contributed to the completion of this thesis for the past six years.

Sincere appreciation goes to my advisor, Assoc. Prof. Dr. Chuwong Phongcharoenpanich, for his professional guidance in antenna theory, support encouragement throughout my course of study at King Mongkut's Institute of Technology Ladkrabang. I also appreciate to my co-advisor, Assoc. Prof. Dr. Sompol Kosulvit, for his fruitful guidance and hospitality throughout the project. Additional thanks to my Japanese co-advisor, Prof. Dr. Kazuhiko Hamamoto and Prof. Dr. Toshio Wakabayashi for their helpful discussion and comments, not to mention their advice and unsurpassed knowledge has been invaluable on both an academic and a personal level, for which I am extremely grateful.

I am particularly grateful to AUN/Seed-Net for highly continues support during the time I have been studying on my doctoral degree. I also extend my sincere appreciation to KMITL for giving me the great opportunity to do research in a warmly environment.

Furthermore, I would like to extend my thankful to co-advisors Prof. Dr. Kazuhiko Hamamoto and Prof. Dr. Toshio Wakabayashi at the Tokai University to give me a good opportunity to do the research at their Laboratory.

In addition, I would like to thank all of my colleagues all alumnae and present members in the Wireless Communication Laboratory and acknowledged for their support, helpful discussions and friendship. I would love to thanks to especially Dr. Suthasinee Lamultree, Dr. Phairote Wounchoum, Dr. Kittisak Pheabua, Dr. Rattapong Suwaluk, Dr. Supakit Kawdungta, Mr. Tajchai Pumpoung and Mr. Sitthichai Dentri for their helpful discussions and experiments. To all my friends and colleagues in Laos, Thailand, Cambodia, and Indonesia, I wish to express many thanks for enjoyable and stimulating atmosphere that their helped to provide with their companion and friendship.

Last, but by no means least, I am deepest grateful goes to my beloved parents, elder brothers and elder sisters for their unflagging love, always stand by my side and encourage for everything, have given me their unequivocal support throughout, as

always, for which my mere expression of thanks likewise does not suffice. It is their tolerance and love that carry me through the peaks and through of my entire life.

Finally, I dedicate this dissertation to my beloved husband Vilathep Vivavong, who raised me to be the person I am today. You have been with me every step of the way, through good times and bad. Thank you for all the unconditional love, support that you have always given me, helping me to succeed and great patience at all times until your last breathes. Thank you for everything. I love you!

Without whom none of my success would be possible.

Souphanna Vongsack

TABLE OF CONTENTS

TABLE OF CONTENTS (CONTINUE)

TABLE OF CONTENTS (CONTINUE)

LIST OF TABLES

LIST OF FIGURES

LIST OF FIGURES (CONTINUE)

LIST OF FIGURES (CONTINUE)

CHAPTER 1
INTRODUCTION

1.1 Rationale

Presently, the wireless communications are essential for human activities in various aspects and have grown rapidly. Besides an integral part of wireless communications, a wideband antenna is a crucial technology in the short-range, high speed and indoor data wireless communications. According to the frequency bands of WiMAX system in three bands are allocated in the frequency bands of 2.300-2.400 GHz, 3.400-3.690 GHz, and 5.150-5.825 GHz (2.50/3.50/5.50 GHz) [1]-[4]. Over the past decades, a greater number of countries have utilized cellular base stations for installation of WiMAX antennas. Moreover, advances in mobile communications technology and rapid urbanization help promote the growth of indoor base stations, for example, in buildings, underground train systems, and tunnels. On distinct characteristic of indoor base stations is their omnidirectional radiation pattern, which is however their main drawback since an omnidirectional antenna can cover a limited circular area. This renders the omnidirectional antenna unsuitable for applications in the environment characterized by long and confined spaces in which a unidirectional antenna is more appropriate. In addition, unidirectional antennas are applicable to point-to-point communications. In these environments, for example, streets, highways, tunnels, and corridors, a unidirectional or bidirectional antenna performs better than an omnidirectional antenna [5]-[13]. To generate a unidirectional beam, a planar reflector [14]-[15], corner reflector [16]-[17], parabolic reflector [18], or conical reflector [19] was used with an omnidirectional monopole antenna. The unidirectional bandwidth is narrow and could be enhanced by replacing the linear monopole with surface monopole, for example, circular, triangular, square, or rectangular monopole [20]-[24]. To achieve the unidirectional pattern along the WiMAX frequency range of 2.300 GHz to 5.825 GHz, this research proposes a rectangular ring antenna excited by a CDM mounted in front of a square reflector. The simulations and experiments were carried out along the WiMAX frequency band.

Moreover, to design the dual-band unidirectional antenna this thesis proposes a rectangular ring antenna excited by U-shaped slot CDM are placed above the square

reflector with 3.600 GHz to 4.900 GHz rejection band. The U-shaped slot in the CDM, band-rejected filtering property in the WiMAX band is achieved. The antenna is proposed for the dual-band point-to-point communication of Wireless Local Area Network (WLAN) system according to the IEEE 802.11a standard in which the allocated frequency band ranges from 2.400-2.484 GHz and 5.150-5.825 GHz, of which the center frequency are 2.45 GHz and 5.50 GHz [25]-[27]. Over the designed bandwidth of wideband system, there are some other existing narrowband services that already occupy frequencies in the wideband, such as World interoperability for Microwave Access (WiMAX) service from 3.400-3.700 GHz also operates in the wideband [28]. Along with the wideband, some narrow band systems operate. The dual band antenna with unidirectional or bidirectional pattern is very useful for base station applications such as WLAN system [29-33]. Based on the background of the researches above, this thesis proposes a simple and compact U-shaped slot CDM fed rectangular ring antenna above square reflector with dual band-notched characteristics in 4.00 GHz (3.600-4.860 GHz). The dual band-notched operations are achieved by etching U-shaped slot in the CDM.

In addition, this thesis also presents a circular ring antenna fed by two perpendicular probes, both of which are placed above the square reflector. The antenna is employed to radiate unidirectional beam for polarization diversity reception. The Wireless LAN system plays an important role in connecting users in the community of a given service area [34]. Based on IEEE 802.11a standard, the operating frequency band covers 5.150 GHz to 5.825 GHz, of which the center frequency is 5.50 GHz. Typically, the communication network of WLAN system can be classified into two topologies, i.e., point-to-multipoint and point-to-point connections as illustrated in Fig. 1.1. The point-to-multipoint connection is the typical topology in which the root or base station is able to communicate to a number of clients located around it. In this configuration, the omnidirectional antenna is suitable for the base station [35]-[36]. For the point-to-point connection topology, the unidirectional antenna is a promising candidate [37]-[39]. In the case of only line of sight (LOS) situation, the signal can be directly propagated from the transmitter to the receiver. However, in some environments in which the transmitter and receiver are obstructed by various objects, the multipath signal occurs due to obstacles, such as buildings and trees, which cause the signal to reflect and diffract. The multiple components of transmitted signal reach the receiver at slightly different time points,

thereby producing multipath fading which not only varies with time and physical motion but also affects the channel performance and thus reduces the data rate [40]. To mitigate the fading problem, the diversity reception techniques have been applied [41]-[42]. A number of diversity antennas have been discussed in the existing literature [43]-[44]. The space diversity with proper spacing between two antennas is the simplest geometry [45]. However, since large spacing is required, the overall antenna dimension needs to be relatively large [46]. The polarization diversity with two orthogonal excitations in the same antenna body has been proposed to minimize the whole antenna size [47]-[50]. The polarization diversity antenna with unidirectional pattern is very useful for base station applications such as WLAN system [51]-[54]. This thesis presents the unidirectional antenna for polarization diversity of WLAN system following IEEE 802.11a standard with the operating frequency band between 5.150 GHz and 5.825 GHz. The antenna evolution starts from the circular ring excited by a probe that radiates bidirectional pattern in two opposite directions along two ring apertures with single polarization. This structure is located above the square reflector to confine the main beam to single direction. The excitation with two perpendicular probes is introduced for polarization diversity. To improve the isolation between two excited probes, the linear isolator with proper angle is added. The antenna characteristics in terms of the reflection ($|S_{11}|$ and $|S_{22}|$), isolation ($|S_{21}|$ and $|S_{12}|$), radiation pattern, and gain are presented. The simulation was performed using CST Microwave Studio [55]. The prototype antenna was fabricated and measured to confirm the theoretical principle.

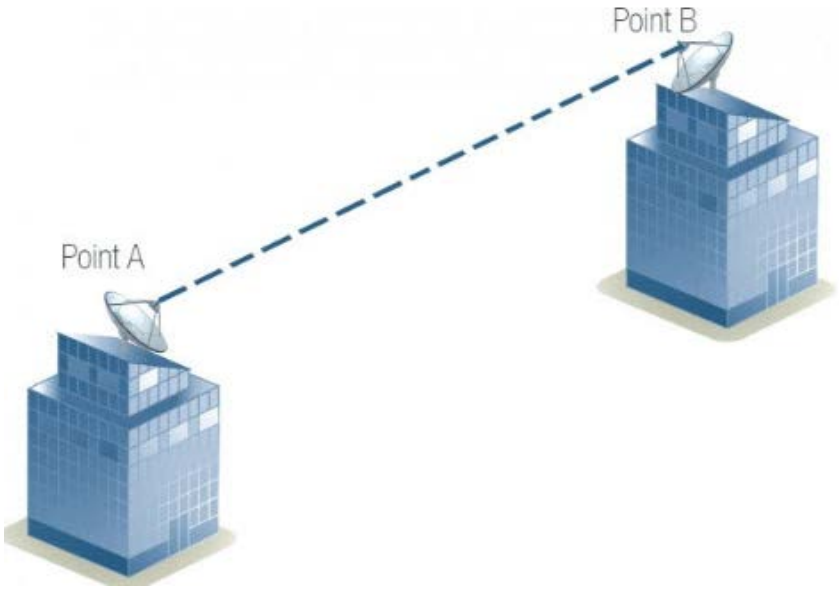

(a)

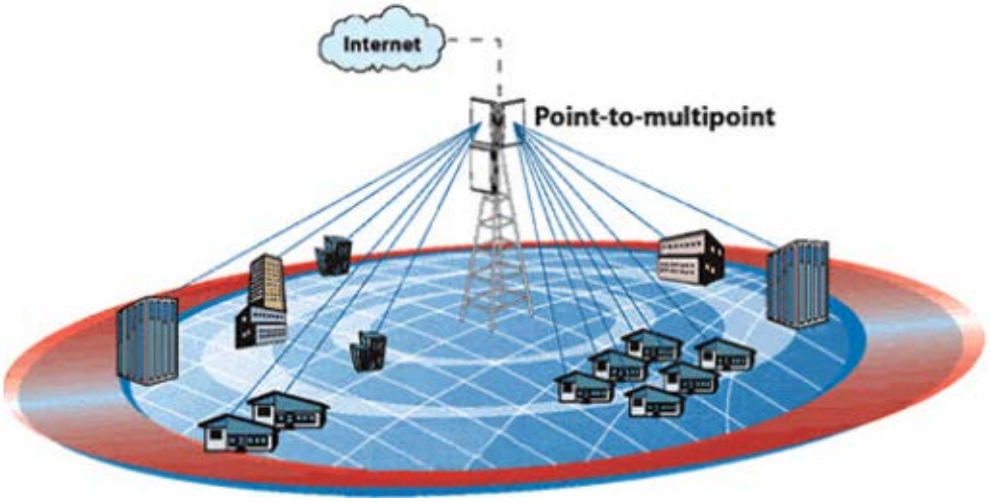

(b)

Figure 1.1 Wireless Local Area Network (WLAN) communication systems.
(a) Point-to-point communications, and (b) Point-to-multipoint communications.

1.2 The Objective and Scope of the Thesis

The objectives and the scope of the thesis is the development of the antenna for WLAN and WiMAX and given as follows:

1. The rectangular and circular ring antennas are selected because they have simple structure and easy to fabricate. The conventional antenna radiates bidirectional narrow bandwidth.

2. The gain improvement using square reflector to confine the beam to be the unidirectional pattern for bridging outdoor connection.

3. The bandwidth enhancement using the CDM feeder to achieve wideband operation for both WLAN and WiMAX application

4. The band notch using U-slot inside CDM to obtain dual-band frequency for WLAN application

5. The polarization diversity using two perpendicular probe feeders with linear isolator to yield high isolation.

1.3 Organization of the Thesis

To fulfill the purpose of this thesis, numerous works must be carried out both theoretically and experimentally. Recently, WiFi is no longer used merely for internet

connectivity; it is further used to broadcast quality multimedia content throughout the entire home. WiMAX is an approaching wireless technology that is designed for Metropolitan Area Networks (MAN) based on the IEEE 802.16 specifications. It aims to provide high speed wireless internet connections over long distances. Hence, this thesis is divided into three models. The first model is a unidirectional wideband antenna using circular disc monopole (CDM) excited rectangular ring above square reflector for WiMAX and WLAN systems is introduce in Chapter 3. Chapter 4 proposes a unidirectional dual-band antenna using U-shaped slot circular disc monopole (CDM) excited rectangular ring above square reflector for WLAN systems with 3.600 GHz to 4.870 GHz rejection band. In addition, to mitigate the fading problem, a unidirectional antenna using two-probe excited circular ring above square reflector for polarization diversity with high isolation for WLAN system is present in Chapter 5. The conclusions are drown and detailed in Chapter 6. The organization of this thesis is as follows:

In Chapter 2, the literature review of the unidirectional antenna using a probe excited ring.

Chapter 3 a unidirectional wideband antenna using circular disc monopole (CDM) excited rectangular ring above square reflector for WiMAX and WLAN system. The antenna is designed to cover the frequency range from 2.300 GHz to 5.825 GHz. The radiation pattern, gain antenna, and impedance bandwidth is analyzed in terms of antenna parametric study, such as the dimension of the rectangular ring, ring width a, ring height b, and ring length d. The space between the CDM and the square reflector is denoted by h. The radius of CDM r_c and the delta gap δ. The rectangular ring is used to confine the CDM radiating omnidirectional pattern to become bidirectional beam. After that, to realize the unidirectional pattern the reflector should be place near the one side of the ring aperture.

Chapter 4 a unidirectional dual-band antenna using U-shaped slot circular disc monopole (CDM) excited rectangular ring above square reflector for WLAN system. The dual-band notched operations are achieved by etching U-shaped slot from CDM element with can rejection band at 3.600 GHz to 4.870 GHz is proposed and discussed.

Chapter 5 presents the simulation and measurement of a unidirectional antenna using two-probe excited circular ring above square reflector for polarization diversity

with high isolation. The impedance bandwidth $|S_{11}|$, the isolation between probes $|S_{21}|$, the radiation pattern, and the gain is analyzed in terms of antenna parameters, such as radius and length of circular ring, probe length and the spacing between the probe and the reflector, the position and the length of isolator. These results are shown in figures and variations of their characteristics on frequency are also discussed. The proposed antenna is operated at the center frequency of 5.50 GHz for point-to-point communication systems to cover the frequency range from 5.150 GHz to 5.825 GHz. From the results, it is found that the good radiation characteristics of the proposed antenna have been obtained that is polarization diversity with high isolation, front-to-back ratio in both in *xy*-plane and *xz*-plane and large bandwidth of better than 20 dB.

Chapter 6 summarizes the consequence of the preceding chapters with the discussion of the future studies.

CHAPTER 2
ANTENNA PRINCIPLE

2.1 Introduction

In this chapter, the concept of the main keywords is necessary that related to this thesis are introduced and organized in five keywords as follows:

❖ First keyword: The design principle starts with exciting the rectangular ring with a circular-disc monopole (CDM) are also considered and discussed.

❖ Second keyword: In this step, to model the bidirectional radiation pattern one important candidate is the ring such as rectangular ring, circular ring and others, which are used to form beam from omnidirectional to radiate in two aperture ring. Thus, the bidirectional antenna using ring structure with monopole is introduced.

❖ Third keyword: To obtain the unidirectional pattern, the structure should be place near the one side of the ring aperture to focus the main beam into the one direction. The unidirectional antenna using ring structure above reflector is described in this section.

❖ Fourth keyword: Application of the unidirectional antenna for point-to-point WLAN and WiMAX systems.

❖ Fifth keyword: As well-known that, it is cannot deny that in some environments in which the transmitter and receiver are set up in location lower than the surrounding buildings or are obstructed by various objects, the multipath signal will be occurs due to obstacles such as buildings, trees and many other obstacles, which case the signal to reflect and diffract. But in the case of only line of sight (LOS) situation, the signal can be directly propagated from the transmitter to the receiver. Hence, to mitigate or reduce the fading problem the diversity reception techniques have been applied and discussed.

2.2 The Bandwidth Enhancement Using a Planar Monopole Antenna

A fundamental thin wire monopole antenna and its variants have the common features to be omnidirectional and structurally, but narrowband. Hence, a planar plate monopole antenna is a candidate. They are interesting due to their broad impedance

bandwidth, linearly polarized omnidirectional radiation pattern and very cost effective to construct. They are planar structure, where a thin planar metal element can be used instead of the traditional wire element of a monopole antenna. There are various ways to express bandwidth, the basic antenna structures considered include a circular plate, elliptical (with different elliptical ratios), square, rectangular, and hexagonal disc monopole antennas which yield very large impedance bandwidth as shown in Fig. 2.1 [21]-[23].

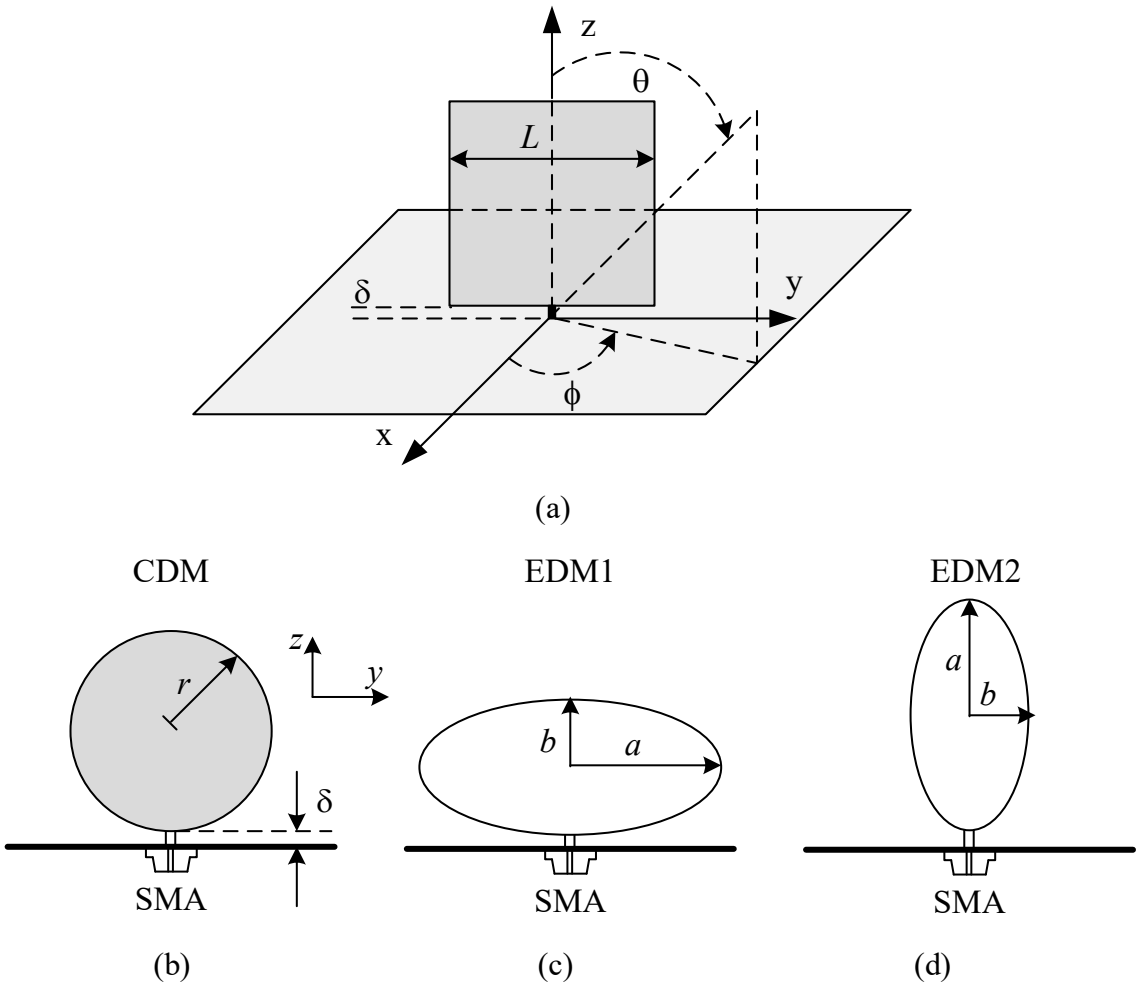

Figure 2.1 The geometry of planar monopole antenna mounted above ground plane. (a) Square disc monopole, (b) Circular disc monopole, (c) and (d) elliptical disc monopoles.

2.2.1 A Square Planar Monopole Antenna

One of the simple planar monopole shapes that have received a lot of attentions is a square or rectangular plate as shown in Fig. 2.1 (a). One of the most popular antennas employed in mobile and wireless communications systems is the

monopole antenna and its family. The planar element is located a distance δ mounted a ground plane, and is fed by a SMA connector. The bandwidth of the planar monopole antenna is set mainly by the radiating element dimensions, L and to obtain the maximum impedance bandwidth a suitable feed gap separation, δ is required.

The effect that a square planar monopole antenna dimension and its separation from ground have on the impedance bandwidth can be obtained through the study of the return loss results, were described in 2003 by M.J. Ammann and Z. N. Chen [20]. In all cases the thickness of a planar plate monopole is 0.5 mm copper sheet and the square ground plane considered is of side 100 mm and the SMA connector has a feed-probe diameter of 1.2 mm. Table 2.1 gives for a square plate planar monopole of various dimensions, L, the lower and upper frequency limits, and hence, the bandwidth based on 10 dB return loss. In each case the feed gap has been optimized for the highest bandwidth.

As is typical for monopole antennas, the lower edge of the impedance bandwidth is inversely proportional to the overall length of the element. In the case of planar monopole antenna, the overall length also includes the feed gap (i.e. $L+\delta$). Typically, the length of the square planar monopole antenna corresponds to about 0.21 of a free space wavelength at the lower-edge frequency; this is shorter than a quarter-wave monopole due to a reduced length-to-radius factor.

Table 2.1 The impedance bandwidth for the square elements of various dimensions, L

Square Side L (mm)	Frequency Limits (GHz)	Bandwidth (MHz)	Optimum Feed Gap (mm)
60	1.16 – 2.08	920	3
55	1.23 – 2.19	960	3
50	1.34 – 2.35	1010	3
45	1.44 – 2.59	1150	2.5
40	1.59 – 2.96	1370	2.5
35	1.86 – 3.53	1670	2.5
30	1.98 – 4.05	2090	2.5
25	2.38 – 5.20	2820	2.5
20	2.68 – 6.50	3820	2.2

2.2.2 A Planar Circular Monopole Antenna

One of the earliest monopole shaped whose properties were studied in the literature is the circular disc monopole antenna was introduced in 1998 by N.P. Agrawall, G. Kumar, and K.P. Ray [22]. Fig. 2.1 (b)-(d) shows a metallic circular disc monopole (CDM), and a elliptical disc monopole (EDM), placed above a flat ground plane and fed through a coaxial feed via a narrow strip.

From the verification simulations and experiments have been carried out on various planar monopole antennas such as square, circular and elliptical disc monopole. Among all the configurations studied, not merely the square planar monopole, the CDM and EDM are also yield maximum bandwidth as shown in Table 2.2. Table 2.2 shows the frequency corresponding to the lower edge of the bandwidth of this monopole antennas VSWR bandwidth of CDM and EDM. Upon comparison of the square planar monopole antenna with the circular planar monopole antenna one can see that the circular plate provides higher impedance bandwidth but, unlike the circular planar monopole antenna the patterns of the square or rectangular plate monopole are fairly stable with frequency. As such, majority of the works, reported in the literature, carried out on the planar monopole antennas use the square or rectangular shaped plates.

Table 2.2 The impedance bandwidth for the square elements of various dimensions, *L*

Config.	***a* (mm)**	***b* (mm)**	**Freq. range for VSWR<2 (GHz)**	**Theory lower freq. for VSWR<2 (GHz)**	**Bandwidth ratio**
CDM	25	25	1.17 – 12.00	1.28	1:10.2
EDM1	26	24	1.21 – 13.00	1.31	1:10.7
EDM2			1.20 – 12.50	1.24	1:10.4
EDM1	27	23	1.38 – 11.49	1.37	1:8.3
EDM2			1.13 – 12.00	1.20	1:10.6
EDM1	28	22	1.37 – 11.30	1.41	1:8.2
EDM2			1.08 – 11.43	1.17	1:10.6
EDM1	29	21	1.58 – 10.45	1.46	1:6.6
EDM2			1.09 – 10.45	1.13	1:9.6

2.3 Bidirectional Antenna Using Ring Structure with Monopole

In general, the base station antennas in microcellular system for the urban areas are located lower than the surrounded buildings along the streets and located in the underground area; the communicable cell is formed along the street, subway station, tunnel etc. For these environments the bidirectional antenna is suitable more than the omnidirectional one because its radiation pattern can be formed along the street. Therefore, before discussing the principle of a bidirectional antenna using a ring structure with monopole, the meaning of the term principle of a waveguide as it is used in this section must be established. Waveguides are basically a device "a guide" for transporting electromagnetic energy from one region to another. Typically, waveguides are hollow metal tubes such as rectangular, circular, elliptical ring and others, but rectangular and circular are the most popular, because of ease of analysis and fabrication and their attractive radiation characteristics, especially low cross-polarization radiation as shown in Fig. 2.2. They are capable of directing power precisely to where it is needed, can handle large amounts of power. Moreover, the waveguide has a cutoff frequency f_c and acts as a high pass filter in that most of the energy above the cutoff frequency will pass through the waveguide, whereas most of the energy that is below the cutoff frequency will be attenuated by the waveguide. The cutoff frequency defines the high-pass filter characteristic of the waveguide: above this frequency, the waveguide passes power, below this frequency the waveguide attenuated or blocks power.

(a) (b)

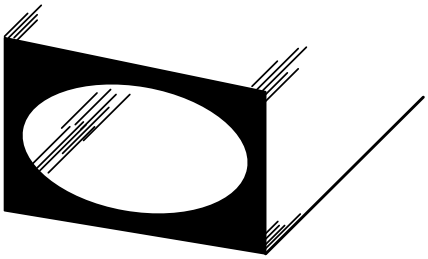

(c)

Figure 2.2 Waveguide shapes. (a) Circular waveguide, (b) Rectangular waveguide, and (c) Elliptical waveguide.

2.3.1 Rectangular Ring Waveguide

The cutoff frequency depends on the shape and size of the cross section of the waveguide. The formula for the cutoff frequency of a rectangular cross sectioned waveguide is given by

$$f_c = \frac{1}{2a\sqrt{\mu\varepsilon}} = \frac{c}{2a} \tag{2.1}$$

whereas c is the speed of light within the waveguide, μ is the permeability, and ε is the permittivity of the material that fills the waveguide. Note that the cutoff frequency is independent of the short length b of the waveguide.

Let us consider from the literature review [7]-[8] the characteristics of a bidirectional antenna using a linear probe excited a rectangular ring is proposed. The ring height and width are first chosen to achieve the dominant mode propagation and ring length to obtain the optimum radiation pattern condition, respectively. For the standard waveguide that has the ratio between the widths to the height equals to 2, the criterion for selecting the ring width should be greater than half wavelength and less than on wavelength to let only TE_{10} mode propagation. However, the evanescent wave of the higher order mode near the probe still has a significant level. Therefore, they contribute to the aperture field and the radiate field. On the other hand, as the length is increased these higher modes can be vanished at an expense of the long aperture separation. We can conclude that the ring width and height is selected based on the dominant mode propagation. The ring length is optimized to achieve the optimum radiation pattern. The polarization is vertical linear polarization at the

boresight direction. The impedance matching can be achieved by adjusting the probe length.

2.3.2 Circular Ring Waveguide

For the cutoff frequency for a waveguide with a circular cross section of radius *a* is given by

$$f_c = \frac{1.8412}{2\pi a\sqrt{\mu\varepsilon}} = \frac{1.8412c}{2\pi a} \tag{2.2}$$

From the previous work, a simple structure and cost-effectiveness linear monopole excited a circular ring antenna [6]. The principle to design of this research work is to use a circular structure in which the excited probe is located at the center between two open apertures. The ring radius that yields the shortest ring width that the higher modes die out at the apertures is selected as the design criterion. It is well-know that the ring as a part of circular waveguide which electromagnetic fields propagate in both *z* and *–z* directions and they radiate from the apertures at the ends of the ring. These aperture fields correspond to the composite field consisting of various modes accommodating in the waveguide. Since the ring width and radius are choose that cutoff all the higher modes but dominant mode (TE_{11}), the field near the probe is still consisting of composite modes. Generally, the higher modes are evanescent and their amplitudes are decreased rapidly as the distance from the probe is increased. The distance is chosen such that the amplitudes of the higher modes are negligible small at the apertures. Hence, the apertures radiate the fields according to only the dominant mode. To let only the dominant mode accommodated in the ring, the radius is chosen such that the lowest cutoff frequency is the dominant mode (TE_{11}). The adjacent mode (TE_{21}) is cutoff [56].

$$0.293\lambda < a < 0.486\lambda \tag{2.3}$$

whereas λ is the wavelength at the operating frequency.

From these aforementioned literatures, it is apparent that all of the optimum parameters from the literature review are very useful as the guideline for the antenna design.

We now know what a waveguide is. Since the ring as a part of rectangular and circular waveguide which electromagnetic fields propagate in both z and *–z* directions and they radiate from the apertures at the ends of the ring. On other hand, it is can say that the bidirectional pattern can be achieved because the omnidirectional beam of linear monopole is forced by the rectangular or circular ring to radiate the bidirectional beam, beam peaks direct only in forward and reverse directions as shown in Fig. 2.3. Thus, many researches and developments on bidirectional antenna have been continuously conducted as illustrated from literature reviews. Unfortunately, the bandwidth is relative narrow. Afterwards, many techniques have been reported to enlarge the impedance bandwidth of the conventional narrow-band antenna such as using planar or disk monopole. In 2008 by S. Lamultree [57], from this work presents a bidirectional UWB antenna using rectangular ring fed by stepped monopole instead of linear monopole to enhance the impedance bandwidth. Apparently, the bandwidth can be enhanced by using stepped monopole excited compared to the conventionally linear monopole. Furthermore, the return loss is lower than -10 dB, and it provides the fairly stable directional radiation pattern over the frequency range from 3.1 GHz to 10.6 GHz. At the desired direction, the simulated gain of 2.33 dBi to 5.21 dBi. These results are very useful to design a bidirectional UWB antenna as well as for others wide band applications. However, for some specific application that requires the long range service area such as point-to-point communication between the buildings, when the mobiles move along the confined paths such as street, highways, tunnels and corridors; for these environments, a unidirectional antenna is more suitable than the bidirectional or omnidirectional one to serve these demands. Hence, the bidirectional antenna is modified by adding different shapes of reflectors will describe in the next section.

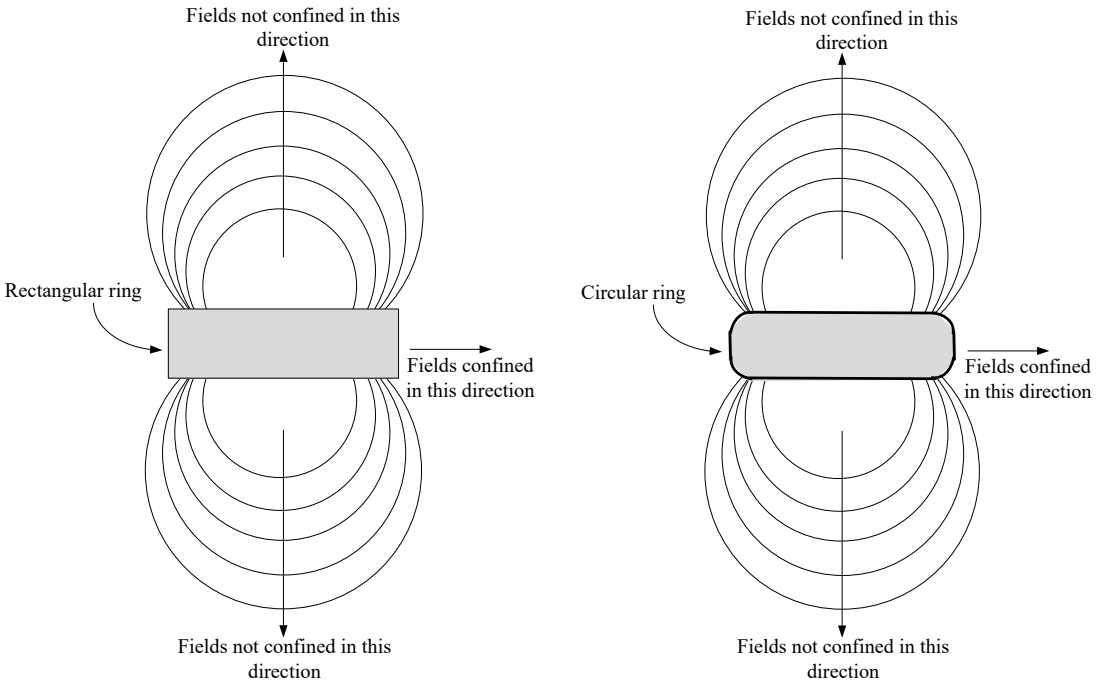

Figure 2.3 Top view of fields confined in two directions only. (a) Rectangular ring, and (b) Circular ring.

2.4 Unidirectional Antenna Using Ring Structure above Reflector

Directional antennas as the name implies refers to signal coverage in a specified direction. Unlike omnidirectional antennas, directional antennas are used for point-to-point or sometimes for multi-point systems. If you are trying to transmit the signal from one location to another location, the directional antenna is recommended. According to aforementioned in the last section, for some specific application that we requires the long and narrow path service area such as point-to-point communication between the buildings, street, highways, tunnels and others; for these environments, the unidirectional antenna is desirable than the omnidirectional and bidirectional. Recently, several researchers have devoted large efforts to develop antennas that satisfy the demands of the wireless communication industry for improving performances, especially in term of multiband operations and miniaturization. Anyway, the bidirectional antenna is modified by adding different shapes of reflectors such as planar reflector [14]-[15], corner reflectors [16]-[17], parabolic reflector [18], or conical reflector [19], Others often met in practice are the cylindrical reflector, spherical reflector, and others to obtain the unidirectional beam. Although

reflector antennas take many geometrical configurations, each of which such as plane reflector will be discussed in this section.

The simplest type of reflector is a plane reflector introduced to direct energy in a desired direction as shown in Fig. 2.4. The advantage of this structure is simple and easy to fabricate. In addition, there is no dielectric component and it has low loss. From literature review, it is evident that the probe excited rectangular ring near the reflector yields the better characteristics. Moreover, the spacing between the probe and plane reflector have been considered, because it is influence to directivity, radiation pattern, and side lobe level. However, the radiation characteristics of the antenna for various spacing between a probe excited rectangular ring and reflector was introduced in 2002 by C. Phongcharoenpanich [15]. The results of the analysis are very useful for designing the high directivity unidirectional beam antenna.

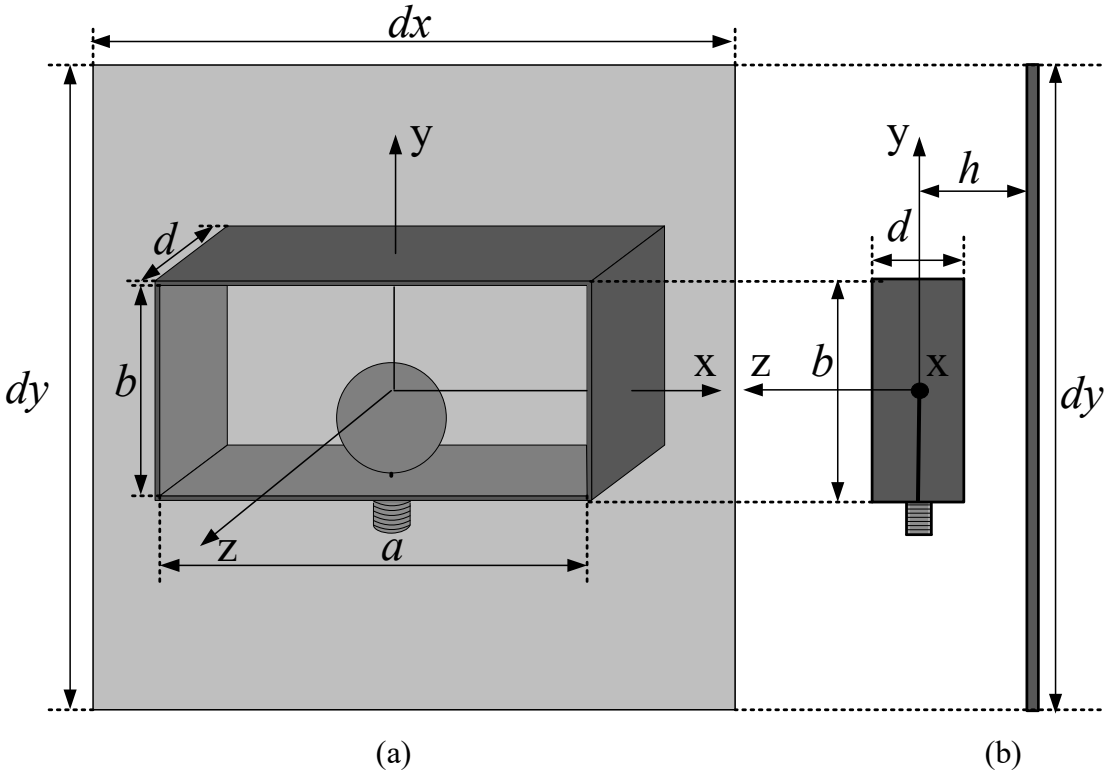

Figure 2.4 A unidirectional beam antenna using the CDM excited rectangular ring above plane reflector. (a) Perspective view, and (b) Side view.

2.5 Application of a Unidirectional Antenna for Point-to-point WiMAX and WLAN Systems

Worldwide interoperability for microwave access (WiMAX) is a wireless communications standard designed for creating metropolitan area networks (MANs). It is similar to the WiFi standard, but supports a far greater range of coverage. While a WiFi signal can cover a radius of several hundred feet, which WiMAX station can cover a range of up to 30 miles. WiMAX is also known by its technical name, "IEEE 802.16," which is similar to WiFi's technical specification of 802.11. It is considered the second generation broadband wireless access standard and will most likely be used along with WiFi, rather than replace it. Since WiMAX has such as large signal range, it will potentially be used to provide wireless internet access to entire cities and other large areas. WiMAX, on the other hand, can cover several miles using a single station. The WiMAX forum has published three licenses spectrum profiles, namely the 2.50 GHz (2.50-2.69 GHz), 3.50 GHz (3.40-3.69 GHz), and 5.50 GHz (5.25-5.85 GHz) varying country to country.

As we known-well that a Wireless Local Area Network (WLAN) is one of the faster growing networking technologies. Apart from mobile communication technology, WLAN technology has also made a giant stride by introducing WiFi. WiFi is a part of product compatibility standards for WLAN technology based on the IEEE 802.11 specifications. WLAN today are being used or a wide variety of traffic types and applications. WLAN is a wireless distribution method for two or more devices that use high-frequency radio waves and often include an access point to the internet and some of the application of WLANs include, hotspots, medical facilities using VoIP over WLAN phones and badges, department stores using wireless barcode scanners, consumer electronics using wireless communications like wireless TVs, wireless cameras etc., Moreover, WLAN allows users to move around the coverage area, often a home or small office, while maintaining a network connection. Hence, modern communication requires the antenna satisfy the technical request for high performance, being lightweight and low profiles, simplicity, and reliability. The multi-frequency antenna has become one of the most important devices and attracted much interest. The most popular are those defined by the IEEE 802.11b/g WLAN standards allocate the license-free spectrum of 2.400 GHz to 2.484 GHz and IEEE 802.11a of 5.150 GHz to 5.825 GHz, multiband antennas with good performance are

needed. Many techniques have been reported in the literatures. The standardized WiFi and WiMAX operating bands are listed in Table 2.3.

As mentioned above, the design and development of a single antenna working in wideband or more frequency bands, called multiband antenna, is generally not easy task. To answer these challenges, many antennas with wideband and/or multiband performances have been published in literatures. The possibility of covering the standardized WiMAX and WLAN by using probe excited ring with modified feeder and shaped of ring. Therefore, the design of a unidirectional antenna by using CDM excited rectangular ring mounted in front of a square reflector with low cost, lightweight, and good performance for WiMAX application have been discussed in Chapter 3. In order to obtain dual-band (2.40 GHz and 5.20 GHz) and broadband operations, a rectangular ring unidirectional antenna by using U-shaped slot CDM placed above square reflector for WLAN operation is presented in Chapter 4. Then, in order to achieve a unidirectional radiation for base station antennas with decrease the multipath, two-perpendicular probe excited circular ring antenna are placed above the square reflector are designed and discussed in Chapter 5.

Table 2.3 The designed operating frequency and corresponding frequency range of WiFi and WiMAX [28]

System	Designed Operating Frequency	Frequency Range (GHz)
WiFi IEEE 802.11	2.4 GHz	2.400 – 2.485
	5.0 GHz	5.150 - 5.825
Mobile WiMAX IEEE 802.16 2005	2.3 GHz	2.300 – 2.400
	2.5 GHz	2.500 – 2.690
	3.3 GHz	3.300 – 3.400
	3.5 GHz	3.400 – 3.600
	3.7 GHz	3.600 – 3.800
Fixed WiMAX IEEE 802.16 2004	3.7 GHz	3.600 – 3.800
	5.8 GHz	5.725 – 5.850

2.6 To Mitigation of Multipath Effect Using Diversity Antenna

In the new generation of mobile communication systems it is of concern to increase the performance of the mobile terminals and their antennas to be able to answer the demand of faster and more various communicational services. However, the issue of signal fading in a multipath environment still stands as obstacle major problem today.

2.6.1 Propagation Environment

The propagation mechanism of radio waves in a mobile environment is a vital aspect in modern wireless communication systems. Since the transmission paths between the transmitter and receiver vary from simple line-of-sight (LOS) to one that is obstructed by buildings, trees, and many other obstacles, the radio channels are extremely random and unpredictable. Fading and shadowing are the most important phenomena which cause significant worsening to the quality of a mobile radio channel or can say that the fading is an attenuation that varies between a maximum and minimum value in an irregular way.

2.6.2 Diversity

The major cause of the poor performance on fading channels in the occasional fading dips, are not only achieved by spaced receiving antennas. To overcome the effect of fading dips, diversity techniques are introduced. Other mechanisms are as brief introduction some of them, in which Space diversity, Time diversity, Frequency diversity, and Polarization diversity can be utilized in antenna systems.

2.6.2.1 Space Diversity

The most common and simple mechanism used in wireless communication is space or spatial diversity. Using two or more antennas with a distance between them the phase delay makes multipath signals arriving at the antennas diverge in fading.

2.6.2.2 Time Diversity

Time diversity is related mechanisms applicable in digital data transmission. In time diversity is achieved by transmitting the same bits of information repeatedly

at time intervals. So, the fading variations for these different repetitions of a signal will be independent. Diversity can be obtained [56].

2.6.2.3 Frequency Diversity

Frequency diversity is implemented by transmitting information on more than one carrier frequency. It is a costly mechanism to use because of the difficulties to generate several transmitted signals and the combining signals received at several different frequencies at the same time.

2.6.2.4 Polarization Diversity

Two polarizations, vertical and horizontal, from two antennas can carry two signals on one radio frequency over wireless links. Polarization diversity can be exploited by using orthogonal polarization. This diversity mechanism is very practical because of the very small size of antennas that can be used.

Moreover, there are many other types of diversity mechanisms, such as Pattern diversity, Energy diversity and so on.

Hence, accomplished by increasing capacity or reducing the fading problem and multipath interference many researchers and developments on the diversity reception techniques have been applied. The diversity antenna has conventionally been implemented at the base station for current mobile communications to mitigate the fading effects of a multipath environment. Hence, the main purpose of this thesis work is introducing polarization diversity technique as a promising way of improving the performance and another merit is that the antennas used are usually of compact dimensions suitable for installing at the base station applications such as WLAN system is presented in Chapter 5. The studies and evaluation of the diversity performance have been conducted both in simulations and measurements. The measured results compare well with those from simulation cases using computer program.

2.7 Summary

These are the important five keywords that related to this thesis. The main purpose of this thesis to design antenna has a simple structure unidirectional antenna using a CDM excited rectangular ring above square reflector to cover the frequency

2.300 GHz to 5.825 GHz for WiMAX. To obtain the dual-band unidirectional antenna by using the same as structure in the previous Chapter, but the feeding is replaced to U-shaped slot CDM instead of conventional a CDM. Moreover, the polarization diversity unidirectional antenna is propose by using two perpendicular probe excited circular ring mounted above square reflector to cover the frequency range of 5.15 GHz to 5.825 GHz for WLAN applications and to apply those antenna for installing at the base station in the street cell.

CHAPTER 3
A UNIDIRECTIONAL ANTENNA BY USING CIRCULAR DISC MONOPOLE EXCITED RECTANGULAR RING FOR WIMAX SYSTEMS

3.1 Introduction

Besides an integral part of wireless communications, a wide-band antenna is a crucial technology in the short-range, high-speed, and indoor wireless communications. According to the WiMAX frequency bands are classified into three frequency bands of 2.300-2.400 GHz, 3.400-3.690 GHz, and 5.250-5.850 GHz (2.5/3.5/5.5 GHz). Over the past decades, a greater number of countries have utilized cellular base stations for installation of WiMAX antennas. Moreover, advances in mobile communications technology and rapid urbanization help promote the growth of indoor base stations, for example, in buildings, underground train systems, and tunnels. One distinct characteristic of indoor base stations is their omnidirectional radiation pattern, which is however their main drawback since an omnidirectional antenna can cover a limited circular area. This renders the omnidirectional antenna unsuitable for applications in the environment characterized by long and confined spaces in which a unidirectional antenna is more appropriate. In addition, unidirectional antennas are applicable to point-to-point communications. In these environments, for example, streets, highways, tunnels, and corridors, a unidirectional or bidirectional antenna performs better than an omnicational antenna. To generate a unidirectional beam, a planar reflector, corner reflector, parabolic reflector or conical reflector was used with an omnidirectional monopole antenna. The unisirectional bandwidth is narrow and could be enhanced by replacing the linear monopole with a surface, for example, circular, triangular, square, or rectangular monopole. To achieve the unidirectional pattern along the WiMAX frequency range of 2.300 GHz to 5.825 GHz, this chapter proposes a rectangular ring antenna excited by a CDM mounted in front of a square reflector. The simulations and experiments were carried out along the WiMAX frequency band. The proposed antenna's $|S_{11}|$, radiation pattern, and gain along the WiMAX frequency were simulated using the CST Microwave Studio.

Based on the simulation results, the optimal rectangular ring dimensions and CDM radius are a = 7.20 cm, $b = a/2$, d = 2.60 cm, and r_c = 1.10 cm, respectively, as $|S_{11}| <$ -10 dB along the WiMAX band. It is however found that the beam direction beyond a higher frequency of 5.5 GHz tilts upward as a result of the asymmetrical areas between the upper and lower portions of the rectangular ring chamber.

The organization of this Chapter is as follows. Section 3.1 is the introduction. Section 3.2 details the structure and parameters of the proposed antenna. Section 3.3 presents the design principle and the parametric study, while Section 3.4 compares the simulation and measured results. The concluding remarks are provided in Section 3.5.

3.2 Geometry of the Proposed Antenna

Figure 3.1(a) illustrates the structure of the proposed antenna, which consists of a CDM and a rectangular ring with width a, height b, length d, and thickness t. The rectangular ring center is at the yz-plane origin. The ring is excited by the CDM on the y-axis via a 50 Ω SMA connector to generate vertical polarization. The CDM radius r_c and the delta gap δ are 1.10 cm and 1.00 mm, respectively. The structure is mounted in front of an $L \times L$ square reflector. The space between the rectangular ring and the reflector is denoted by h, as illustrated in Fig. 3.1(b). The antenna radiation pattern is unidirectional with the beam peak pointing in the z direction.

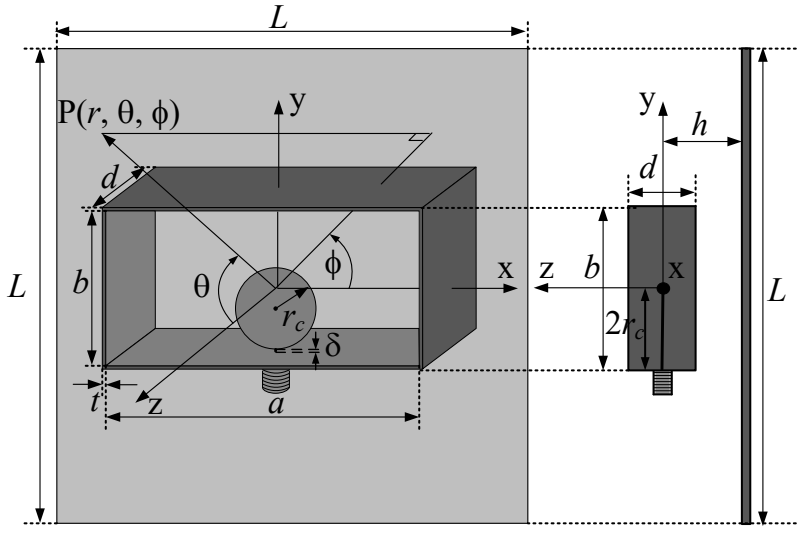

(a) (b)

Figure 3.1 The proposed antenna structure of unidirectional wideband antenna using CDM excited rectangular ring above square reflector.
(a) Perspective view, and (b) Side view.

3.3 Design Principle and Parametric Study

The antenna is designed to operate in the WiMAX frequency range of 2.300 GHz to 5.825 GHz. The design principle starts with exciting the rectangular ring with a circular-disc monopole (CDM), as shown in Fig. 3.1. The initial ring width a of the 2.3 GHz frequency is slightly greater than λ/2 (i.e., 6.60 cm). The ring height b is proportional to the ring width a; that is, $b = a/2$. The ring length d and thickness t are 3.25 cm (λ/4) and 2.00 mm, respectively. The rectangular ring is excited by a circular-disc monopole with an r_c radius 1.30 cm (0.1λ). The selected square reflectors is 16×16 cm (L×L) in dimension with the space (h) between the rectangular ring and the reflector of 3.90 cm (0.3λ). Both the rectangular ring and the reflector are made of aluminum. Ideally, the width a and height b of a rectangular ring should be minimal to obtain an antenna of a size as compact as possible.

The width a of the proposed rectangular ring follows the following rule, where λ (i.e., 13.00 cm) is the wavelength at the 2.3 GHz frequency:

$$0.5\lambda < a < \lambda \tag{1}$$

whereas λ is the wavelength at the operating frequency of 2.3 GHz.

To enhance the bandwidth, the rectangular ring is thus excited by a circular-disc monopole with an r_c radius. The initial circular monopole radius (r_c) is determined by (2) with the predetermined feed gap (δ) of 1.00 mm and 0.21λ being referenced from [20]:

$$r_c = (0.21\lambda - \delta)/2 \tag{2}$$

3.3.1 Effect of Dimension of Rectangular Ring

Parametric studies were carried out to determine the optimal ring dimensions that produce an optimal combination of resonant frequency, radiation pattern, and gain and also are of compact size. Fig. 3.2 illustrates the fractional bandwidths of resonant frequency (closest to the 2.3 GHz frequency) by varying a and d of the rectangular ring antenna which is excited by a CDM. Both the ring antenna and the CDM are together mounted in front of the square reflector. As shown in Fig. 3.2, the

fractional bandwidth of resonant frequencies at 2.3 GHz is achieved with *a* of 7.20 cm (0.553λ), *b* of 3.60 cm, and *d* of 2.60 cm, which are selected as the design parameters. It is noted that the ring width *a* of 7.20 cm (0.553λ) is selected because of the wide bandwidth, compact antenna size, and available material in the market suitable for the mass production.

To determine an optimal matching condition with a wide bandwidth, the space between the CDM and the square reflector *h* is varied from 1.65 (0.21λ) to 3.90 cm (0.30λ). The simulated unidirectional beam is achieved at *h* of 0.10λ-0.30λ and 0.60λ-0.70λ, while that the widest bandwidth is achieved at $h < 0.30\lambda$. The beam splits occur when *h* is between 0.30λ and 0.60λ. According to [15], the unidirectional beam can also be realized when *h* is ≥0.70λ. It is found that the radiation pattern becomes split for *h* between 0.30λ and 0.60λ. The simulation results are shown for *h* of 1.65-2.90 cm because while *h* is >2.90 cm the $|S_{11}|$ cannot cover the frequency bandwidth (e.g., $h = 3.15$ cm, the $|S_{11}| > -10$ dB from 4.92 to 5.91 GHz). Based in the simulation results (Fig. 3.3), *h* of 2.40 cm (0.184λ) is selected as it produces a unidirectional beam with wide bandwidth.

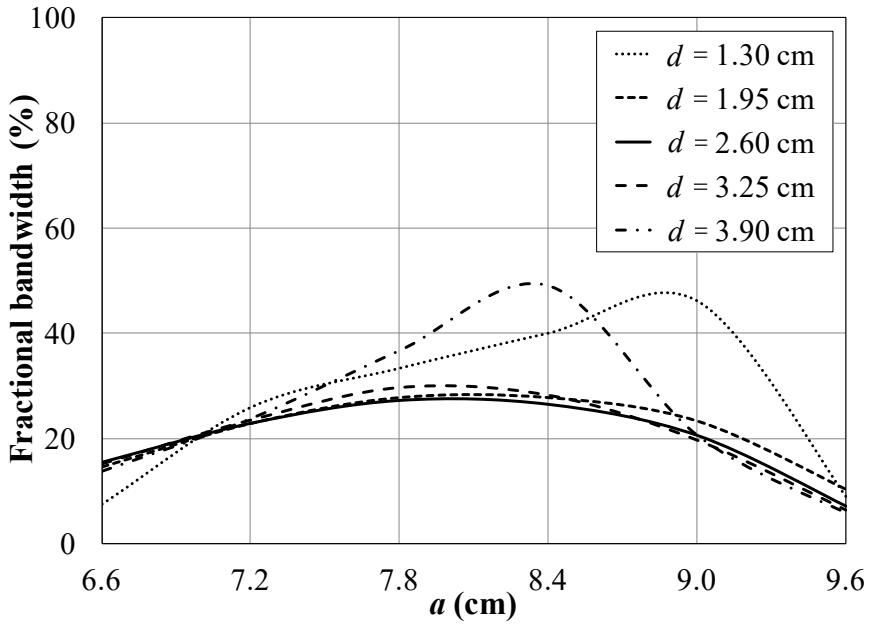

Figure 3.2 Fractional bandwidth of the resonant frequency at 2.3 GHz versus *a* as a function of *d* ($r_c = 1.30$ cm and $h = 3.90$ cm).

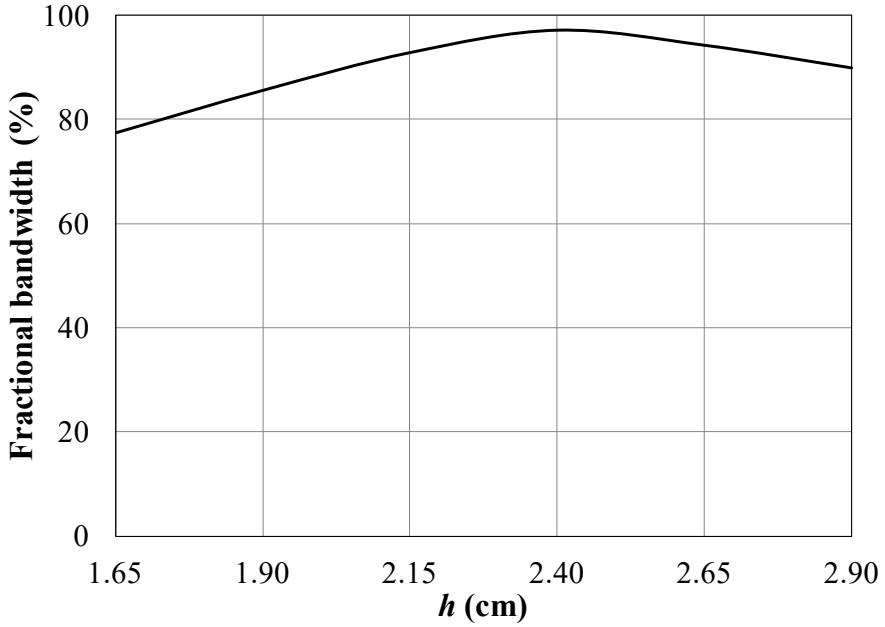

Figure 3.3 Fractional bandwidth of the resonant frequency at 2.3 GHz as a function of h (a = 7.20 cm, b = 3.60 cm, d = 2.60 cm and r_c = 1.30 cm).

Figures 3.4(a) and 4(b) show, respectively, the minimum and maximum frequencies ($|S_{11}|$ < -10 dB) of resonance at 2.3 GHz as a function of b/a by varying r_c, where b/a is the ring height. The radius of CDM (r_c) is varied between 1.00 and 1.40 cm to determine a ring height (b/a) that gives good resonance at the 2.3 GHz frequency. To produce the rectangular ring of a size as compact as possible, r_c = 1.10 cm for $b = 0.48a$ or 3.40 cm is selected.

Figure 3.5 illustrates the impedance bandwidth $|S_{11}|$ of the resonant frequency closest to 2.3 GHz as a function of b/a of the rectangular ring antenna, assuming a constant r_c of 1.10 cm. To achieve the goal of a compact ring antenna with the widest bandwidth, the ring width (a) and ring height (b) of 7.20 and 3.40 cm are chosen for experiment.

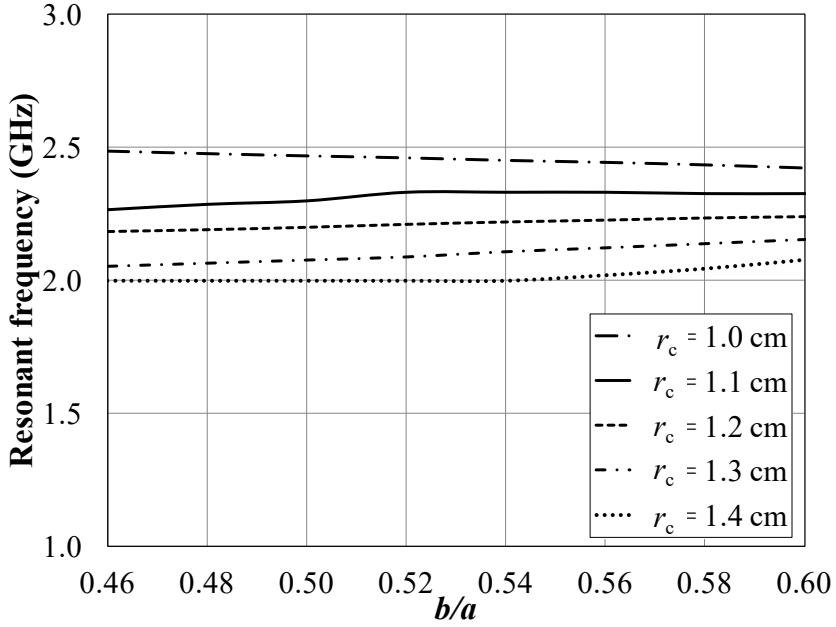

(a) The minimum frequency of resonance at 2.3 GHz by varying r_c

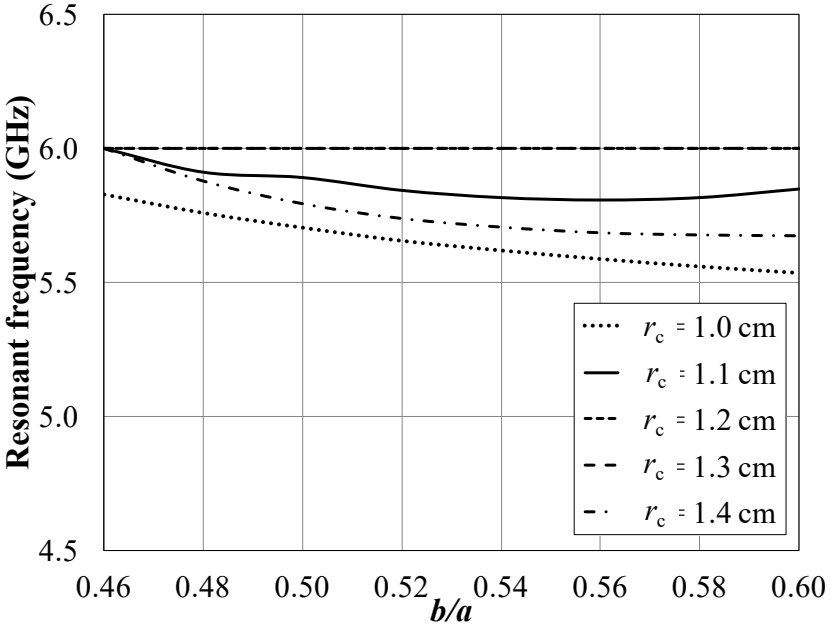

(b) The maximum frequency of resonance at 2.3 GHz by varying r_c

Figure 3.4 The resonant frequency relative to b/a for various r_c (a = 7.20 cm, d = 2.60 cm, and h = 2.40 cm).

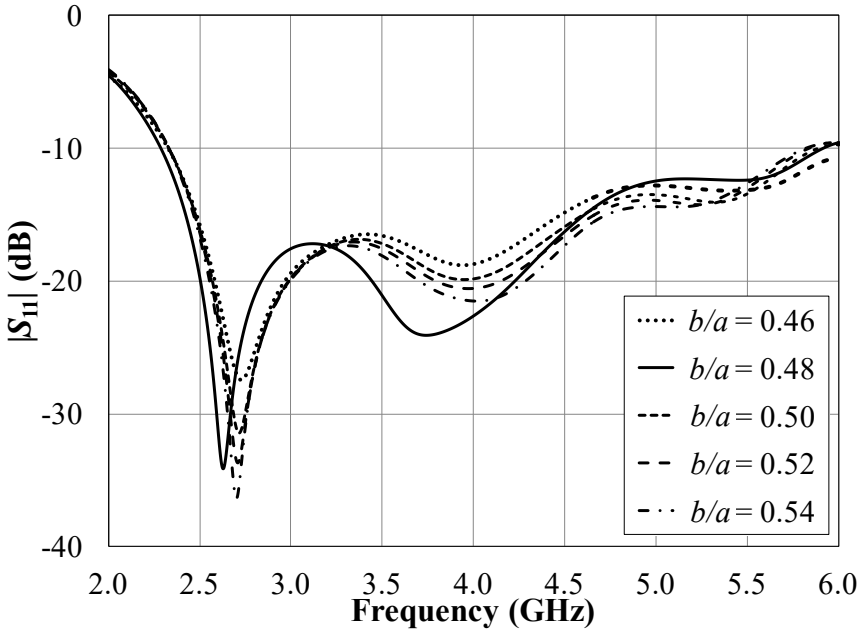

Figure 3.5 $|S_{11}|$ versus frequency as a function of b/a (a = 7.20 cm, d = 2.60 cm, h = 2.40 cm, and r_c = 1.10 cm).

3.3.2 Effect of Circular Disc Monopole

The inclusion of the CDM into the rectangular ring antenna is to increase the antenna's frequency bandwidth to cover the WiMAX band of 2.300 GHz to 5.825 GHz. Fig. 3.6 illustrates the frequency response curves as a function of $|S_{11}|$ and the frequency for the CDM radii of 1.00 cm to 1.40 cm and constant feed gap (δ) of 1.00 mm. Even though the $|S_{11}|$ curves for five CDM radii follow a similar pattern, an r_c of 1.10 cm is selected as it gives the highest overall efficiency in terms of impedance bandwidth, radiation pattern, and gain.

In addition, the effect of the feeding gap (δ) is examined and the results are depicted in Fig. 3.7. It is found that varying the feeding (δ) impacts the impedance bandwidth. That is, a reduction in δ from 1.50 mm to 0.50 mm causes the impedance bandwidth to become narrower and thereby fails to cover the entire WiMAX frequency band. Based on Fig.3.7, the feeding gap (δ) of 1.00 mm is chosen for the widest impedance bandwidth which covers the entire WiMAX band. Table 3.1 presents the optimal parametric values from the simulation of the proposed antenna.

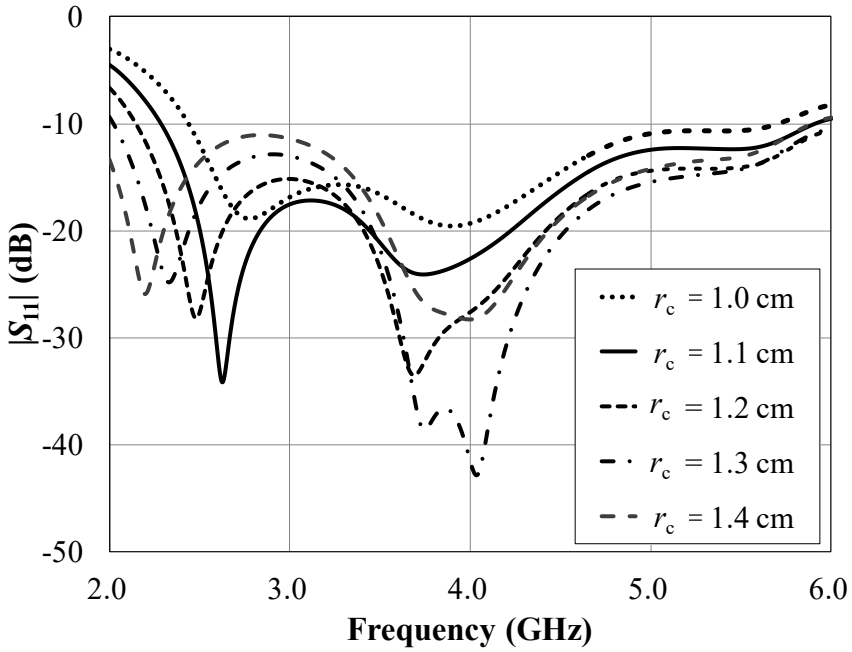

Figure 3.6 $|S_{11}|$ relative to frequency as a function of r_c (δ = 1.00 mm).

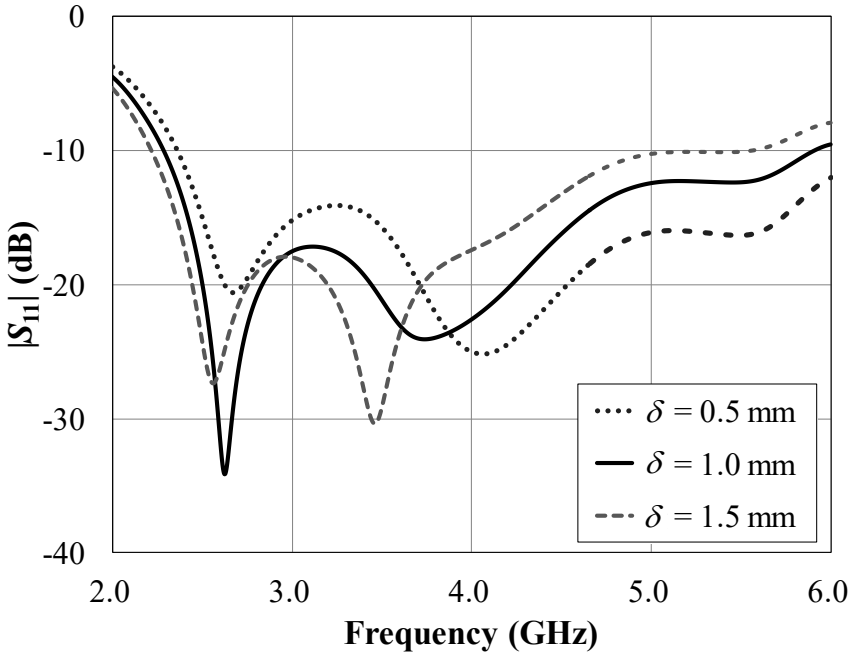

Figure 3.7 $|S_{11}|$ relative to frequency as a function of δ.

Table 3.1 The optimal parametric values of the proposed antenna.

Parameters	Physical size	Electrical size (λ)
L	16.0 cm	1.2307
a	7.2 cm	0.5538
b	3.4 cm	0.2615
d	2.6 cm	0.2000
h	2.4 cm	0.1846
r_c	1.1 cm	0.0846
t	2.0 mm	0.0153
δ	1.0 mm	

3.4 Measured Results

To validate the simulation results, a prototype antenna was fabricated based on the optimal parameters in Table 3.1. Fig. 3.8 is a photograph image of the prototype antenna.

3.4.1 Impedance Bandwidth

The measurements of impedance bandwidth, radiation pattern, and gain were taken using an HP8720C Network Analyzer. A comparison of the simulated and measured $|S_{11}|$, represented, respectively, by a solid line and a dashed line, is presented in Fig. 3.9. The simulated impedance bandwidth ($|S_{11}| < -10$ dB) of 88% was achieved in a frequency range of 2.28 GHz to 5.91 GHz (central frequency of 4.095 GHz), while that of the prototype antenna of 93% was in a frequency of 2.16 GHz to 5.96 GHz (central frequency of 4.06 GHz). It is found that the simulation and measured results are in reasonable agreement. In addition, the frequency ranges of both simulation and experiment satisfy the WiMAX requirement.

Figure 3.10 illustrates a comparison of the gain along the 2.300 GHz to 5.825 GHz frequency range of the prototype antenna and that of the simulation, in which the former is represented by a solid line and the latter by a dashed line. The minimum and maximum gains are 3.4 dBi and 9.3 dBi for the simulation and 3.7 dBi and 8.7 dBi for the prototype antenna.

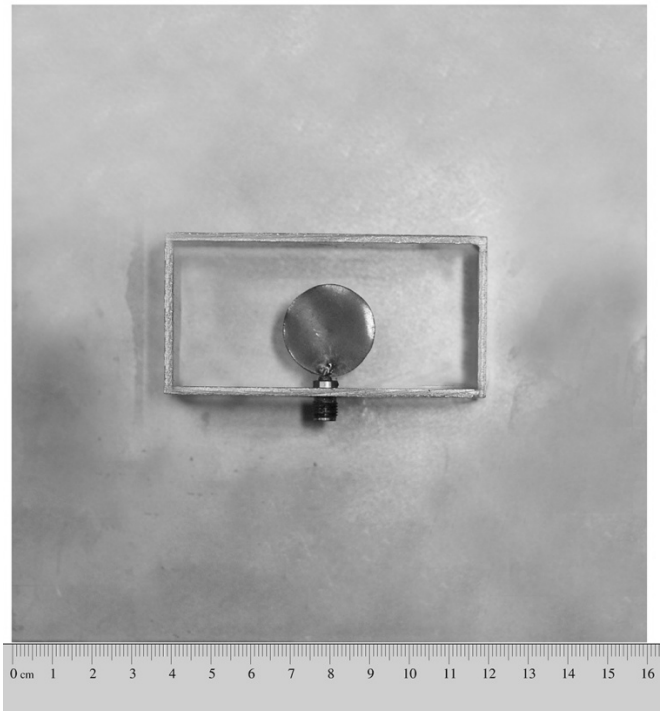

Figure 3.8 A unidirectional wideband antenna using CDM excited rectangular ring above square reflector prototype antenna.

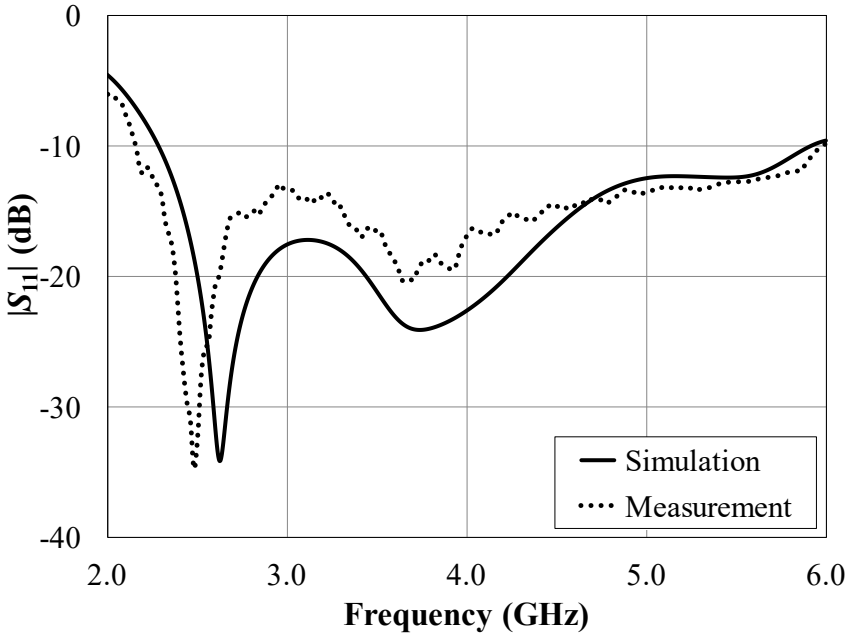

Figure 3.9 The comparison of the simulation and measured $|S_{11}|$ of unidirectional wideband antenna using CDM excited rectangular ring above square reflector relative to frequency.

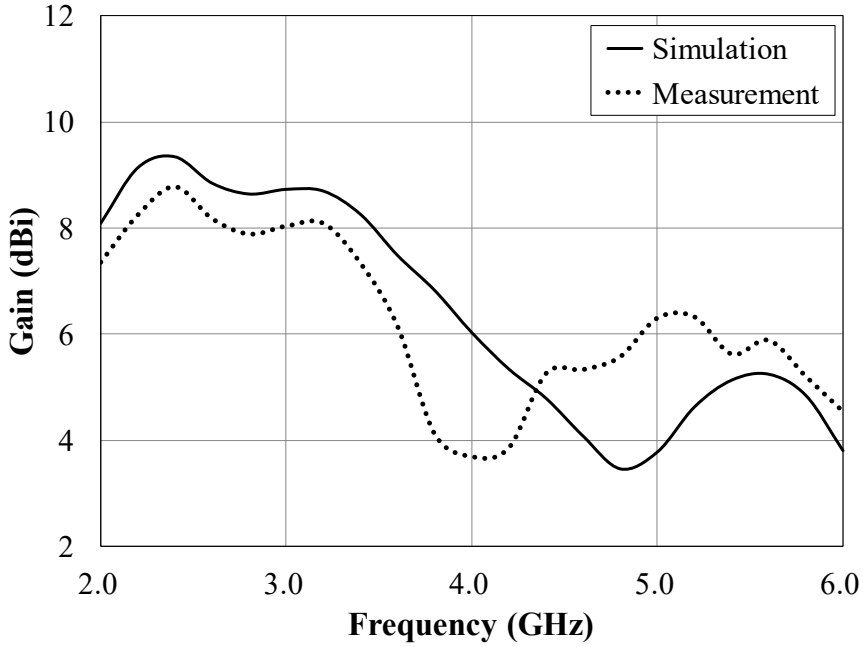

Figure 3.10 The simulated and measured gains of unidirectional wideband antenna using CDM excited rectangular ring above square reflector relative to frequency.

3.4.2 Radiation Pattern

Figures 3.11 and 3.12 illustrate the simulation and measured radiation patterns in the *yz*- and *xz*-planes, respectively, at 2.5, 3.5, and 5.5 GHz. In Fig. 3.11, the beam peaks direct in the +*z* direction. The radiation pattern in the *yz*-plane at 5.5 GHz slightly tilts upward from the *z*-axis as a result of the CDM installation on the rectangular ring base. The CDM contributes to the asymmetrical areas between the upper and lower portions of the ring chamber. However, the radiation pattern in the *xz*-plane is symmetrical because of the symmetrical areas between the left and right portions of the ring chamber. The simulation and measured radiation patterns show good agreement. At 2.5 GHz, the measured half-power beamwidth (HPBW) in the *yz*- and *xz*-planes is 73 and 62 degrees. At 3.5 GHz, the measured HPBWs in the *yz*- and *xz*-planes are identical at 80 degrees, while those at 5.5 GHz are 28 and 40 degrees, respectively. The measured front-to-back ratio (*F*/*B*) in both *yz*- and *xz*-planes is greater than 20 dB. Thus, the proposed antenna produces a good radiation pattern and is a very good unidirectional antenna.

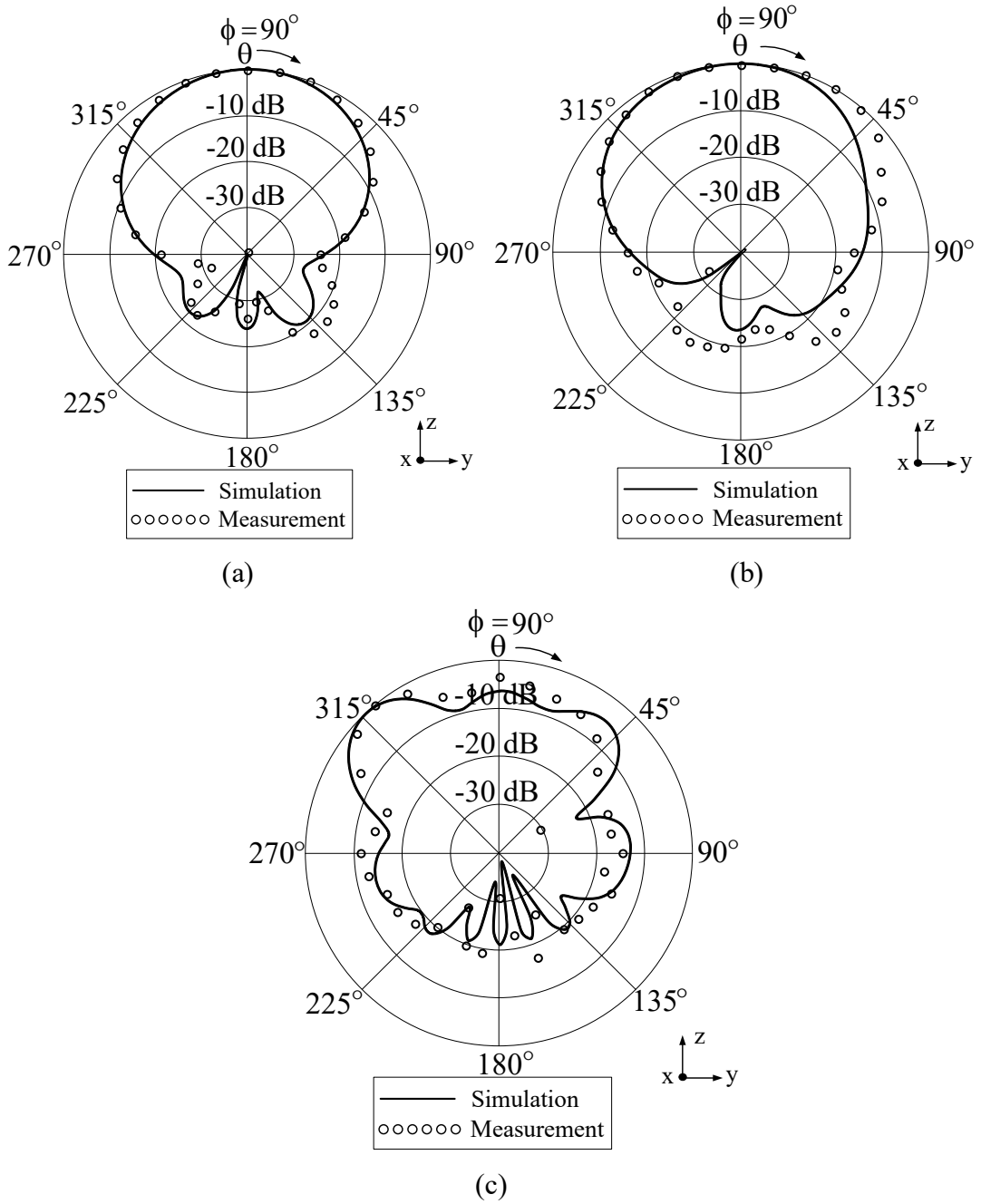

Figure 3.11 The comparison between the simulated and measured radiation pattern in the *yz*-plane. (a) 2.5 GHz, (b) 3.5 GHz, and (c) 5.5 GHz.

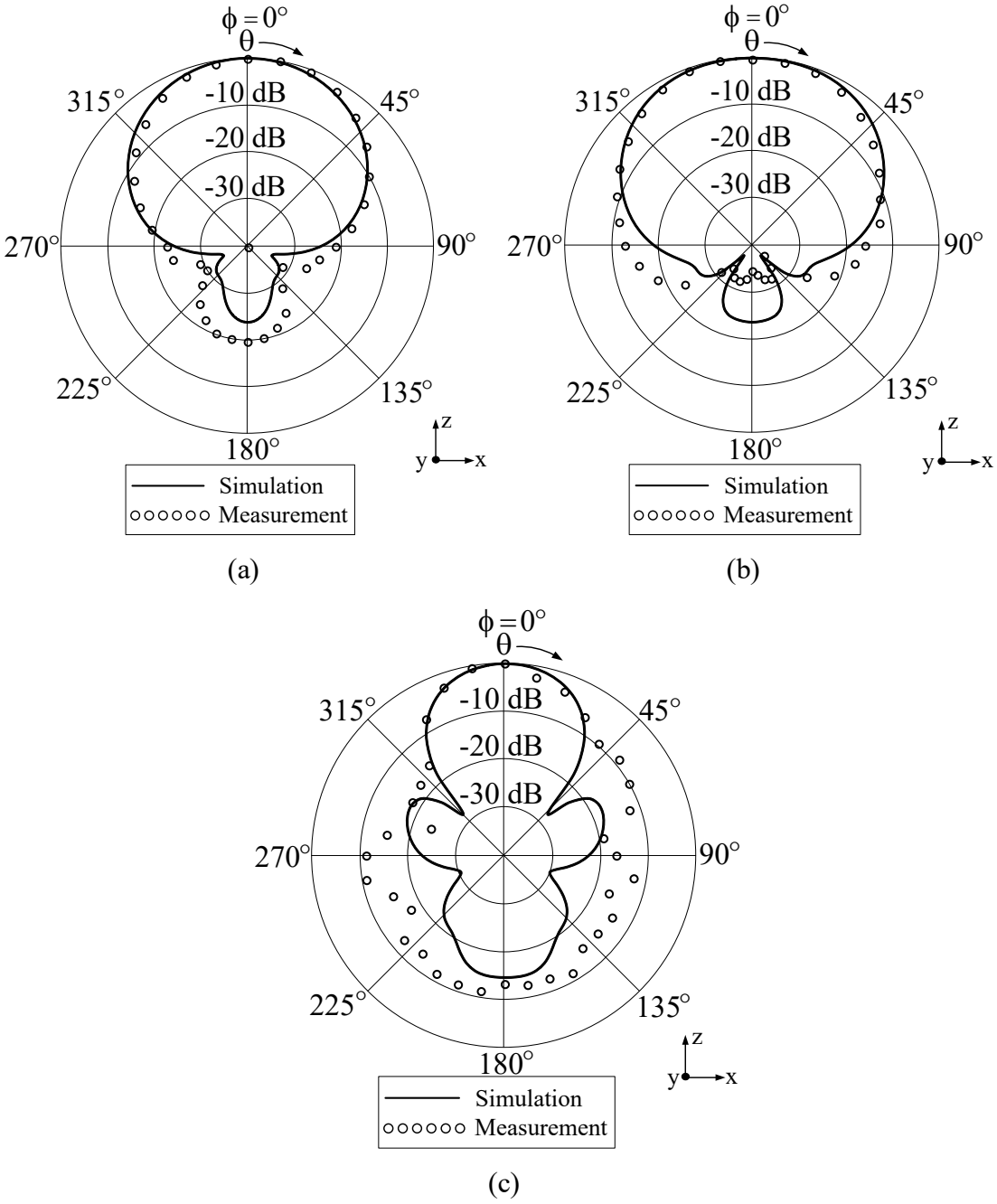

Figure 3.12 The comparison between the simulated and measured radiation pattern in the *xz*-plane. (a) 2.5 GHz, (b) 3.5 GHz, and (c) 5.5 GHz.

3.5 Summary

The unidirectional antenna suitable for WiMAX is developed using the CDM-excited rectangular ring mounted in front of the square reflector. The design principle is simple and straightforward. In addition, the antenna can be fabricated and manufactured on a large scale. At 2.5 GHz, the measured HPBWs in the *yz*- and *xz*-

planes are 72 and 62 degrees, respectively. At 3.5 GHz, the measured HPBWs in both planes are identical at 80 degrees, while those at 5.5 GHz are 28 and 40 degrees, respectively. The measured *F*/*B* in both *yz*- and *xz*-planes are greater than 20 dB. The antenna has a good radiation pattern suitable for the point-to-point communications and can achieve the impedance bandwidth ($|S_{11}|$ < -10 dB) of 93% covering the frequency range of 2.16 GHz to 5.96 GHz. Its compact size and good radiation performance render the proposed antenna suitable for the WiMAX applications.

CHAPTER 4
A UNIDIRECTIONAL DUAL-BAND ANTENNA USING U-SHAPED SLOT CDM EXCITED RECTANGULAR RING ABOVE SQUARE REFLECTOR FOR WLAN SYSTEM

4.1 Introduction

Based on the background of the researches [25]-[30], this chapter proposes a simple and compact U-shaped slot CDM fed rectangular ring antenna above square reflector with dual band-notched characteristics in 4.00 GHz (3.60 GHz to 4.87 GHz), by applying the antenna structure design criteria have already been presented in Chapter 3. The dual band-notched operations are achieved by etching U-shaped slot in the CDM surrounded by rectangular ring above square reflector and fed by a 50-Ω SMA connector. It is found that by tuning the total length of the U-shaped slot. The antenna is employed to radiate unidirectional beam for dual band with linear polarization. The U-shaped slot in the CDM, band-rejected filtering property in the WiMAX band is achieved. The antenna is proposed for the dual band point-to-point communication of Wireless Local Area Network (WLAN) system according to the IEEE 802.11a standard in which the allocated frequency band ranges from 2.400 GHz to 2.500 GHz and 5.150 GHz to 5.825 GHz. The prototype antenna was fabricated and measured to verify the theoretical principle.

The organization of this chapter is as follows. The proposed antenna structure and its associated parameters are discussed in Section 4.2. Section 4.3 described the design principle and parametric study. To confirm the simulated results, Section 4.4 presents the measured results. The conclusions are present in Section 4.5.

4.2 Geometry of the Proposed Antenna

Design criteria have already been presented in Chapter 3. The parameters are appropriately selected so that maximum gain and matched impedance can be

obtained. Hence, this chapter would like to design unidirectional beam for dual band antenna by applying the appropriate unidirectional antenna in Chapter 3 by etching U-shaped slot in CDM as illustrated in Fig. 4.1(a). The rectangular ring is excited by U-shaped slot CDM aligned on *y*-axis to generate vertical polarization with the radius of CDM is r_c via 50-Ω SMA connector with gap δ. The U-shaped slot height (t_4) from lower wall of rectangular ring, the spacing (t_2) between 2 branches of U-shaped slot from origin, U-shaped slot gap t_3 and the distance between U-shaped bottom and lower wall of rectangular ring is t_1, both of which are placed above square reflector of size $L \times L$. The spacing between the ring and the square reflector is denoted with h as illustrated in Fig. 4.1(b). The radiation pattern of this antenna is unidirectional with the beam peak pointing *z* direction.

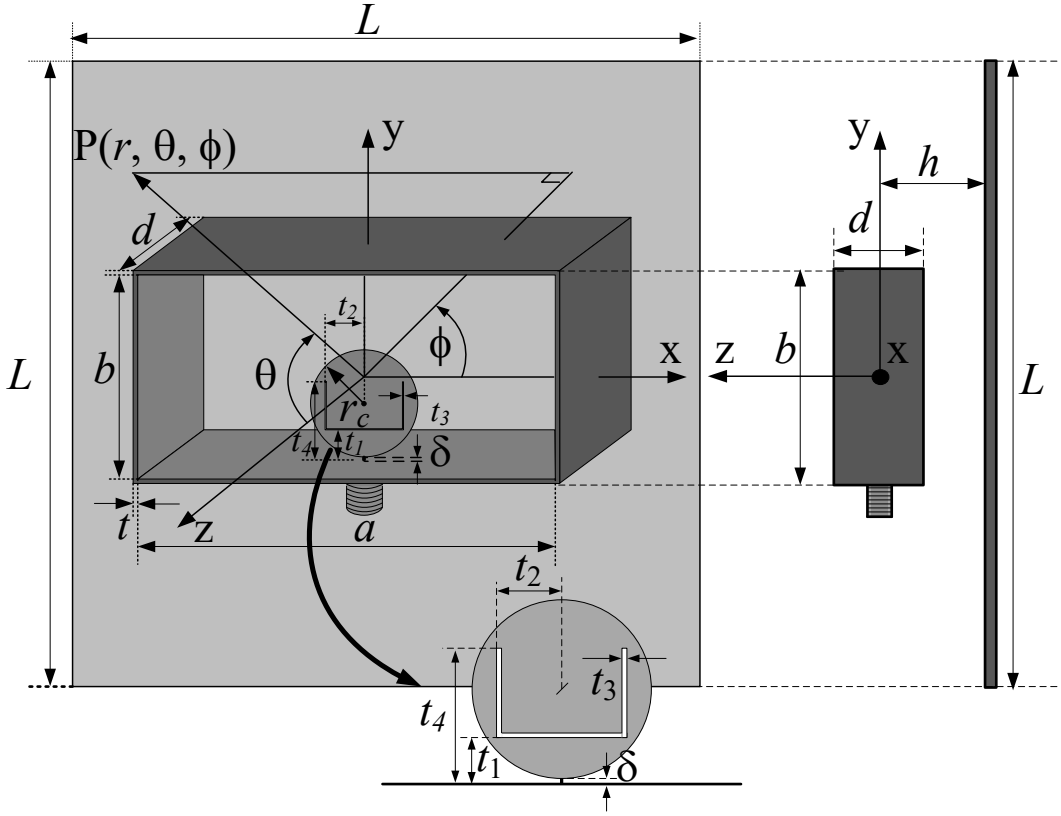

(a) (b)

Figure 4.1 The proposed antenna structure unidirectional antenna using U-shaped slot CDM excited rectangular ring above square reflector.
(a) Perspective view, and (b) Side view.

According to the design criteria in Fig. 4.1, the antenna structure is designed to operate in two separate frequency range of 2.400 GHz to 2.500 GHz and 5.150 GHz

to 5.825 GHz, of which the center frequency are 2.45 GHz and 5.50 GHz. The principle of the antenna design starts with the conventional rectangular ring, with the initial ring width (a) $\lambda/2$ of the lower edge frequency 2.3 GHz, which is equal to 6.60 cm. For ring height b is proportional with ring width a, which $b = a/2$. The ring length d of 3.25 cm ($\lambda/4$) excited by a probe of the length (l) $\lambda/4$ or 3.25 cm. It is noted that the ensemble of the antenna was made using 2 types, i.e. the rectangular ring and square reflector are made of aluminum with the thickness t of 2.00 mm and U-shaped slot CDM is made of brass. It is noted that to keep the antenna as compact and also provided the good characteristic and high gain. Hence, the antenna parameters are appropriately selected from Chapter 3 as aforementioned in above. Hereafter, we will discuss only the variation of U-shaped slot characteristic. The initial antenna parameters are determined as tabulated in Table 4.1. In order to study the influence of U-shaped slot gap t_3, the U-shaped slot height from lower wall of rectangular ring t_4, the distance (t_1) between U-shaped slot bottom and lower wall of rectangular ring, and the spacing (t_2) between 2 branches of U-shaped slot from origin, respectively. While all the other parameters are fixed in Table 4.1.

Table 4.1 Initial antenna parameters.

Parameters	**Electrical Size**	**Physical Size at 2.3 GHz**
$L \times L$	1.2307λ	16.00 cm
a	0.5538λ	7.20 cm
b	0.2615λ	3.40 cm
d	0.2000λ	2.60 cm
h	0.1846λ	2.40 cm
r_c	0.0846λ	1.10 cm
t	0.0153λ	2.00 mm
t_4	0.1307λ	1.90 cm
t_2	0.0615λ	0.80 cm
t_1	0.0384λ	0.50 cm
t_3	0.0038λ	0.50 mm

4.3 Design Principle and Parametric Study

4.3.1 Effect of U-shaped Slot Gap

Although the band-notched characteristics in 3.60 GHz to 4.87 GHz are achieved by etching U-shaped slots from the CDM element surrounded by rectangular ring placed above square reflector and fed by a 50-Ω SMA connector. It is observed that by tuning the total length of the U-shaped slot to the approximately 0.3 of the guided wavelength (λ_g) of the desired notch frequency, a destructive interference takes place causing the antenna non-radiating at the frequency. The notch center frequency can be easily tunable by changing the total length of the U-shaped slot. From the simulated results, it is found that the U-shaped slot gap slightly affected to level of $|S_{11}|$ as can be seen from Fig. 4.2. It is found that $|S_{11}|$ at t_3 of 0.05 cm has widest rejection the frequency from 2.572 GHz to 4.371 GHz. When t_3 increase, $|S_{11}|$ becomes worse cannot cover the higher band. Therefore, U-shaped slot gap t_3 of 0.05 cm is chosen as the design parameter. As observed that the length adjustment of the band-notched frequency can be carried out by varying the U-shaped slot height (t_4) from lower wall of rectangular ring from 1.50 cm to 1.90 cm. The t_4 is adjusted in a decrement fashion of 0.10 cm. The total length L_t for the U-shaped slot characteristic is denoted as $L_t = 2t_4 + 2t_2 + 2t_3$ [33], where t_2 of 0.80 cm and t_3 of 0.05 cm.

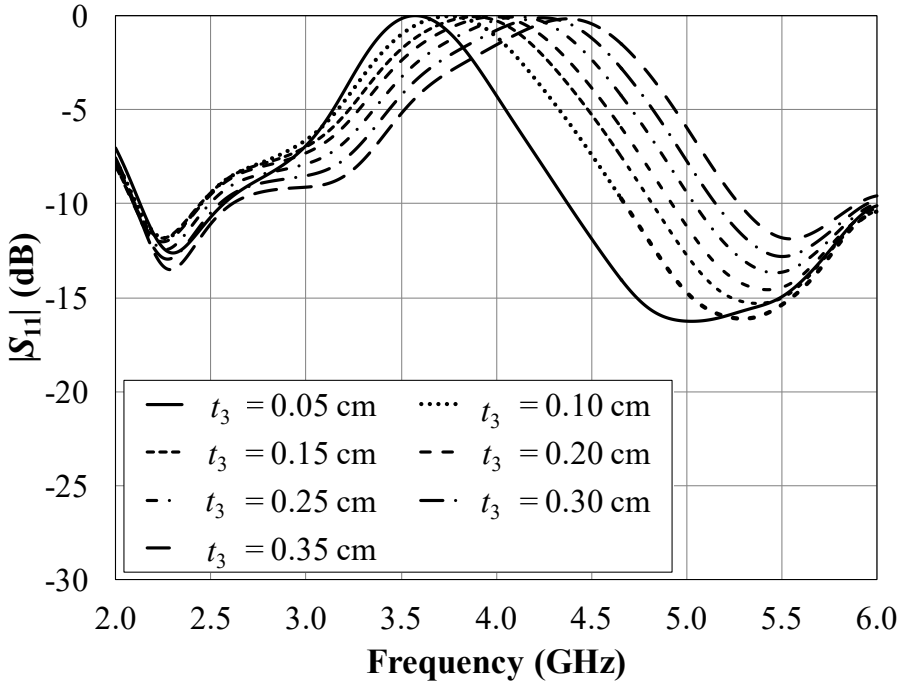

Figure 4.2 $|S_{11}|$ versus frequency as a function of the U-shaped slot gap t_3.

4.3.2 Effect of the U-shaped Slot Height and the Distance between the U-shaped Bottom and Lower Wall of Rectangular Ring

The U-shaped slot height must be varied to find the appropriate dimension. Fig. 4.3 shows the frequency response curves of $|S_{11}|$ with different the U-shaped slot heights which are varied from 1.50 cm to 1.90 cm by fixing the U-shaped slot gap t_3 of 0.05 cm. It is observed that the $|S_{11}|$ curves have same trend shape for the five different the U-shaped heights and slightly impacted with impedance bandwidth. It is found that when the U-shaped height is small equal to 1.50 cm, the impedance bandwidth at higher edge frequency is narrow and cannot cover the frequency range. It is obvious that t_4 of 1.70 cm is chosen to cover the dual band frequency for WLAN range. Moreover, the effect of the distance between U-shaped bottom and lower wall of rectangular ring t_1 is studied as illustrated in Fig. 4.4. From Fig. 4.4 shows the $|S_{11}|$ versus frequency as a function of the distance between U-shaped bottom and lower wall of rectangular ring t_1 is strong impacted with impedance bandwidth. If the distance between U-shaped bottom and lower wall of rectangular ring t_1 is higher equal to 0.70, 0.80, and 0.90 cm, the impedance bandwidth at higher edge frequency is narrow cannot cover the frequency range from 5.150 GHz to 5.825 GHz. Hence, it is found that t_1 of 0.60 cm is appropriately chosen to obtain widest impedance bandwidth both of frequency range and optimum gain.

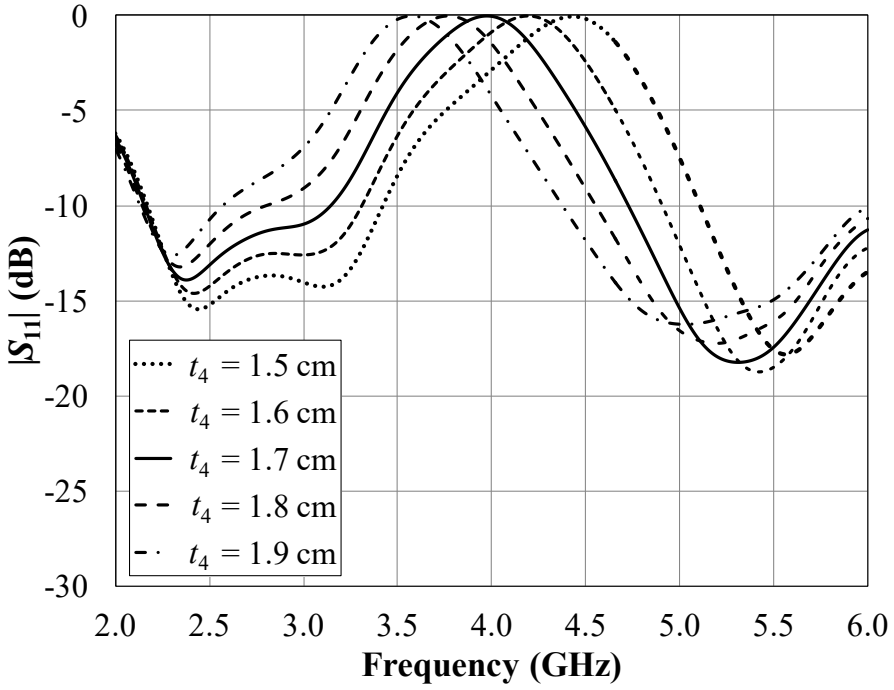

Figure 4.3 $|S_{11}|$ versus frequency as a function of the U-shaped slot height t_4.

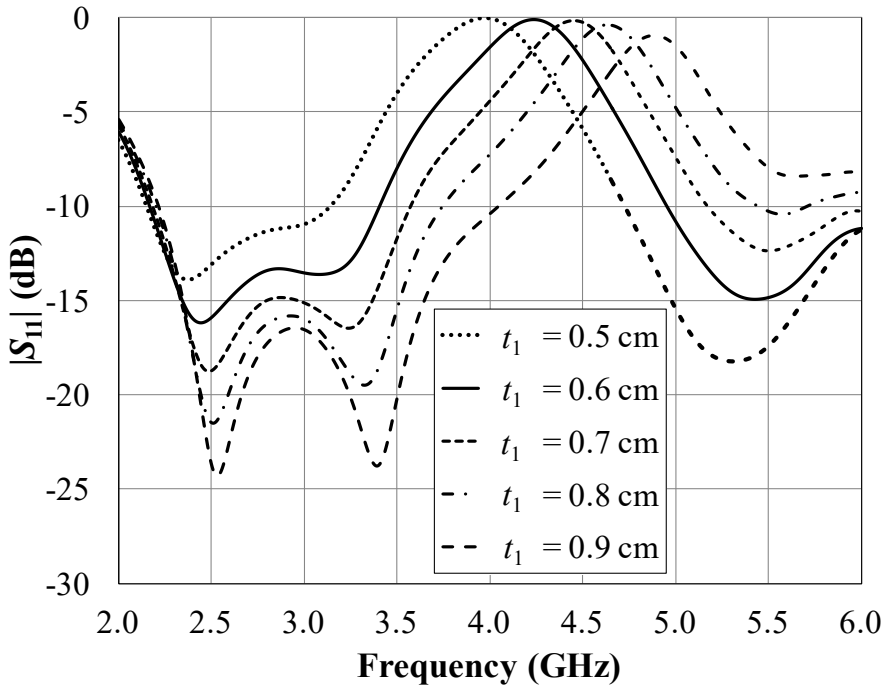

Figure 4.4 $|S_{11}|$ versus frequency as a function of the distance between U-shaped slot bottom and lower wall of rectangular ring t_1.

4.3.3 Effect of the Spacing (t_2) between 2 Branches of U-shaped Slot

Moreover, the most important influence parameter is the spacing between 2 branches of U-shaped slot t_2 from origin as shown in Fig. 4.5. It is can be seen that when t_2 become narrow equal to 0.70 cm, it is found that the $|S_{11}|$ curve become worse and cannot cover the frequency band. To achieve the dual band and cover the frequency range, t_2 of 0.80 cm is selected.

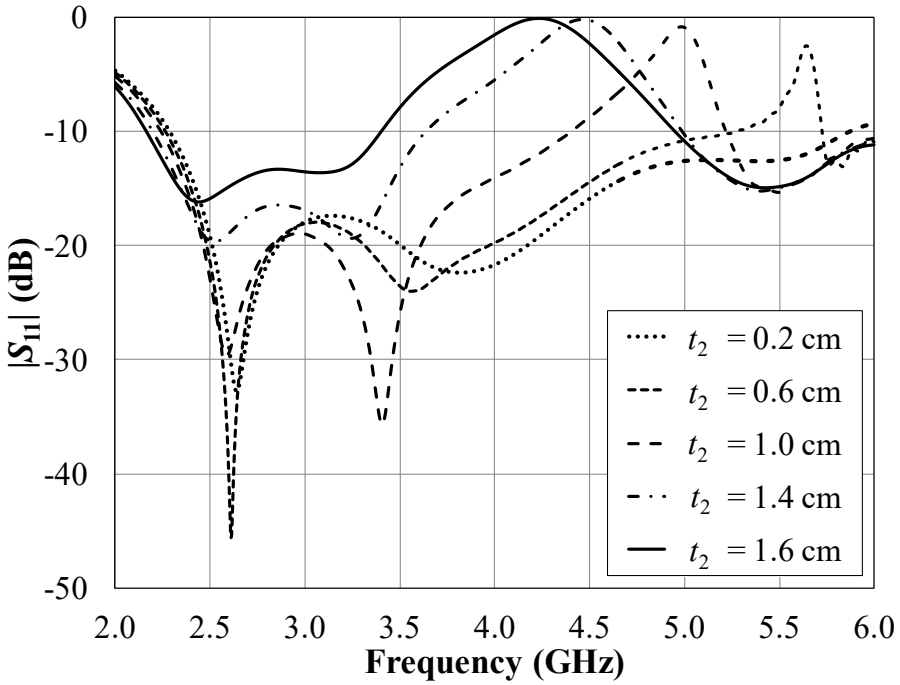

Figure 4.5 $|S_{11}|$ versus frequency as a function of the spacing t_2 between 2 branches of the U-shaped slot.

The final design U-shaped slot parameters are t_1 of 0.60 cm, t_2 of 0.80 cm, t_3 of 0.05 cm, and t_4 of 1.70 cm. Based on the parametric study results, the design parameters of the proposed antenna are tabulate in Table 4.2.

Table 4.2 The Design Parameters.

Parameter	Electrical Size	Physical Size at 2.3 GHz
$L \times L$	1.2307λ	16.00 cm
a	0.5538λ	7.20 cm
b	0.2615λ	3.40 cm
d	0.2000λ	2.60 cm
h	0.1846λ	2.40 cm
r_c	0.0846λ	1.10 cm
t	0.0153λ	2.00 mm
t_4	0.1307λ	1.70 cm
t_2	0.0615λ	0.80 cm
t_1	0.0461λ	0.60 cm
t_3	0.0038λ	0.50 mm

4.4 Measured Results

The experiment is performed to confirm the theoretical principle the prototype antenna with the design parameters tabulated in Table 2 was fabricated as depicted in Fig. 4.6. A unidirectional antenna by using U-shaped slot CDM excited rectangular ring above square reflector was fabricated to operate at the dual-band frequency of 2.45 GHz and 5.50 GHz. The ensemble of the antenna was made using 2 material types, i.e. the rectangular ring and square reflector are made of aluminum and the U-shaped slot CDM is made of brass. The antenna can be easily designed with the low production cost material and available in the market. The impedance bandwidth characteristics, the radiation pattern and the gain were measured using an HP872C Network Analyzer.

Figure 4.6 Photograph of the prototype of a unidirectional antenna by using U-shaped slot CDM excited rectangular ring above square reflector.

4.4.1 Impedance Characteristics

This chapter proposes a unidirectional antenna excited by U-shaped slot CDM are placed above the square reflector with 3.60 GHz to 4.87 GHz rejection band. The antenna is employed to radiate unidirectional beam for dual-band with linear polarization. The U-shaped slot in the CDM, band rejected filtering property in the WiMAX band is achieved. Fig. 4.7 illustrated the $|S_{11}|$ compared between the simulation and measured results. The solid and dashed lines represent the simulated and measured results, respectively. The simulated and measured results are in reasonable agreement. At the center frequency of 2.45 GHz, the simulated and measured $|S_{11}|$ are respectively -16.197 dB and -14.635 dB, whereas the simulated and measured $|S_{11}|$ at 5.50 GHz are -15.335 dB and -15.800 dB, respectively. The measured return loss is compared with the simulated results in Fig. 4.7 and good agreement is observed. The impedance bandwidth ($|S_{11}|$ < -10 dB) from the measured results are 2.06 GHz to 3.58 GHz for the 2.4 GHz band and 4.88 to 6.00 GHz for the 5.0 GHz band, which covers the 2.4 GHz and 5.0 GHz band the requirement of WLAN system according to the IEEE 802.11a standard.

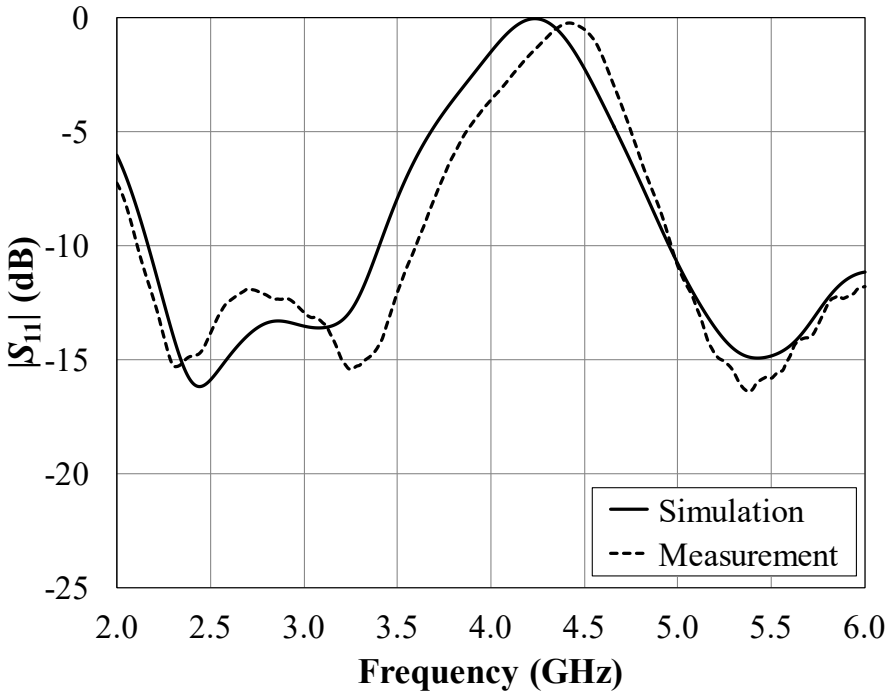

Figure 4.7 The comparison of the simulation and measured $|S_{11}|$ a unidirectional antenna by using U-shaped slot CDM excited rectangular ring above square reflector relative to frequency.

4.4.2 Radiation Pattern

The simulation and measured radiation patterns in the *yz*- and *xz*-planes at 2.45 GHz and 5.50 GHz are plotted in Figs. 4.8 and 4.9, respectively. It is obvious that the beam peak directs to the +*z* directions. Furthermore, it is found that the radiation pattern in the *yz*-plane is slightly tilted from *z* axis at the higher frequency because of the present U-shaped slot CDM located at the lower wall of rectangular ring making unsymmetrical structure the upper and lower parts of the ring. Due to the symmetrical structure along left and right part of the ring, the radiation pattern is symmetrical in *xz*-plane. The good agreement between the simulation and measurement is achieved. The simulated and measured HPBW at 2.45 GHz in *yz*- and *xz*-planes agree very well are 69 and 68 degrees, respectively. For higher frequency at 5.50 GHz the simulated and measured HPBW in both planed *yz*- and *xz*-planes are 26.6 and 26.0 degrees, respectively. The simulated and measured *F*/*B* at 2.45 GHz in *yz*-plane is 15.8 dB and 15.5 dB, respectively. For the *F*/*B* at 5.50 GHz in *yz*-plane are 16.59 dB and 18.05 dB, respectively. From the obtained results, it is apparent that this antenna possesses the good radiation pattern for dual-band of point-to-point communication.

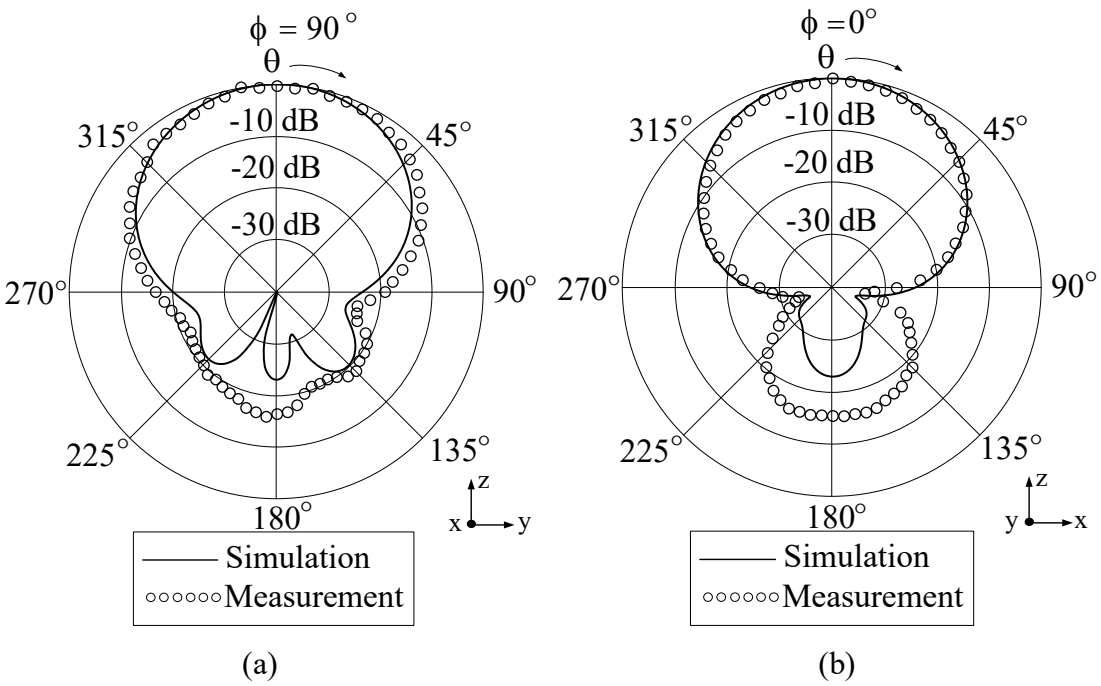

Figure 4.8 The comparison between the simulated and measured radiation patterns. (a) *yz*-plane at 2.45 GHz, and (b) *xz*-plane at 2.45 GHz.

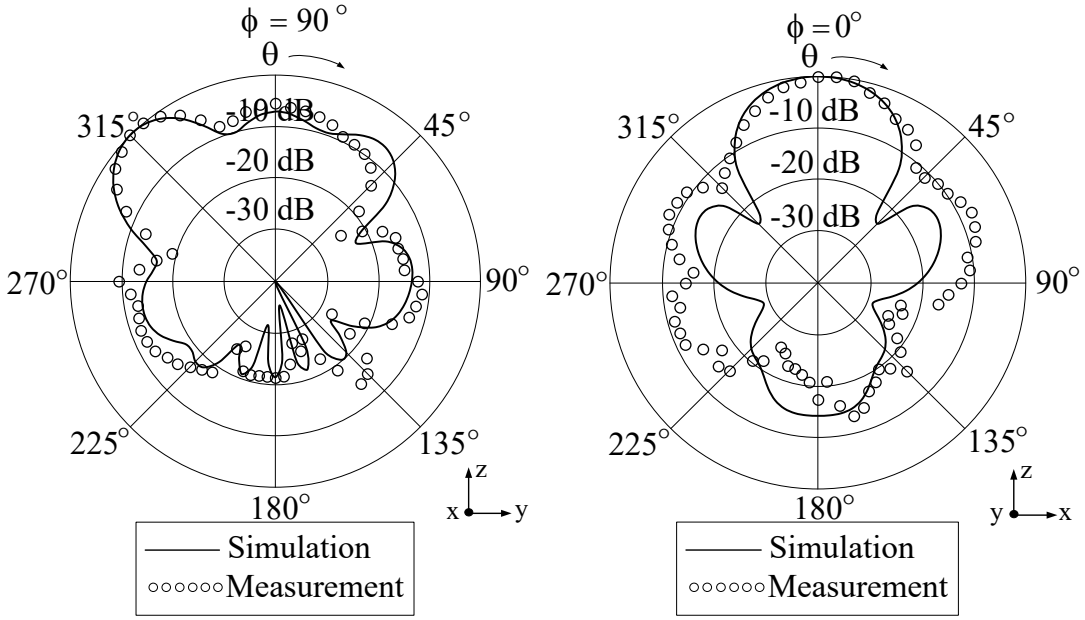

(a) (b)

Figure 4.9 The comparison between the simulated and measured radiation patterns. (a) *yz*-plane at 5.50 GHz, and (b) *xz*-plane at 5.50 GHz.

4.4.3 Gain

The antenna gain was measured and compared with the simulated results as shown in Fig. 4.10. From the both results display an identical trend. It is obvious that the simulated (solid line) and measured (dashed line) gains at the 2.45 GHz band is about 7.49 dBi, 2.68 dB higher than that in the 5.50 GHz band (4.81 dBi). The lower gain in the higher band is due to the unsymmetrical structure as aforementioned at above. This antenna thus has sufficient gain for point-to-point communication of WLAN system.

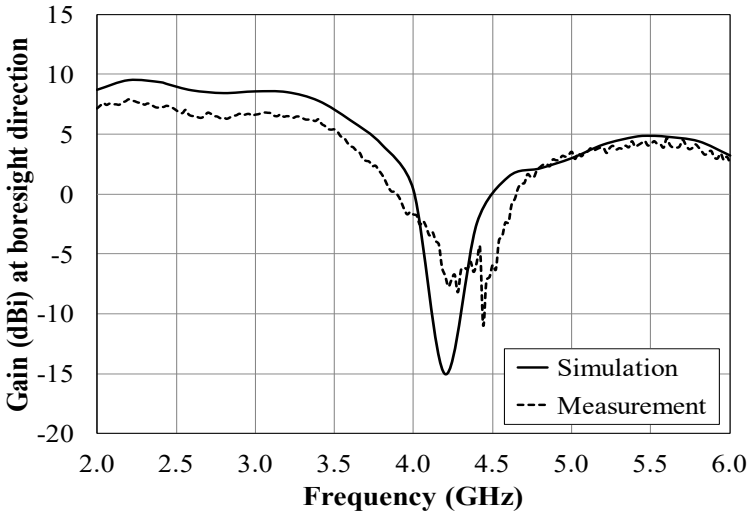

Figure 4.10 The comparison of simulated and measured gains of a unidirectional antenna by using U-shaped slot CDM excited rectangular ring above square reflector relative to frequency.

4.5 Summary

A unidirectional antenna for dual-band of WLAN system is achieved by using U-shaped slot CDM excited the rectangular ring above the square reflector. The dual-band notched operations are achieved by etching U-shaped slot from CDM element with can rejection band at 3.60 GHz to 4.87 GHz is proposed and discussed. The antenna principle is uncomplicated and the design straightforward. In addition, the prototype antenna is readily fabricated and conveniently produced on a mass scale. At the center frequency of 2.45 GHz band, the measured results HPBW 69 and 68 degrees, respectively. For higher frequency at 5.50 GHz the measured results HPBW are 26.6 and 26.0 degrees, respectively. At the frequency 2.45 GHz band the measured *F*/*B* in both planes *yz*- and *xz*-planes are 15.8 dB and 15.5 dB, for 5.50 GHz are 16.59 dB and 18.05 dB, respectively. The antenna provides good radiation characteristics suitable for the point-to-point communication. The $|S_{11}|$ at 2.45 GHz and 5.50 GHz are -14.635 dB and -15.800 dB, respectively. The impedance bandwidth ($|S_{11}| < -10$ dB) from the measured results are 2.06 GHz to 3.58 GHz for the 2.40 GHz band and 4.88 GHz to 6.00 GHz for the 5.50 GHz band, which covers the 2.40 GHz and 5.00 GHz band the requirement of WLAN system according to the IEEE802.11a standard. Furthermore, based in the antenna principle and design, the antenna parameters can be varied to realize the dual-band antenna of point-to-point communication in other wireless communication systems.

CHPTER 5

A UNIDIRECTIONAL ANTENNA USING TWO-PROBE EXCITED CIRCULAR RING ABOVE SQUARE REFLECTOR FOR POLARIZATION DIVERSITY WITH HIGH ISOLATION

5.1 Introduction

Presently, wireless communications have grown rapidly. It is well-known that the antenna is a significant part of wireless system to make the communication successfully. In microcell communication systems, when the base stations are placed in urban areas, the typical topology in which the root or base station is able to communicate to a number of clients located around it. In the case of only line of sight (LOS) situation, the signal can be directly propagated from the transmitter or from base station to the receiver. However, in some environments in which the transmitter or base station and receiver are set up in locations lower than the surrounding buildings or are obstructed by various objects, the multipath signal occurs due to obstacles, such buildings, trees and many other obstacles, which case the signal to reflect and diffract. The multiple components of transmitted signal reach the receiver at slightly different time points. These signals produce multipath fading, which not various with time and physical motion but also affects the channel performance and reduces the data rate. To mitigate the fading problem, many researchers and developments on the diversity reception techniques have been applied. Particularly from literature review, it is found that a number of diversity antennas, space diversity, the polarization diversity antenna have been discussed and conducted. Moreover, the polarization diversity antenna with unidirectional pattern is very useful for base station applications such as WLAN system. Hence, this chapter presents the unidirectional antenna for polarization diversity of WLAN system following IEEE 802.11a standard with the operating frequency band between 5.150 GHz and 5.825 GHz. The antenna evolution is started from the circular ring excited by a probe that radiate bidirectional pattern in two opposite directions along two ring apertures with

single polarization. This structure is located above the square reflector to confine the main beam into one direction. The excitation with two perpendicular probes is introduced for vertical/horizontal polarization diversity. To improve the isolation between two excited, the linear isolator with proper angle is added. The antenna characteristics in terms of the reflection ($|S_{11}|$ and $|S_{22}|$), isolation ($|S_{21}|$ and $|S_{12}|$), radiation pattern, and gain are presented. The simulation was performed using CST Microwave Studio. The prototype antenna was fabricated and measured to confirm the theoretical principle.

The organization of this chapter is as follows. The proposed antenna structure and its associated parameters are discussed in Section 5.2, Section 5.3 addresses the design principle and in Section 5.4 the measured results are presented. The conclusions are drawn and detailed in Section 5.5

5.2 Antenna Structure

The antenna configuration consists of the circular ring with radius r_a, length d and thickness t as shown in Fig. 5.1(a). The circular ring is made of metallic material. The center of the ring is located at the origin of yz-plane. This ring is excited by two identical probes perpendicular to each other along the radial direction via 50-Ω SMA connector with gap δ. The first probe (Probe1) is aligned on z-axis to generate vertical polarization whereas the other probe (Probe2) is oriented along y-axis to create horizontal polarization. The linear isolator of the length l_p and radius r_p is situated inside the ring in the radial direction between two probes. The position of the isolator is at an angle α relative to the Probe1. This structure is placed above the square reflector of size L. The spacing between the ring and the reflector is denoted by h as illustrated in Fig. 5.1(b). The radiation pattern of this antenna is unidirectional with the beam peak pointing x direction. Furthermore, the dimension of the circular ring is reasonably chosen to perform the dominant mode.

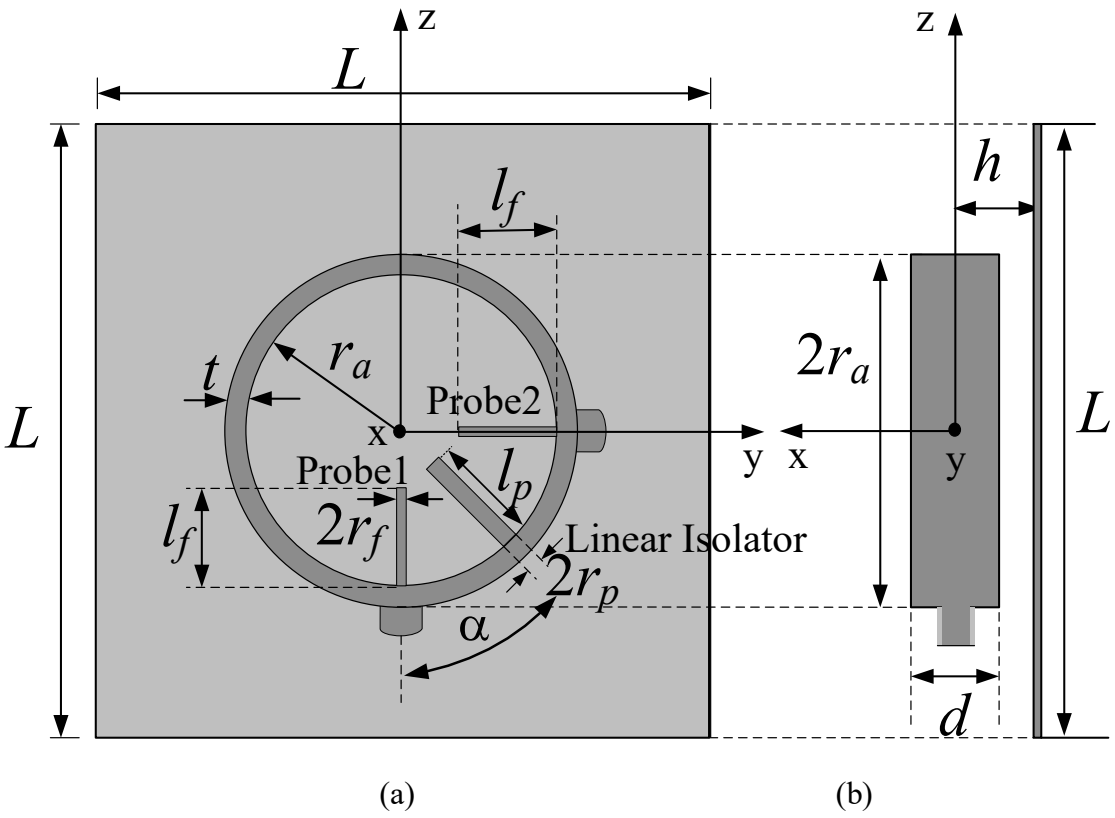

Figure 5.1 The proposed antenna structure. (a) Perspective view, and (b) Side view.

5.3 Design Principle and Parametric Study

The antenna structure is designed to be operated along the frequency range of 5.150 GHz to 5.825 GHz, of which the center frequency is 5.5 GHz. The principle of the antenna design starts with the conventional circular ring as shown in Fig. 5.2, with the initial radius (r_a) of the half-wavelength (λ/2) of the center frequency, which is equal to 2.727 cm. This ring is excited by a single probe along *z* direction to produce vertical polarization. The initial probe length l_f is λ/4 or 1.363 cm. It is noted that the ring in this chapter is made of aluminum with the thickness *t* of 3 mm. The ring length *d* of 1.527 cm (0.28λ) and probe radius r_f of 0.65 mm (0.011λ) are selected and used throughout the design due to its ubiquity as fabrication material. The ring length (*d*) affects to the directivity of the antenna. The guideline for the selection of *d* for the desired directivity can be found in [6]. To keep the antenna as compact as possible, the size of the square reflector is chosen to be 8 cm with the spacing between the circular ring and the square reflector will be clarified in this section. It is noted that the infinitesimal gap between the circular ring and the linear isolator is separated with

dielectric supporter. There is no electrical contact between the circular ring and the linear isolator.

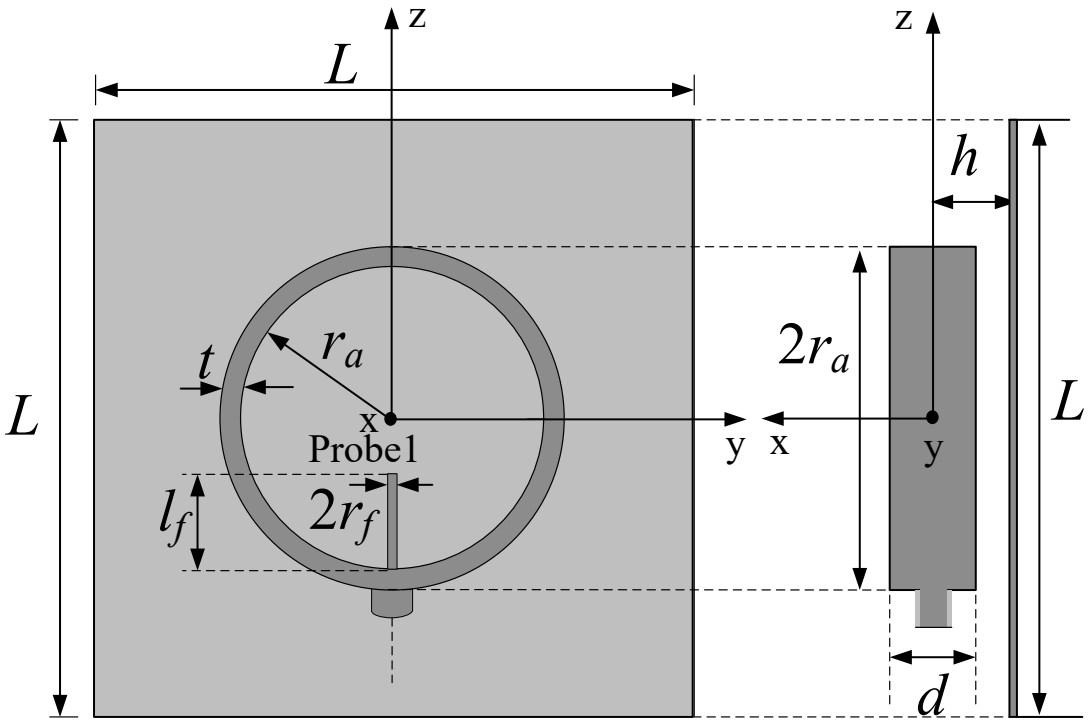

(a) (b)

Figure 5.2 An initial antenna structure. (a) Perspective view, and (b) Side view.

5.3.1 Variation the Radius of Ring and Probe

To determine the proper antenna dimensions that meet the optimum characteristics and are of compact size, the antenna parametric study will be carried out. Fig. 5.3 illustrates the gain at the boresight direction (θ = 90°, ϕ = 0°) of the circular ring antenna excited by the single probe above the square reflector for various ring radii r_a. It is evident that the radius of 0.4λ yields the maximum gain. Therefore, the ring radius r_a of 2.18 cm (0.4λ) is selected as the design parameter.

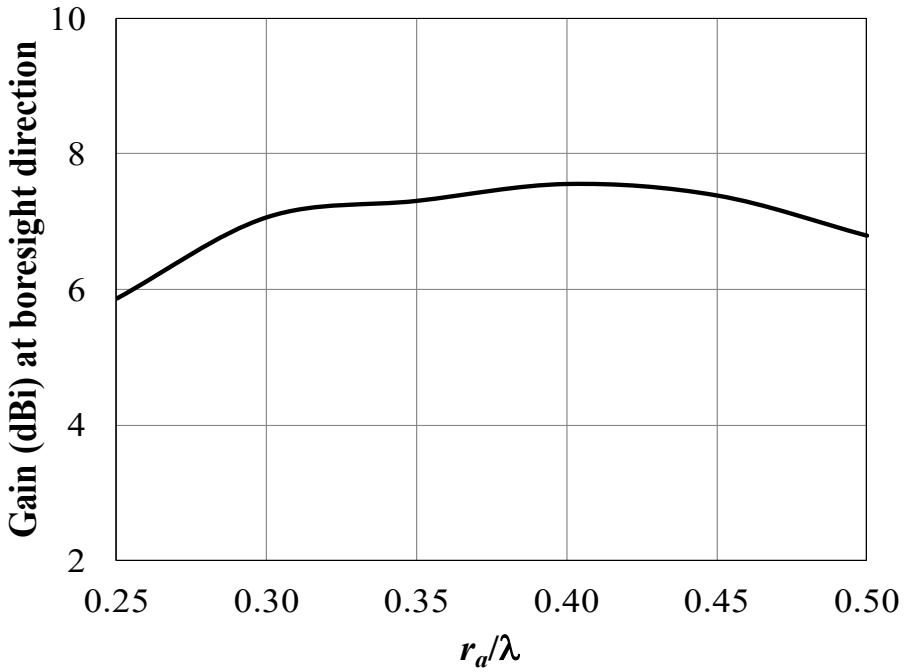

Figure 5.3 The gain at boresight direction versus ring radius r_a (l_f = 1.36 cm and r_f = 0.65 mm).

To obtain the good matching condition with efficiently wide bandwidth, the probe radius is adjusted in an incremental fashion of 0.1 mm. Fig. 5.4 shows the $|S_{11}|$ at single probe excitation versus frequency of the proposed antenna for various probe radii r_f. It is obvious that the probe radius affects the frequency of the minimum $|S_{11}|$. For r_f = 0.65 mm, the $|S_{11}|$ is unacceptable due to the reflection level greater than -10 dB throughout the desired frequency band. When r_f is increased to 0.75 mm or higher, the level of the minimum $|S_{11}|$ at 5.5 GHz is less than -15 dB. To achieve the minimum $|S_{11}|$ at the center frequency, r_f of 0.75 mm is selected. The bandwidth coverage is from 5 GHz to 6 GHz.

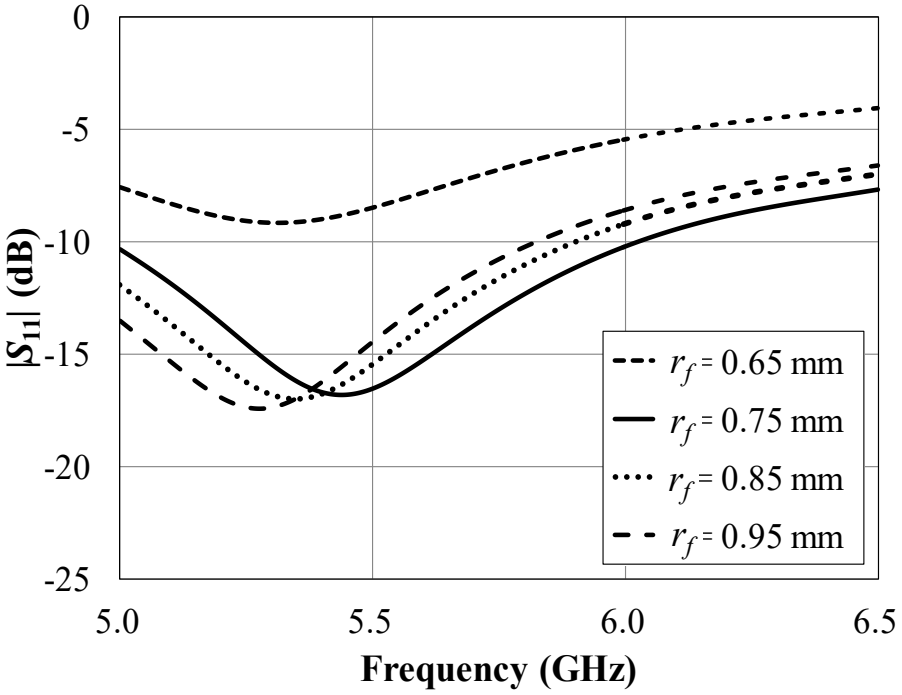

Figure 5.4 The $|S_{11}|$ versus frequency for various probe radii r_f (r_a = 2.18 cm and l_f = 1.36 cm).

5.3.2 Variation of Two Perpendicular Probes with and without Linear Isolator

To develop the circular ring antenna above square reflector for polarization diversity reception, two perpendicular excitation probes in *z* direction (Probe1) and y direction (Probe2) are introduced as shown in Fig. 5.1. By adding Probe2 inside the ring, the reflection at each probe (in terms of $|S_{11}|$ and $|S_{22}|$) is degraded compared with when merely Probe1 excitation is employed. Fig. 5.5 illustrates the frequency response of the reflection of each probe (in terms of $|S_{ij}|$). It is noted that $|S_{11}|$ and $|S_{22}|$ are identical because of their symmetrical structure while $|S_{21}|$ and $|S_{12}|$ are identical due to reciprocal property. The solid line indicates the $|S_{11}|$ and $|S_{22}|$ when two perpendicular probes are employed. It is noted that $|S_{11}|$ is taken into account when Probe1 is excited and while Probe2 is terminated with the matched load. Meanwhile, $|S_{22}|$ is the result of excitation at Probe2 whereas Probe1 is matched with the dummy load termination. As illustrated by the solid line in Fig. 5.5, $|S_{11}|$ worsens with merely one probe excitation due to the coupling effect from Probe2. In terms of $|S_{ij}|$ of the isolation (inverse of coupling) where $I \neq j$, it could be observed from the dotted line that $|S_{21}|$ is around -14 dB along the frequency band. The isolation in this case is

relatively low and insufficient for practical applications. To improve the isolation, the simple linear isolator is symmetrically oriented between the two probes at an angle α of 45°. The linear isolator is made of the copper rod. It is a resonant component that is used to block the surface current from Probe1 to Probe2. Note that the infinitesimal gap between the circular ring and the linear isolator is separated with dielectric supporter to prevent the electrical connection. The current from Probe1 will be stored by this linear isolator. By considering the dashed line and dash-dotted line in Fig. 5.5, the $|S_{11}|$ and $|S_{21}|$ with the linear isolator included are remarkably improved. However, the $|S_{11}|$ and $|S_{21}|$ are not optimum at the center frequency.

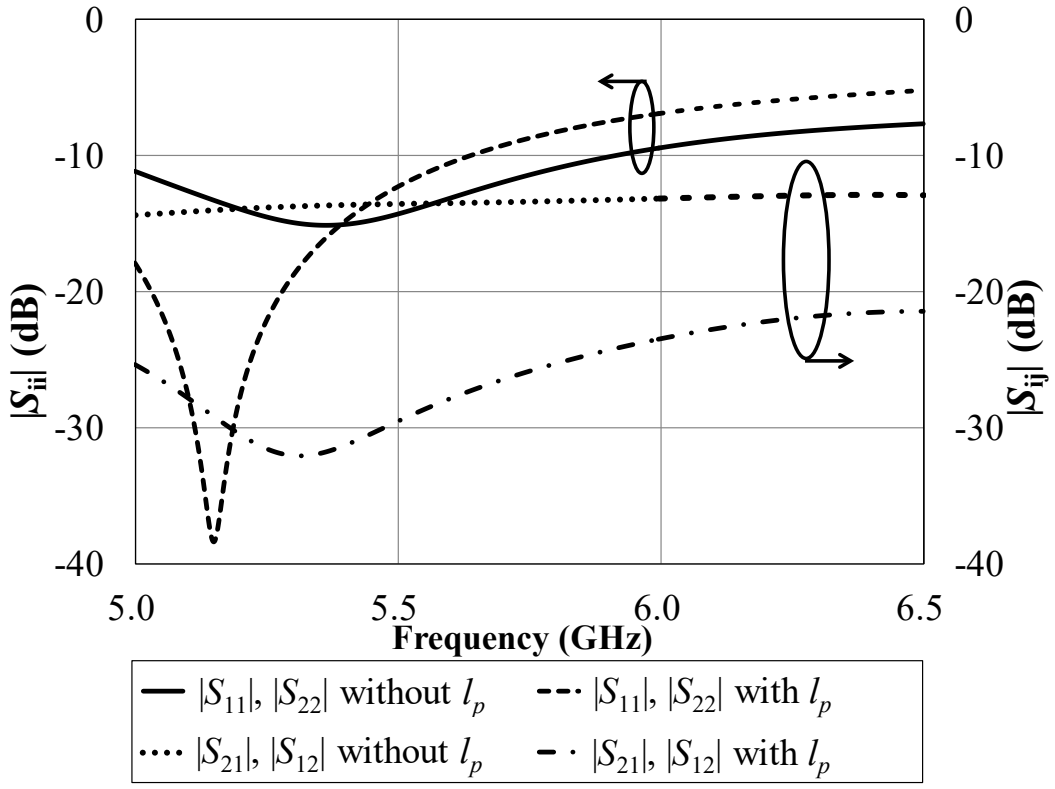

Figure 5.5 The reflection ($|S_{ii}|$) and the isolation ($|S_{ij}|$) versus frequency with and without linear isolator (r_a = 2.18 cm, l_f = 1.36 cm, r_f = 0.75 mm, l_p = 1.60 cm, r_p = 2.50 mm, and α = 45°).

5.3.3 Variation of the Probe Length

The parametric study of the probe length l_f, isolator length l_p and angle α between the isolator and Probe1 will be the focus of this section. Fig. 5.6 shows the $|S_{11}|$ and $|S_{22}|$ along the frequency range of 5.0 GHz to 6.5 GHz for different probe

lengths l_f. The probe length influences both the frequency and the level of minimum $|S_{11}|$. To obtain the minimum $|S_{11}|$ at the center frequency of 5.5 GHz, l_f of 1.25 cm is explicitly chosen. However, when the probe length is varied, the level of $|S_{21}|$ only slightly changes. In particular, at the center frequency, $|S_{21}|$ of different probe lengths are almost identical. The level of $|S_{21}|$ is around -30 dB; therefore, l_f of 1.25 cm is the optimum length.

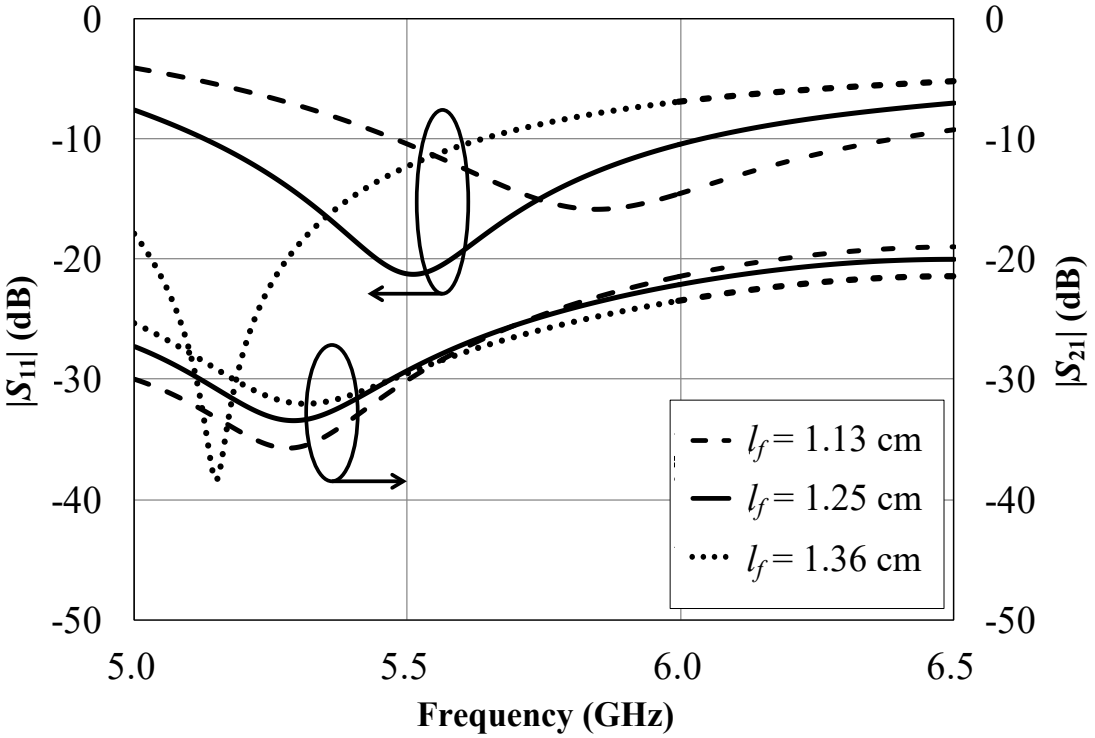

Figure 5.6 The $|S_{11}|$ and the $|S_{21}|$ versus frequency for various probe length l_f (r_a = 2.18 cm, r_f = 0.75 mm, l_p = 1.60 cm, r_p = 2.50 mm, and α = 45°).

5.3.4 Variation of the Linear Isolator Position and Length

The angle α between the linear isolator and Probe1 is another parameter to be investigated. Fig. 5.7 shows the $|S_{11}|$ and $|S_{21}|$ versus frequency for various angles α. It is noted that the $|S_{11}|$ of angle α between the isolator and Probe1 and the $|S_{22}|$ of angle 90° -α between the isolator and Probe2 are identical because Probe1 and Probe2 are perpendicular to each other. It is found that $|S_{11}|$ at α of 45° has the minimum $|S_{11}|$ of -21.25 dB. When the isolator is located offset from the middle between two probes, $|S_{11}|$ becomes worse. The angle between the isolator and the probe has no influence upon the isolation. Therefore, α = 45° is chosen as the design parameter.

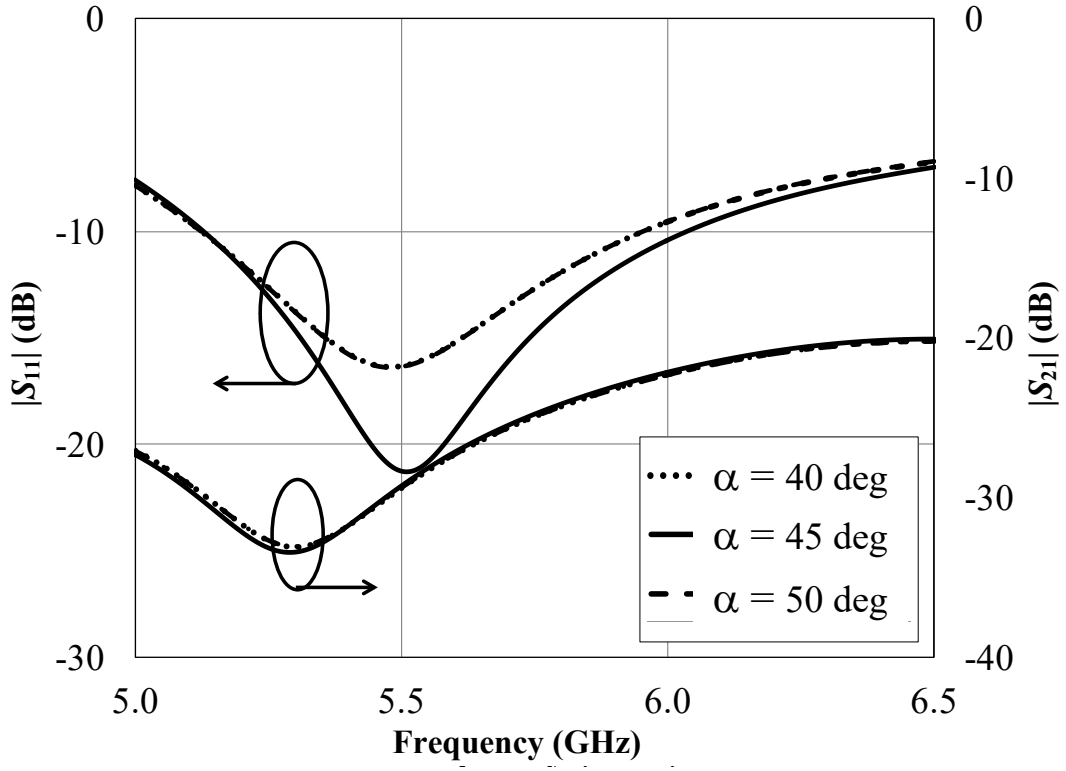

Figure 5.7 The $|S_{11}|$ and the $|S_{21}|$ versus frequency for various angles α between the isolator and Probe1 (r_a = 2.18 cm, l_f = 1.25 cm, r_f = 0.75 mm, l_p = 1.60 mm, and r_p = 2.50 mm).

The isolator length l_p is subsequently varied to achieve the optimum reflection and isolation. Fig. 5.8 shows the $|S_{11}|$ and $|S_{21}|$ of the antenna for various isolator lengths. It is apparent that the isolator length had affected the level of minimum $|S_{11}|$. For $|S_{21}|$ characteristic, when the isolator length is increased, the frequency of minimum $|S_{21}|$ is lower. To achieve the minimum $|S_{21}|$ at 5.5 GHz, the isolator length l_p of 1.43 cm is selected. At the center frequency of 5.5 GHz, the obtained $|S_{11}|$ and $|S_{21}|$ are respectively -22.79 dB and -46.54 dB. It is explicit that the added linear isolator can significantly improve the isolation between the two probes with good reflection at each probe.

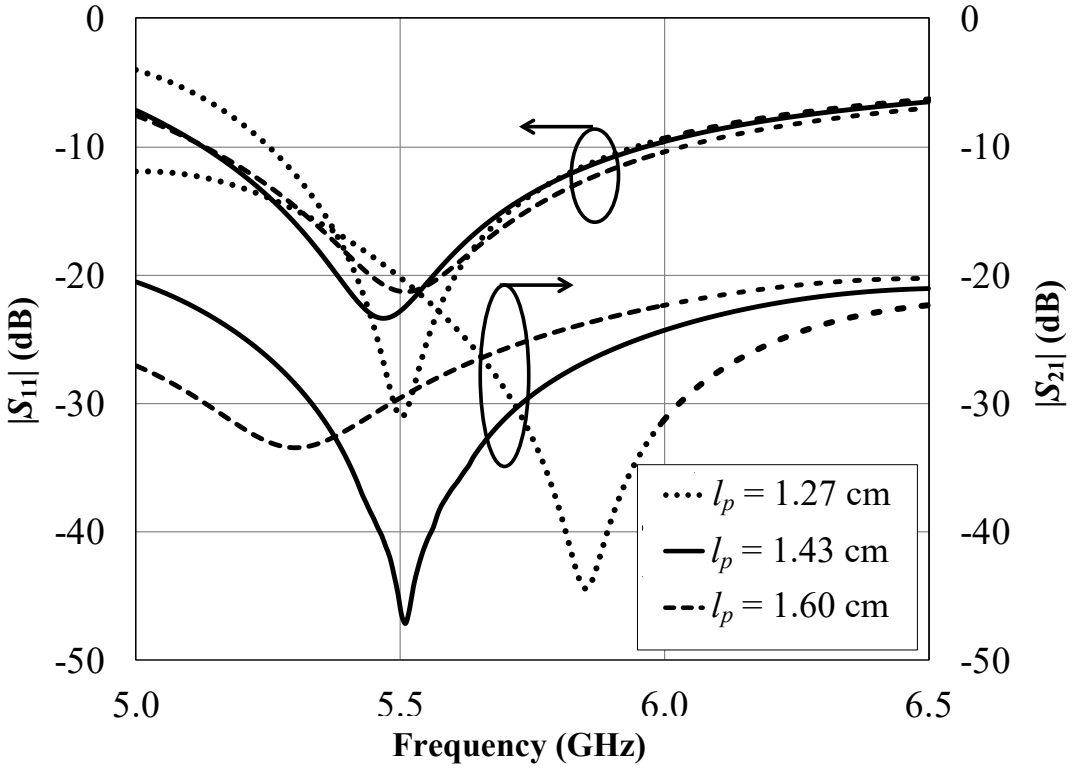

Figure 5.8 The $|S_{11}|$ and the $|S_{21}|$ versus frequency for various isolator lengths l_p (r_a = 2.18 cm, l_f = 1.25 cm, r_f = 0.75 mm, r_p = 2.50 mm, and $\alpha = 45°$).

5.3.5 Variation of the Spacing the Circular Ring and the Size of Square Reflector

The spacing between the circular ring and the square reflector (h) is another parameter that is necessary to be appropriately determined. Fig. 5.9 shows the $|S_{11}|$ and $|S_{21}|$ of the proposed antenna versus frequency for various spacing between the circular ring and the square reflector h. The reflection and isolation of the antenna are changed with the variation of h. To achieve the optimum $|S_{11}|$ and $|S_{21}|$, h of 1.41 cm is obviously chosen. When h is smaller, the $|S_{11}|$ is slightly lower, but the minimum $|S_{11}|$ is occurred at the higher frequency. The isolation of the smaller h is drastically lower. For h of larger than 1.41 cm, the reflection and isolation become worse.

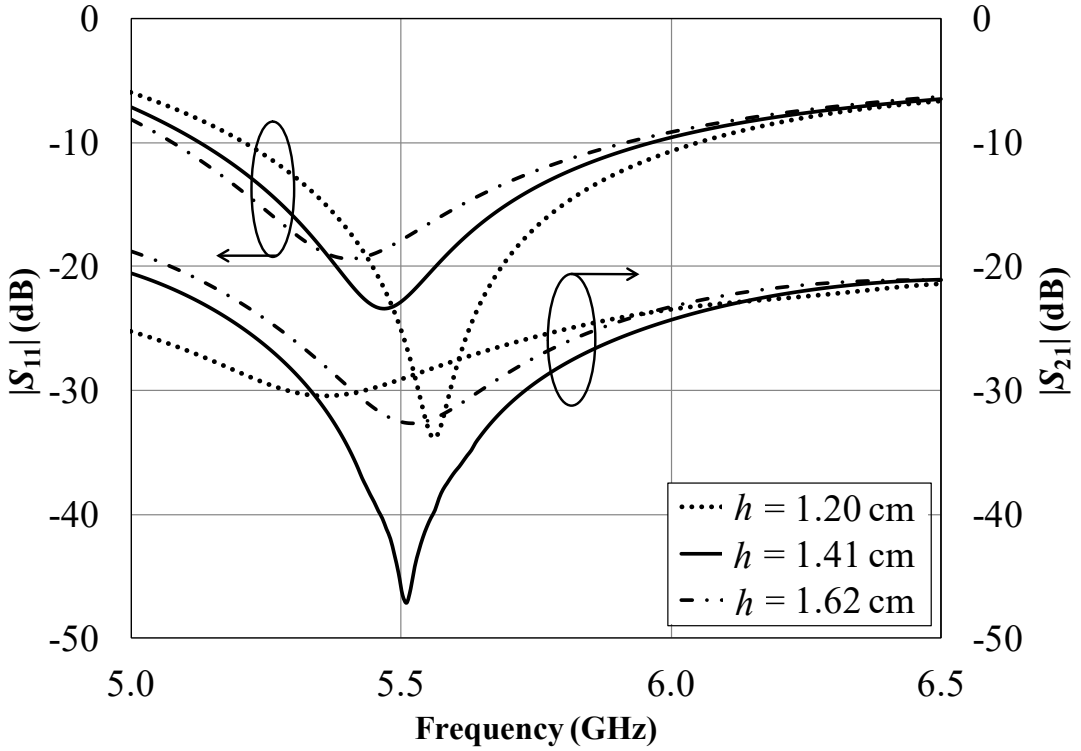

Figure 5.9 The $|S_{11}|$ and the $|S_{21}|$ versus frequency for various spacing between probe and reflector h (r_a = 2.18 cm, l_f = 1.25 cm, r_f = 0.75 mm, r_p = 2.50 mm, α = 45°, and l_p = 1.43 cm).

The unidirectional beam is achieved by placing the circular ring above the square reflector. The square reflector size must be selected according to the compact size and good electrical characteristics. The $|S_{11}|$ and $|S_{21}|$ for various sizes of the square reflector is illustrated in Fig. 5.10. It is apparent that the reflection and isolation are not significantly sensitive with the size of the square reflector. To obtain the optimum $|S_{11}|$ and $|S_{21}|$, the square reflector size of 8 cm is chosen. Generally, the square reflector size has impacted on the radiation pattern especially the front-to-back (F/B) ratio. Fig. 5.11 shows the radiation pattern of the antenna in *xy*- and *xz*-plane for either Probe1 or Probe2 excitation. The unidirectional pattern with similar beamwidth is obtained with the square reflector size of 6 cm, 8 cm and 10 cm. As expected, the F/B ratio is lower when the square reflector size is smaller. To obtain the compact size with F/B ratio higher than 20 dB, the square reflector size L of 8 cm is accordingly chosen.

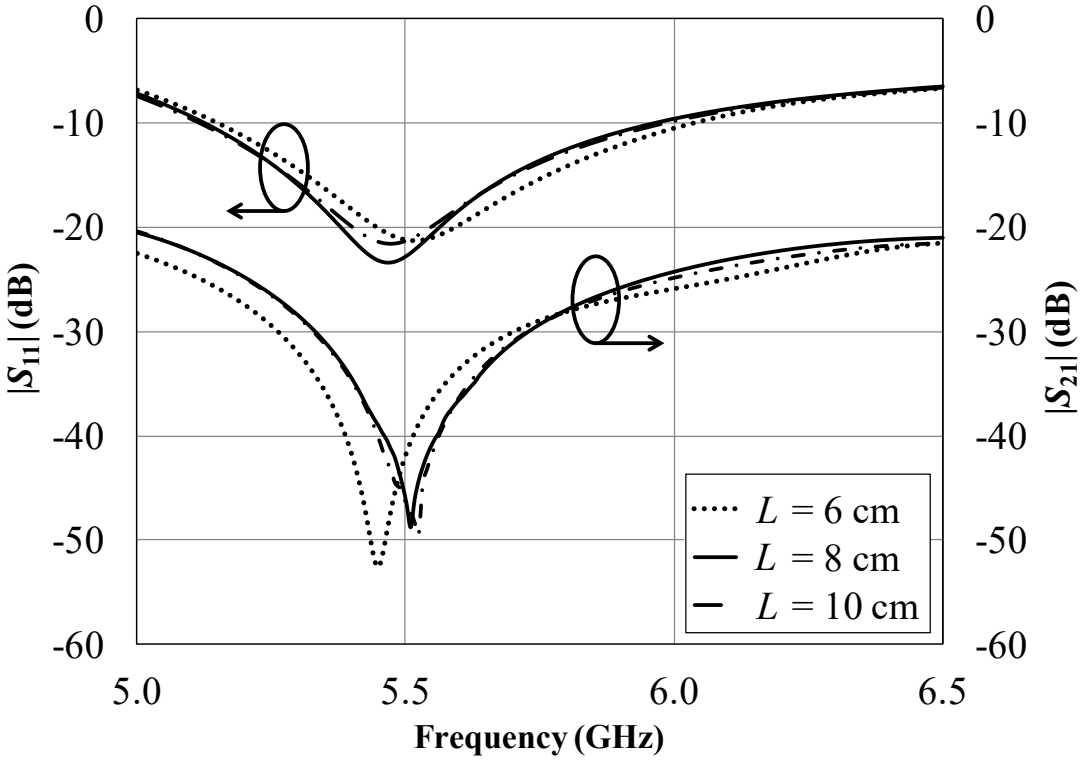

Figure 5.10 The $|S_{11}|$ and the $|S_{21}|$ versus frequency for various square reflector size L (r_a = 2.18 cm, l_f = 1.25 cm, r_f = 0.75 mm, r_p = 2.50 mm, α = 45°, and l_p = 1.43 cm).

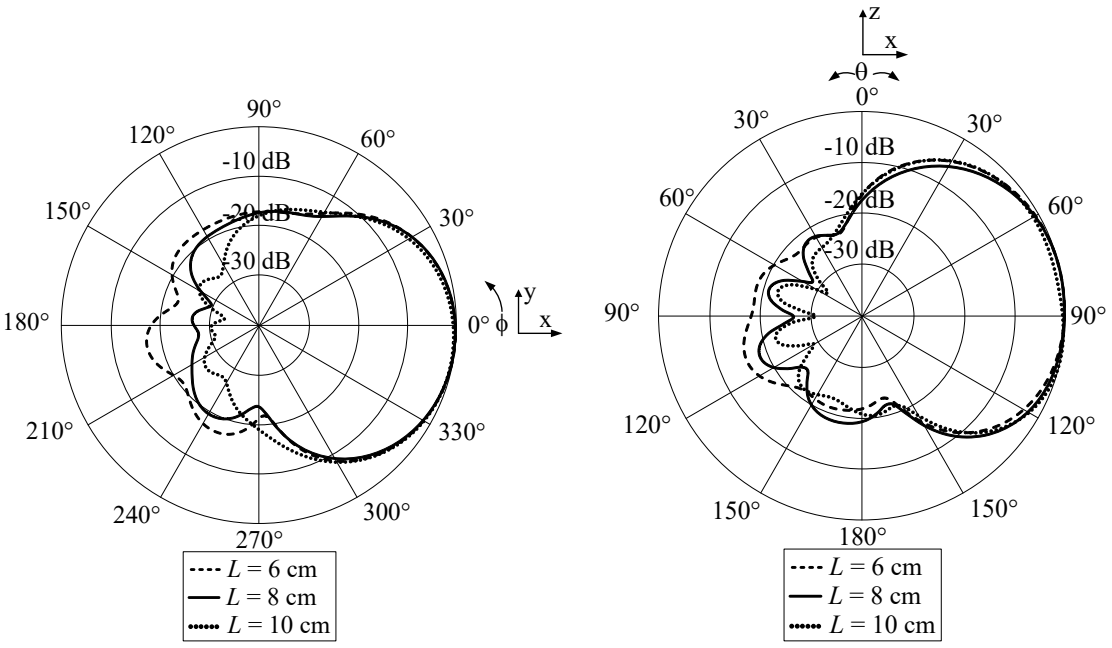

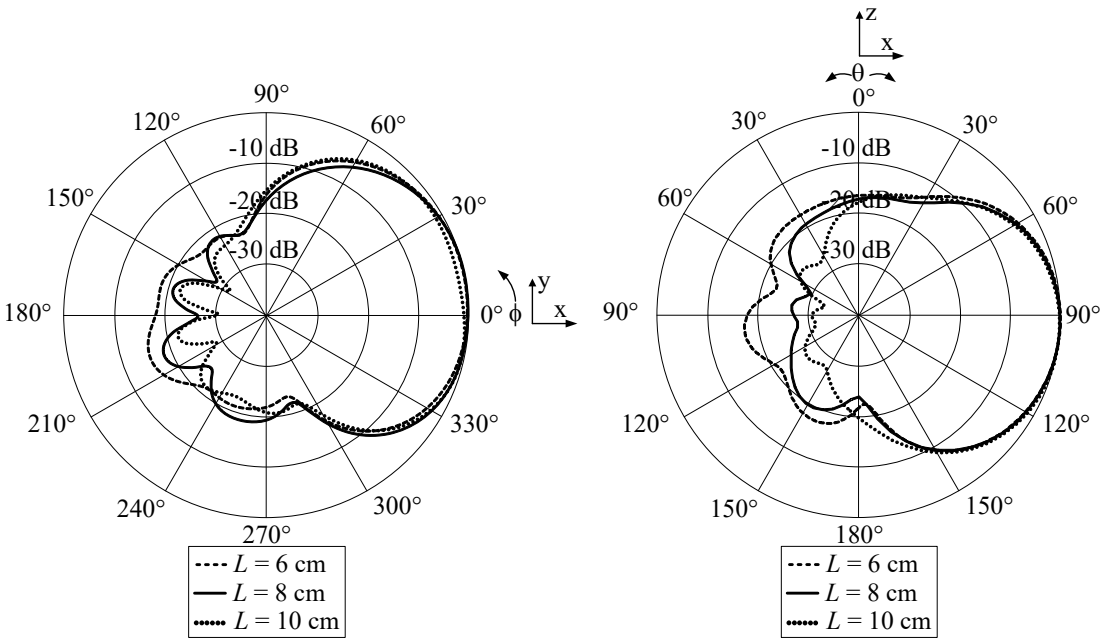

Figure 5.11 The radiation pattern at 5.5 GHz for various L (r_a = 2.18 cm, l_f = 1.25 cm, r_f = 0.75 mm, l_p = 1.43 cm, r_p = 2.50 mm, and α = 45°). (a) Probe1 excitation in *xy*-plane, (b) Probe1 excitation in *xz*-plane, (c) Probe2 excitation in *xy*-plane, and (d) Probe2 excitation in *xz*-plane.

Based on the parametric study results, the design parameters of the proposed antenna are tabulated in Table 5.1.

The radiation pattern of the antenna in two principal planes for excitation of Probe1 and Probe2 is illustrated in Figs. 5.12(a) and 5.12(b) in which the radiation patterns in *xy*-plane and *xz*-plane are respectively shown. The solid line represents the excitation of Probe1 whereas the dashed line is for Probe2 excitation. The unidirectional pattern is achieved for either Probe1 or Probe2 excitation. It is noted that the pattern in *xy*-plane for Probe1 excitation is identical to that in *xz*-plane for Probe2 excitation due to the symmetrical configuration in two principle planes. The half-power beamwidths (HPBW) in *xy*-plane for excitation of Probe1 and Probe2 are 60 degrees and 80 degrees, respectively. The *F*/*B* ratio in both planes is 26 dB.

Table 5.1. The Design Parameters.

Parameter	Electrical size	Physical size at 5.5 GHz
L	1.466λ	8.000 cm
r_a	0.400λ	2.181 cm
d	0.280λ	1.527 cm
t	0.055λ	3.000 mm
h	0.260λ	1.418 cm
l_f	0.229λ	1.250 cm
r_f	0.013λ	0.750 mm
l_p	0.262λ	1.430 cm
r_p	0.045λ	2.500 mm
α	45°	

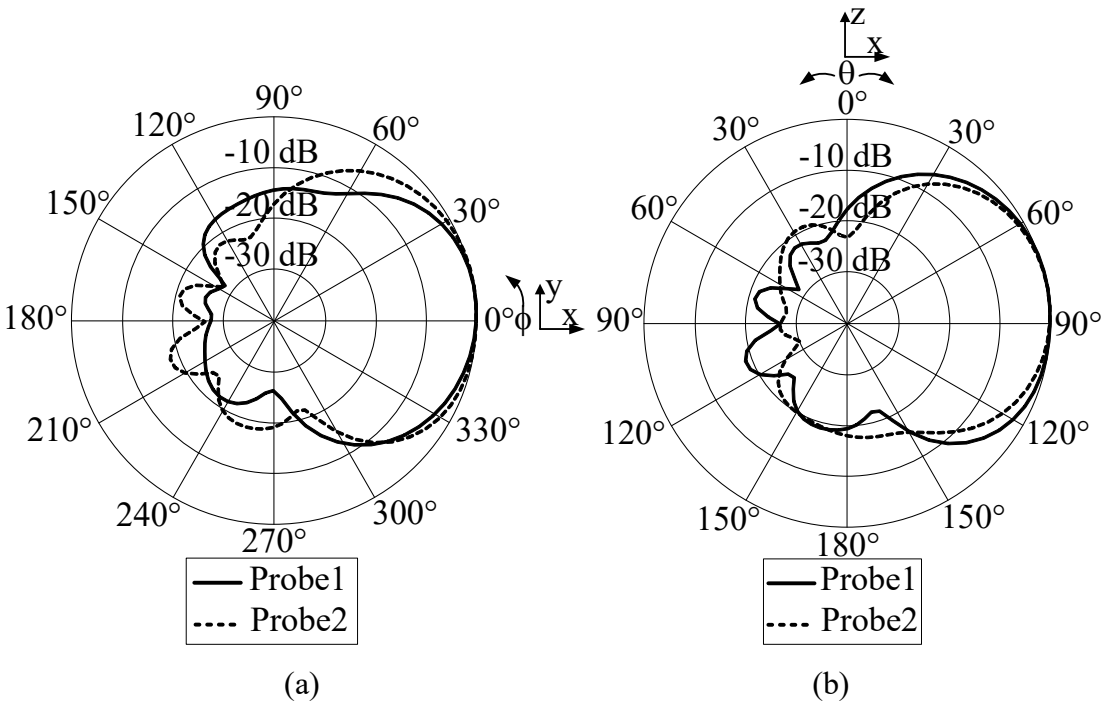

Figure 5.12 The radiation pattern at 5.5 GHz (r_a = 2.18 cm, l_f = 1.25 cm, r_f = 0.75 mm, l_p = 1.43 cm, r_p = 2.50 mm, and α = 45°). (a) *xy*-plane, and (b) *xz*-plane.

5.4 Measured Results

To verify the antenna principle, the prototype antenna with the design parameters tabulated in Table 1 was fabricated as depicted in Fig. 5.13.

5.4.1 Impedance Characteristics

The reflection (in terms of $|S_{11}|$) and isolation (in terms of $|S_{21}|$) were measured using an HP872C Network Analyzer. It is noted that $|S_{11}|$ was measured at input port of Probe1 while Probe2 was terminated with matched load. Fig. 5.14 illustrates $|S_{11}|$ and $|S_{21}|$ compared between the simulated and measured results. The solid and dashed lines represent the simulated and measured results, respectively. The simulated and measured are in reasonable agreement. At the center frequency, the simulated and measured $|S_{11}|$ are respectively -22.79 dB and -23.09 dB, whereas the simulated and measured $|S_{21}|$ are -46.54 dB and -33.99 dB, respectively. The impedance bandwidth ($|S_{11}|$ < -10 dB) from the simulation is 15.16% (5.12 – 5.96 GHz), and that from the measurement is 23.64% (5.11 – 6.48 GHz). The obtained bandwidth can cover the requirement of WLAN system according to the IEEE802.11a standard. In addition, the isolation is relatively high. It thus can be concluded that the proposed antenna can be efficiently applied to polarization diversity reception.

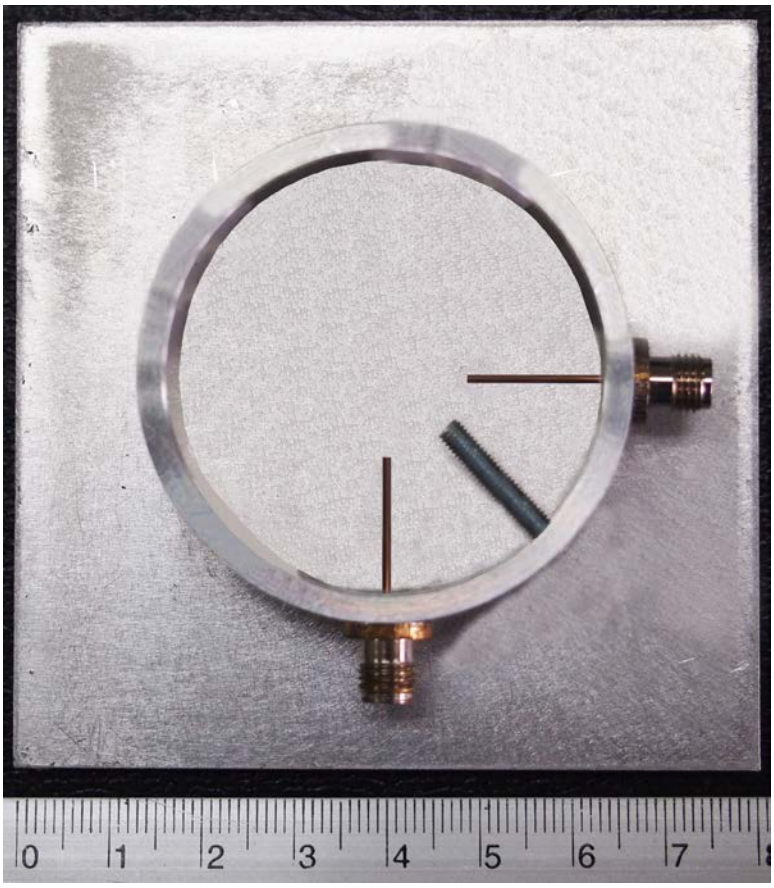

Figure 5.13 Prototype antenna of unidirectional antenna using two-probe excited circular ring above square reflector for polarization diversity.

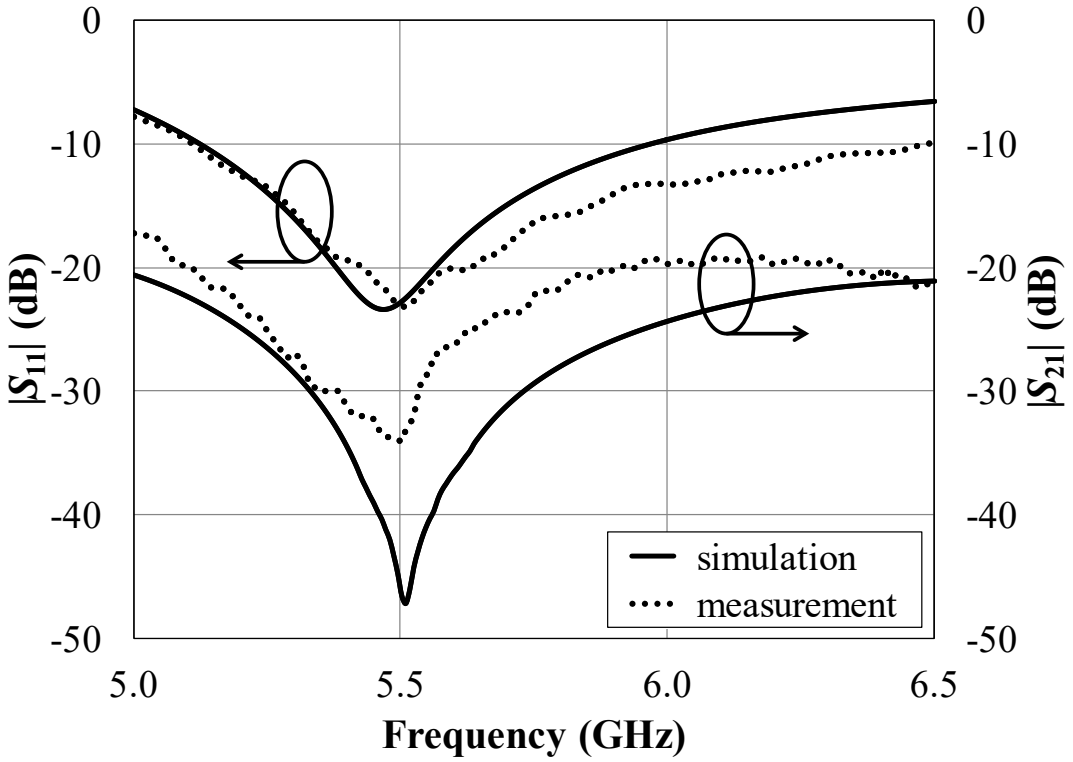

Figure 5.14 The comparison of $|S_{11}|$ and $|S_{21}|$ between simulation and measurement of unidirectional antenna using two-probe excited circular ring above square reflector for polarization diversity.

5.4.2 Radiation Pattern

The radiation patterns of the antenna were also measured. The measurement was carried out in two cases. The first case is performed for Probe1 excitation while Probe2 is terminated with a matched load. The measured results in xy-plane and xz-plane are superimposed with the simulated results as shown in Fig. 5.15. The second case is similar except that the antenna is excited at Probe2 while Probe1 is terminated with a matched load. The results are illustrated in Fig. 5.16. The solid and dashed lines represent the simulated and measured results, respectively. For both cases, the pattern with Probe1 excitation in *xy*-plane coincides with the excitation by Probe2 in *xz*-plane. The good agreement between the simulation and measurement is achieved. The simulated HPBW for Probe1 excitation in *xy*-plane and *xz*-plane are 60 and 80 degrees, respectively. For the measured results the HPBW are 65 and 75 degrees, respectively. The simulated and measured F/B are 26 dB and 31 dB, respectively. From the obtained results, it is apparent that this antenna possesses the good radiation pattern for polarization diversity of point-to-point communication.

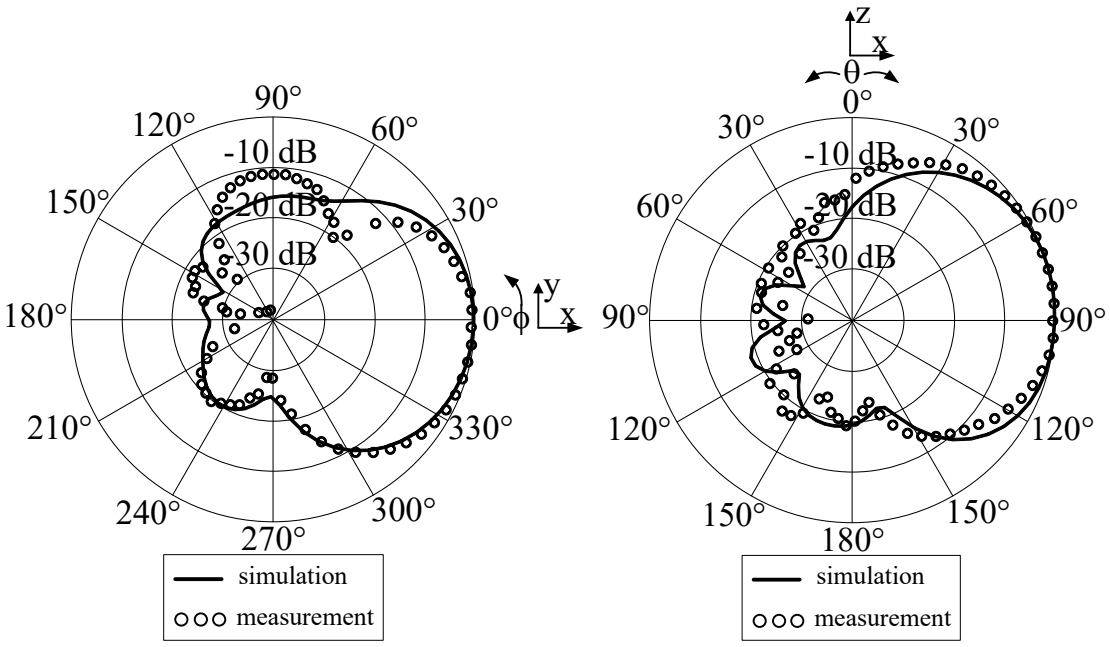

(a) (b)

Figure 5.15 The simulated and measured radiation patterns with Probe1 excitation. (a) *xy*-plane, and (b) *xz*-plane *xy*-plane.

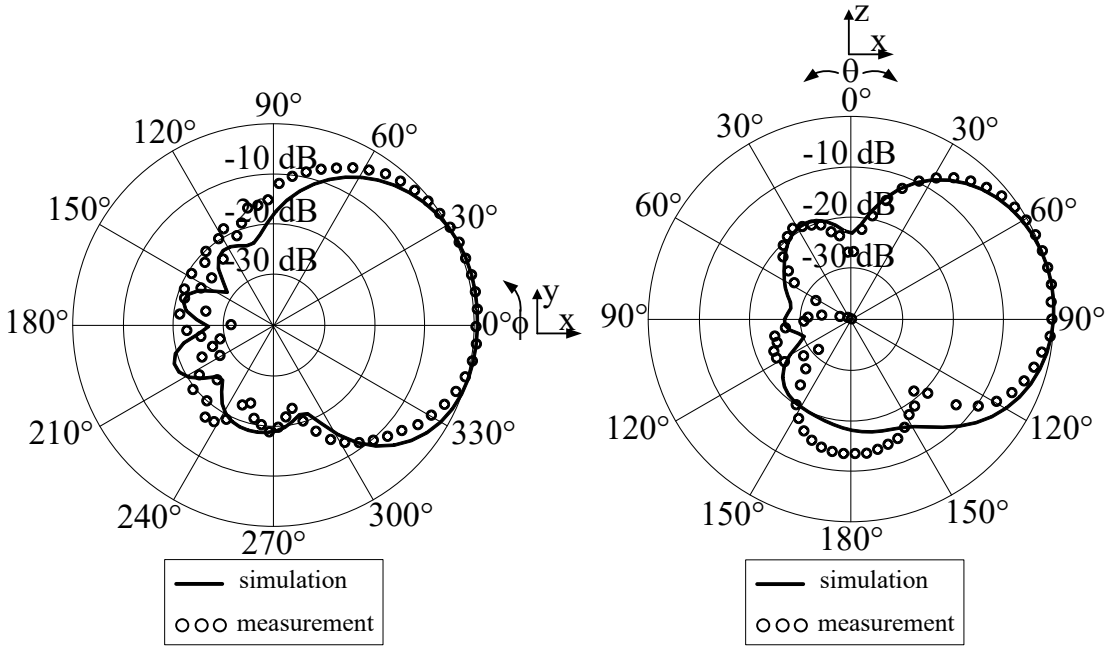

Figure 5.16 The Simulated and measured radiation patterns with Probe2 excitation. (a) xy-plane, and (b) xz-plane xy-plane.

5.4.3 Gain

The antenna gain was measured and compared with the simulated results as shown in Fig. 5.17. Both results display an identical trend with less than 2 dB

difference. This discrepancy is due to the imperfect fabrication compared with the ideal simulation. For example, the loss tangent from the plastic rod that is used as the dielectric supporter between the circular ring and the square reflector was not taken into account in the simulation. It is obvious that the simulated (solid line) and measured (dashed line) gains at the center frequency are 8.35 dBi and 7.42 dBi, respectively. The variation of the gain along the bandwidth of 5.150 – 5.825 GHz is around 1 dB. This antenna thus has sufficient gain for point-to-point communication of WLAN system.

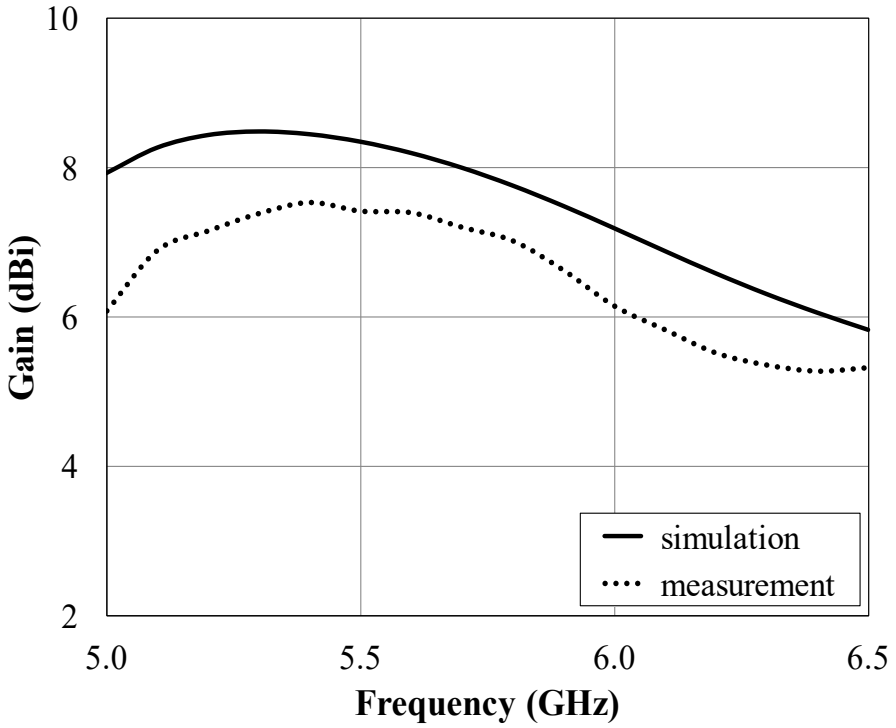

Figure 5.17. The comparison of simulated and measured gains of a unidirectional antenna using two-probe excited circular ring above square reflector for polarization diversity.

5.5 Summary

A unidirectional antenna for polarization diversity of WLAN system is achieved by using the circular ring excited by two perpendicular probes above the square reflector. The isolation is improved by adding a linear isolator at an angle of 45 degrees between two probes. The antenna principle is uncomplicated and the design straightforward. In addition, the prototype antenna is readily fabricated and

conveniently produced on a mass scale. At the center frequency, the HPBW in two principal planes are 65 and 75 degrees, and the *F*/*B* is 31 dB. The obtained gain is 7.42 dBi. The antenna provides good radiation characteristics suitable for the point-to-point communication. $|S_{11}|$ and $|S_{21}|$ are -23.09 dB and -33.99 dB, respectively. The bandwidth can cover 5.11–6.48 GHz. It can be concluded that this antenna is appropriate for polarization diversity of WLAN system according to the IEEE802.11a standard. Furthermore, based on the antenna principle and design, the antenna parameters can be varied to realize the polarization diversity antenna of point-to-point communication in other wireless communication systems.

CHAPTER 6
CONCLUSIONS AND DISCUSSIONS

In this thesis, the author proposed three models are included from 6 chapters as follow, the motivation and literature review of the concept of the main keyword is necessary that related to the thesis i.e. the design principle starts with exciting the rectangular ring with a CDM. To model the bidirectional radiation pattern once important candidate used to form beam from omnidirectional to radiate in two apertures is the ring such as rectangular, circular ring and others. After that, to obtain the unidirectional pattern, the structure should be place above the one side of the ring aperture to focus the main beam into the one direction is call reflector. Moreover, to improve and mitigate or reduce the fading problem the diversity reception techniques have been applied and discussed in Chapter 2.

In Chapter 3, the first model to propose a unidirectional ring antenna for WiMAX systems by using circular disc monopole (CDM) excited rectangular ring mounted in front of a square reflector to operating the frequency range of 2.300 GHz to 5.825 GHz. The rectangular ring is used to confine the CDM radiating omnidirectional pattern to become bidirectional beam. Hence, to realize the unidirectional pattern the reflector was place near the one side of the ring aperture. So, the distance between the CDM and the square reflector was simulated to focus the main beam into the direction along $+z$ axes. The rectangular ring dimensions and the distance between the CDM and the square reflector were determined for a CDM must be appropriately chosen to achieve the wideband and high gain. Based on the simulation results, the rectangular ring width a of 7.2 cm, ring height b of 3.4 cm, ring length d of 2.6 cm, and the distance between the CDM and the square reflector h of 2.4 cm are included from the parametric study. The impedance bandwidth was enhanced by varying the radius of CDM r_c and feed gap δ. Moreover, to confirm the simulation results, the prototype antenna with optimum parameters from simulation results was fabricated. The impedance bandwidth characteristics and radiation patterns are measured. Apparently, the simulation and measured impedance bandwidth of 88% and 93% ($|S_{11}|$<-10 dB) are obtained for the frequency ranges from 2.28 GHz to 5.91 GHz and 2.16 GHz to 5.96 GHz over the WiMAX requirement, respectively. In addition, the simulated and measured gain at the desired direction (θ =

0° and $\phi = 90°$) along the frequency range of 2.300 GHz to 5.825 GHz. The antenna possesses the maximum value of the measured gain of 8.7 dBi at 2.4 GHz. It is noted that the proposed antenna with the advantages of compact size and good radiation performance can be promised for WiMAX systems.

Second model the author propose a rectangular ring antenna excited by U-shaped slot in the CDM, band-rejected filtering property in the WiMAX band is achieved. The dual band-notched operations are achieved by etching U-shaped slot in the CDM by applying the antenna structure design criteria have already been present in Chapter 3. The proposes a simple and compact U-shaped slot in CDM fed rectangular ring antenna are placed above the square reflector with dual band-notched characteristics in 4.0 GHz (3.60 GHz to 4.86 GHz). The antenna is proposed for the dual band point-to-point communication of Wireless Local Area Network (WLAN) system according to the IEEE 802.11a standard in which the allocated frequency band ranges from 2.400 GHz to 2.500 GHz and 5.150 GHz to 5.825 GHz. To verification the simulated results, the prototype antenna was fabricate and measured to compared with simulation results. Although the band-notched characteristics in 3.60 GHz to 4.86 GHz are achieved by tuning the total length of the U-shaped slot, a destructive interference takes place causing the antenna non-radiating at the frequency. From the results, it is found that the most important impact parameters are the distance between the U-shaped bottom and lower wall of the rectangular ring t_1, and the spacing between 2 branched of the U-shaped slot t_2. Based on, the parametric study results, the prototype antenna was fabricated and measured. From the results, the antenna gain at the 2.45 GHz band is 7.49 dBi, 2.68 dB higher than that in the 5.50 GHz band (4.81 dBi) with provides good radiation pattern and *F*/*B* in both planes *yz*- and *xz*-planes are 15.8 dB and 15.5 dB at the frequency 2.45 GHz band. For 5.50 GHz are 16.59 dB and 18.05 dB, respectively. Moreover, the impedance bandwidth ($|S_{11}| < -10$ dB) from the measured results are 2.06 GHz to 3.58 GHz for the 2.4 GHz band and 4.88 GHz to 6.00 GHz for the 5.0 GHz band, which covers the 2.4 GHz and 5.0 GHz band the requirement of WLAN system according to the IEEE 802.11a standard is presented in Chapter 4.

For the third model is a polarization diversity unidirectional antenna by using two-perpendicular probes excited circular ring are placed above the square reflector for polarization diversity with high isolation. The antenna is proposed for the point-to-

point communication of WLAN system according to the IEEE 802.11a standard in which the allocated frequency band ranges from 5.150 GHz to 5.825 GHz. The proposed antenna is compact and suitable for mass production. It is initially described theoretically in term of a unidirectional antenna using a probe excited circular ring above the square reflector. The antenna design and antenna characteristics were done by using CST Microwave Studio simulation tool. The design process was as follow: First, a suitable radius of circular ring was chosen for a single probe antenna. After that, the suitable radius of the ring, probe radius, and the probe length were determined for the two probes antenna. The antenna parameters that are ring radius r_a of 0.4λ, ring length d of 0.28λ, probe radius r_f of 0.75 mm, and probe length l_f of 0.22λ is included from the parametric study. The isolation between the two probes was improved by insertion the linear isolator between two probes. Then, the isolation between the two probes and reflection was enhanced by offsetting the position of linear isolator and isolator length. Moreover, to achieve the optimum $|S_{11}|$ and $|S_{21}|$, the distance between square reflector and two probes h of 0.26λ is obviously chosen. In addition, the square reflector size must be selected according to the compact size and good electrical characteristics. It is apparent that the reflection and isolation are not significantly sensitive with the size of the square reflector. To obtain the optimum $|S_{11}|$ and $|S_{21}|$, the square reflector size of 8 cm is chosen. Based on, the parametric study results, the prototype antenna at the frequency of 5.5 GHz was fabricated and measured to compare with simulated results. It is found that the simulated and measured results were in reasonable agreement. The results showed that the isolation achieved was higher than 30 dB with the gain was 7.42 dBi. The radiation patterns of the antenna were also measured and were carried out in two cases. The measured results in both planes in *xy*-plane and *xz*-plane are superimposed with the simulated results. The measured *F*/*B* is 31 dB while the HPBW in *xy*-plane and *xz*-plane from the measured results are 65 and 75 degrees, respectively. From the obtained results, the two perpendicular probe antenna above square reflector with a linear isolator as the transmitting and receiving antennas provided the highest capacity result. The independent two perpendicular probes could be provided for the polarization diversity antenna. In other hand, it can be said that inserting the linear isolator between two probes can improve the isolation and reflection of the proposed antenna are drawn and detailed in Chapter 5.

As the aforementioned earlier, it is evident that a unidirectional antenna ring antenna for WIFI and WiMAX systems by using the CDM and two perpendicular probes excited rectangular and circular ring above the square reflector are satisfy developed. It is well-known that the antenna is a significant and essential part of wireless communication systems to make the communication successful. Even thought the impedance bandwidth can be enhance by using the CDM excited rectangular ring mounted in front of the square reflector, but the radiation pattern at higher edge frequency still tilt upward. Hence, the antenna characteristics should be improved. Especially, there are some approaches to improve the radiation pattern and gain, for example, change the dimension of rectangular ring or change the feeding structure or position. However, these topics are left for further study.

RELATED PUBLICATIONS

Journal Papers

[1] **Souphanna Vongsack**, Suthasinee Lamultree, Pracha Osklang, Chuwong Phongcharoenpanich, Sompol Kosulvit, Kazuhika Hamamoto, and Toshio Wakabayashi, "A UWB Bidirectional Rectangular Ring Antenna Fed by CDM with a Rod and Ridges for Constant Beam Direction," *International Journal of Microwave Science and Technology,* March 2011.

[2] **Souphanna Vongsack**, Chuwong Phongcharoenpanich, Sompol Kosulvit, Kazuhiko Hamamoto, and Toshio Wakabayashi, "Unidirectional Antenna Using Two-probe Excited Circular Ring above Square Reflector for Polarization Diversity with High Isolation," *Progress In Electromagnetics Research*, *PIER*, vol. 133, pp. 159-176, 2012.

[3] **Souphanna Vongsack**, Chuwong Phoncharoenpanich, Sompol Kosulvit, Kazuhiko Hamamoto, and Toshio Wakabayashi, "Rectangular Ring Antenna Excited by Circular Disc Monopole for WiMAX System," *International Journal of Antennas and Propagation*, vol. 2014, pp. 1-7, 2014.

Conference Papers

[1] Sompol Kosulvit, **Souphanna Vongsack**, Suthasinee Lamultree, Kittisak Phaebua, Tajchai Pumpoung, Krittaya Chawanonphithak, Chuwong Phongcharoenpanich, and Monai Krairiksh, "Rectangular Ring Antenna Fed by Broadband Electric Probe above Elliptical Reflector for WiMAX Systems," *Proceeding of International Symposium on Antenna and Propagation (ISAP09)*, pp. 811-814, October 2009.

[2] Pracha Osklang, **Souphanna Vongsack**, Chuwong Phongcharoenpanich, Sompol Kosulvit, Kazuhiko Hamamoto, and Toshio Wakabayashi, "A UWB Bidirectional Antenna with Stable Beam Peak Direction," *International Workshop on Information Communication Technology*, pp. 1-4, August 2010.

[3] Pracha Osklang, **Souphanna Vongsack**, Chuwong Phongcharoenpanich, Sompol Kosulvit, Kazuhiko Hamamoto, and Toshio Wakabayashi, "Improvement of

Bidirectional Pattern along UWB using Parasitic Structures," *Joint International Conference on Information and Communication Technology, Electronic and Electrical Engineering*, pp. 512-515, December 2010.

[4] **Souphanna Vongsack**, Chuwong Phongcharoenpanich, Sompol Kosulvit, Kazuhika Hamamoto, and Toshio Wakabayashi, "Rectangular Ring Antenna with Square Reflector Fed by CDM," *Proceedings of Technical Meeting on Electromagnetic Theory, IEE Japan,* Kitami, pp.221-225, July 2011.

[5] **Souphanna Vongsack**, Chuwong Phongcharoenpanich, Sompol Kosulvit, Kazuhika Hamamoto, and Toshio Wakabayashi, "Polarization Diversity Unidirectional Antenna for Wireless Applications," *Proceedings of The 6th International Conference on Telecommunication Systems, Services, and Applications 2011(TSSA 2011),* Denpasar, pp.102-105, October 2011.

[6] **Souphanna Vongsack**, Chuwong Phongcharoenpanich, Sompol Kosulvit, Kazuhika Hamamoto, and Toshio Wakabayashi, "Polarization Diversity Unidirectional Antenna for IEEE 802.11a Applications," accepted for presentation in *Progress in Electromagnetics Research Symposium (PIERS 2012),* Kuala Lumpur, Mar. 2012.

Progress In Electromagnetics Research, Vol. 133, 159–176, 2012

UNIDIRECTIONAL ANTENNA USING TWO-PROBE EXCITED CIRCULAR RING ABOVE SQUARE REFLECTOR FOR POLARIZATION DIVERSITY WITH HIGH ISOLATION

S. Vongsack[1], C. Phongcharoenpanich[1, *], S. Kosulvit[1], K. Hamamoto[2], and T. Wakabayashi[3]

[1]Faculty of Engineering, King Mongkut's Institute of Technology Ladkrabang, Bangkok 10520, Thailand

[2]School of Information and Telecommunication Engineering, Tokai University, 1117 Kitakaname, Hiratsuka, Kanagawa 259-1292, Japan

[3]Malaysia-Japan International Institute of Technology, University of Technology Malaysia, Kuala Lumpur 54100, Malaysia

Abstract—This paper presents a circular ring antenna fed by two perpendicular probes, both of which are placed above the square reflector. The antenna is employed to radiate unidirectional beam for polarization diversity reception. A linear isolator is added to improve the isolation between the two probes. The antenna is proposed for the point-to-point communication of Wireless Local Area Network (WLAN) system according to the IEEE 802.11a standard in which the allocated frequency band ranges from 5.150 GHz to 5.825 GHz. The proposed antenna is compact and suitable for mass production. Without the dielectric material, the antenna is free of dielectric loss and capable of high power handling. The prototype antenna was fabricated and measured to verify the theoretical predictions. At the center frequency, the unidirectional pattern with the measured half-power beamwidths in two principal planes of 65 and 75 degrees is achieved. The front-to-back ratio is 31 dB, and the antenna gain is 7.42 dBi. The $|S_{11}|$ and $|S_{21}|$ are respectively -23.09 dB and -33.99 dB; the obtained bandwidth is 23.64%. Based on the aforementioned characteristics, the antenna is a potential candidate for polarization diversity of WLAN applications.

Received 1 August 2012, Accepted 15 October 2012, Scheduled 18 October 2012

* Corresponding author: Chuwong Phongcharoenpanich (pchuwong@gmail.com).

1. INTRODUCTION

Presently, wireless communications are essential for human activities in various aspects. The Wireless Local Area Network (WLAN) system plays an important role in connecting users in the community of a given service area [1]. Based on IEEE 802.11a standard, the operating frequency band covers 5.150 GHz to 5.825 GHz, of which the center frequency is 5.5 GHz [2]. Typically, the communication network of WLAN system can be classified into two topologies, i.e., point-to-multipoint and point-to-point connections. The point-to-multipoint connection is the typical topology in which the root or base station is able to communicate to a number of clients located around it. In this configuration, the omnidirectional antenna is suitable for the base station [3–9]. For the point-to-point connection topology, the unidirectional antenna is a promising candidate [10–12]. In the case of only line of sight (LOS) situation, the signal can be directly propagated from the transmitter to the receiver. However, in some environments in which the transmitter and receiver are obstructed by various objects, the multipath signal occurs due to obstacles, such as buildings and trees, which cause the signal to reflect and diffract. The multiple components of transmitted signal reach the receiver at slightly different time points, thereby producing multipath fading which not only varies with time and physical motion but also affects the channel performance and thus reduces the data rate [13]. To mitigate the fading problem, the diversity reception techniques have been applied [14, 15]. A number of diversity antennas have been discussed in the existing literature [16, 17]. The space diversity with proper spacing between two antennas is the simplest geometry [18]. However, since large spacing is required, the overall antenna dimension needs to be relatively large [19]. The polarization diversity with two orthogonal excitations in the same antenna body has been proposed to minimize the whole antenna size [20–23]. The polarization diversity antenna with unidirectional pattern is very useful for base station applications such as WLAN system [24–35]. This paper presents the unidirectional antenna for polarization diversity of WLAN system following IEEE 802.11a standard with the operating frequency band between 5.150 GHz and 5.825 GHz. The antenna evolution starts from the circular ring excited by a probe that radiates bidirectional pattern in two opposite directions along two ring apertures with single polarization. This structure is located above the square reflector to confine the main beam to single direction. The excitation with two perpendicular probes is introduced for polarization diversity. To improve the isolation between two excited probes, the linear isolator

with proper angle is added. The antenna characteristics in terms of the reflection ($|S_{11}|$ and $|S_{22}|$), isolation ($|S_{21}|$ and $|S_{12}|$), radiation pattern, and gain are presented. The simulation was performed using CST Microwave Studio [36]. The prototype antenna was fabricated and measured to confirm the theoretical principle.

The organization of this paper is as follows. The proposed antenna structure and its associated parameters are discussed in Section 2. Section 3 addresses the design principle and parametric study and in Section 4 the measured results are presented. The conclusions are drawn and detailed in Section 5.

2. ANTENNA STRUCTURE

The antenna configuration consists of a circular ring with radius r_a, length d and thickness t as shown in Fig. 1(a). The center of the ring is located at the origin of yz-plane. This ring is excited by two identical probes in the radial direction of the length l_f and radius r_f via 50-Ω SMA connector. The first probe (Probe1) is aligned on z-axis to generate vertical polarization whereas the other probe (Probe2) is oriented along y-axis to create horizontal polarization. The linear isolator of the length l_p and radius r_p is situated inside the ring in the radial direction between two probes. The position of the isolator is at an angle α relative to the Probe1. This structure is placed above the square reflector of size L. The spacing between the ring and the

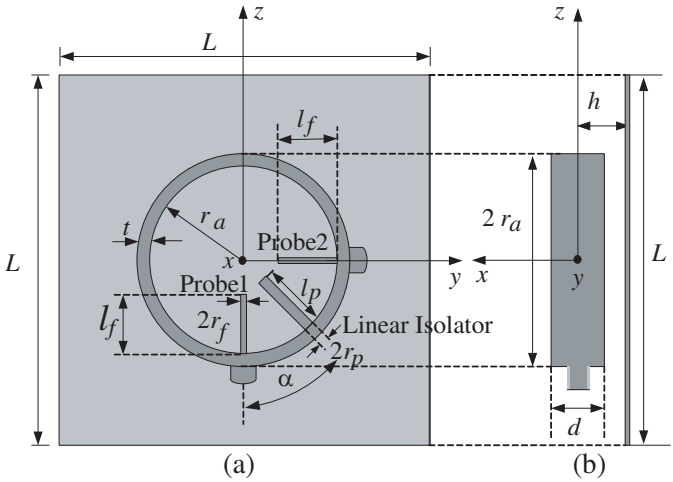

Figure 1. The proposed antenna structure. (a) Perspective view. (b) Side view.

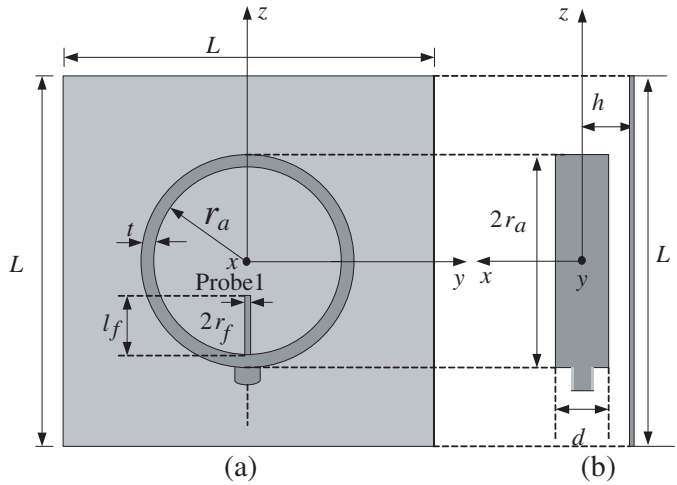

Figure 2. An initial antenna structure. (a) Perspective view. (b) Side view.

reflector is denoted with h as illustrated in Fig. 1(b). The radiation pattern of this antenna is unidirectional with the beam peak pointing x direction.

3. DESIGN PRINCIPLE AND PARAMETRIC STUDY

The antenna structure is designed to operate along the frequency range of 5.150 GHz to 5.825 GHz, of which the center frequency is 5.5 GHz. The principle of the antenna design starts with the conventional circular ring as shown in Fig. 2, with the initial radius $(r_a)\lambda/2$ of the center frequency, which is equal to 2.727 cm. The ring is excited by a single probe of the length $(l_f)\lambda/4$ or 1.363 cm. It is noted that the ring in this paper is made of aluminum with the thickness t of 3 mm. The ring length d of 1.527 cm (0.28λ) and probe radius r_f of 0.65 mm (0.011λ) are selected and used throughout the design due to its ubiquity as fabrication material. The ring length (d) affects to the directivity of the antenna. The guideline for the selection of d for the desired directivity can be found in [37]. To keep the antenna as compact as possible, the size of the square reflector is chosen to be 8 cm with the spacing between the circular ring and the square reflector h of 1.418 cm (0.26λ). In addition, the influence of the size of the square reflector and the spacing between the circular ring and the square reflector will be clarified in this section. It is noted that the infinitesimal gap between the circular ring and the linear isolator is separated with dielectric supporter. There is no electrical contact between the circular ring and the linear isolator.

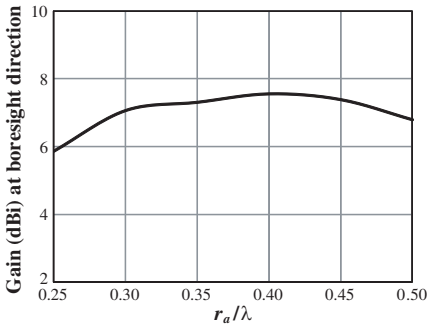

Figure 3. The gain at boresight direction versus ring radius r_a ($l_f = 1.36$ cm and $r_f = 0.65$ mm).

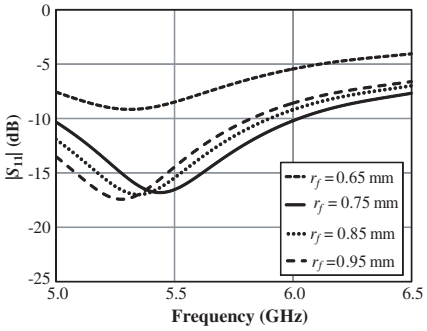

Figure 4. The $|S_{11}|$ versus frequency for various probe radii r_f ($r_a = 2.18$ cm and $l_f = 1.36$ cm).

To determine the proper antenna dimensions that meet the optimum characteristics and are of compact size, the antenna parametric study will be carried out. Fig. 3 illustrates the gain at the boresight direction ($\theta = 90°$, $\phi = 0°$) of the circular ring antenna excited by the single probe above the square reflector for various ring radii r_a. It is evident that the radius of 0.4λ yields the maximum gain. Therefore, the ring radius r_a of 2.18 cm (0.4λ) is selected as the design parameter.

To obtain the good matching condition with efficiently wide bandwidth, the probe radius is adjusted in an incremental fashion of 0.1 mm. Fig. 4 shows the $|S_{11}|$ at single probe excitation versus frequency of the proposed antenna for various probe radii r_f. It is obvious that the probe radius affects the frequency of the minimum $|S_{11}|$. For $r_f = 0.65$ mm, the $|S_{11}|$ is unacceptable due to the reflection level greater than -10 dB throughout the desired frequency band. When r_f is increased to 0.75 mm or higher, the level of the minimum $|S_{11}|$ at 5.5 GHz is less than -15 dB. To achieve the minimum $|S_{11}|$ at the center frequency, r_f of 0.75 mm is selected. The bandwidth coverage is from 5 GHz to 6 GHz.

To develop the circular ring antenna above square reflector for polarization diversity reception, two perpendicular excitation probes in z direction (Probe1) and y direction (Probe2) are introduced as shown in Fig. 1. By adding Probe2 inside the ring, the reflection at each probe (in terms of $|S_{11}|$ and $|S_{22}|$) is degraded compared with when merely Probe1 excitation is employed. Fig. 5 illustrates the frequency response of the reflection of each probe (in terms of $|S_{ii}|$) and the isolation between two probes (in terms of $|S_{ij}|$). It is noted that $|S_{11}|$ and $|S_{22}|$ are identical because of their symmetrical structure while $|S_{21}|$ and

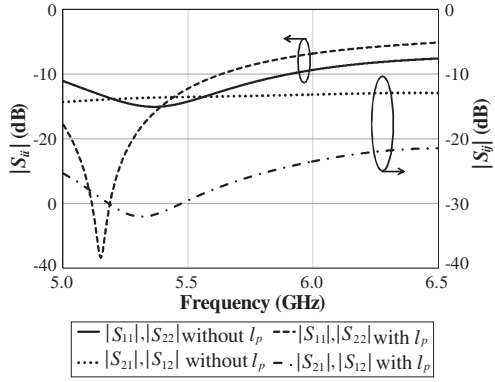

Figure 5. The reflection ($|S_{ii}|$) and the isolation ($|S_{ij}|$) versus frequency with and without linear isolator ($r_a = 2.18\,\text{cm}$, $l_f = 1.36\,\text{cm}$, $r_f = 0.75\,\text{mm}$, $l_p = 1.60\,\text{cm}$, $r_p = 2.50\,\text{mm}$, and $\alpha = 45°$).

$|S_{12}|$ are identical due to reciprocal property. The solid line indicates the $|S_{11}|$ and $|S_{22}|$ when two perpendicular probes are employed. It is noted that $|S_{11}|$ is taken into account when Probe1 is excited and while Probe2 is terminated with the matched load. Meanwhile, $|S_{22}|$ is the result of excitation at Probe2 whereas Probe1 is matched with the dummy load termination. As illustrated by the solid line in Fig. 5, $|S_{11}|$ worsens with merely one probe excitation due to the coupling effect from Probe2. In terms of $|S_{ij}|$ of the isolation (inverse of coupling) where $i \neq j$, it could be observed from the dotted line that $|S_{21}|$ is around $-14\,\text{dB}$ along the frequency band. The isolation in this case is relatively low and insufficient for practical applications. To improve the isolation, the simple linear isolator is symmetrically oriented between the two probes at an angle α of 45°. The linear isolator is made of the copper rod. It is a resonant component that is used to block the surface current from Probe1 to Probe2. Note that the infinitesimal gap between the circular ring and the linear isolator is separated with dielectric supporter to prevent the electrical connection. The current from Probe1 will be stored by this linear isolator. By considering the dashed line and dash-dotted line in Fig. 5, the $|S_{11}|$ and $|S_{21}|$ with the linear isolator included are remarkably improved. However, the $|S_{11}|$ and $|S_{21}|$ are not optimum at the center frequency.

The parametric study of the probe length l_f, isolator length l_p and angle α between the isolator and Probe1 will be the focus of this section. Fig. 6 shows the $|S_{11}|$ and $|S_{21}|$ along the frequency range of 5.0–6.5 GHz for different probe lengths l_f. The probe length influences both the frequency and the level of minimum $|S_{11}|$. To obtain the minimum $|S_{11}|$ at the center frequency of 5.5 GHz, l_f of 1.25 cm is

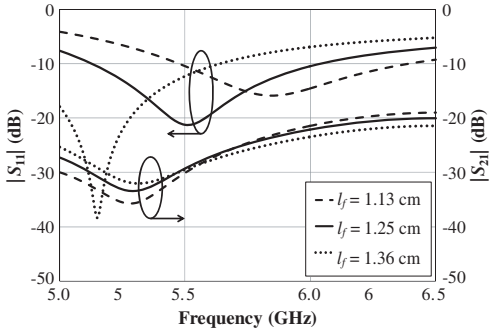

Figure 6. The $|S_{11}|$ and $|S_{21}|$ versus frequency for various probe lengths l_f ($r_a = 2.18\,\text{cm}$, $r_f = 0.75\,\text{mm}$, $l_p = 1.60\,\text{cm}$, $r_p = 2.50\,\text{mm}$ and $\alpha = 45°$).

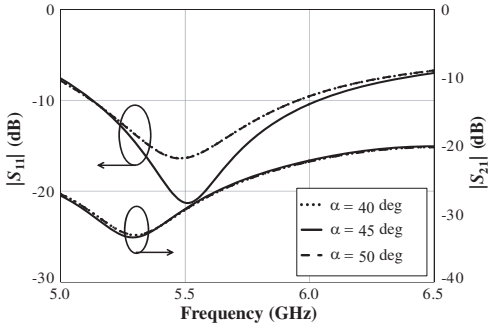

Figure 7. The $|S_{11}|$ and $|S_{21}|$ versus frequency for various angles α between the isolator and Probe1 ($r_a = 2.18\,\text{cm}$, $l_f = 1.25\,\text{cm}$, $r_f = 0.75\,\text{mm}$, $l_p = 1.60\,\text{cm}$ and $r_p = 2.50\,\text{mm}$).

explicitly chosen. However, when the probe length is varied, the level of $|S_{21}|$ only slightly changes. In particular, at the center frequency, $|S_{21}|$ of different probe lengths are almost identical. The level of $|S_{21}|$ is around $-30\,\text{dB}$; therefore, l_f of $1.25\,\text{cm}$ is the optimum length.

The angle α between the linear isolator and Probe1 is another parameter to be investigated. Fig. 7 shows the $|S_{11}|$ and $|S_{21}|$ versus frequency for various angles α. It is noted that the $|S_{11}|$ of angle α between the isolator and Probe1 and the $|S_{22}|$ of angle $90° - \alpha$ between the isolator and Probe2 are identical because Probe1 and Probe2 are perpendicular to each other. It is found that $|S_{11}|$ at α of 45° has the minimum $|S_{11}|$ of $-21.25\,\text{dB}$. When the isolator is located offset from the middle between two probes, $|S_{11}|$ becomes worse. The angle between the isolator and the probe has no influence upon the isolation. Therefore, $\alpha = 45°$ is chosen as the design parameter.

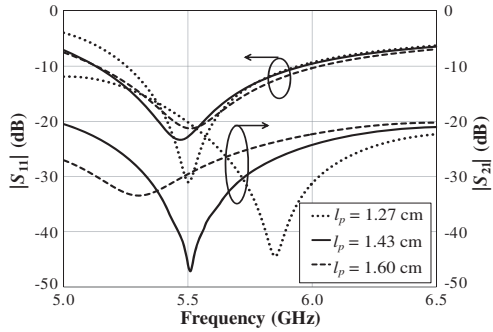

Figure 8. The $|S_{11}|$ and $|S_{21}|$ versus frequency for various isolator lengths l_p ($r_a = 2.18\,\text{cm}$, $l_f = 1.25\,\text{cm}$, $r_f = 0.75\,\text{mm}$, $r_p = 2.50\,\text{mm}$ and $\alpha = 45°$).

The isolator length l_p is subsequently varied to achieve the optimum reflection and isolation. Fig. 8 shows the $|S_{11}|$ and $|S_{21}|$ of the antenna for various isolator lengths. It is apparent that the isolator length has affected the level of minimum $|S_{11}|$. For $|S_{21}|$ characteristic, when the isolator length is increased, the frequency of minimum $|S_{21}|$ is lower. To achieve the minimum $|S_{21}|$ at 5.5 GHz, the isolator length l_p of 1.43 cm is selected. At the center frequency of 5.5 GHz, the obtained $|S_{11}|$ and $|S_{21}|$ are respectively $-22.79\,\text{dB}$ and $-46.54\,\text{dB}$. It is explicit that the added linear isolator can significantly improve the isolation between the two probes with good reflection at each probe.

The spacing between the circular ring and the square reflector (h) is another parameter that is necessary to be appropriately determined. Fig. 9 shows the $|S_{11}|$ and $|S_{21}|$ of the proposed antenna versus frequency for various spacing between the circular ring and the square reflector h. The reflection and isolation of the antenna are changed with the variation of h. To achieve the optimum $|S_{11}|$ and $|S_{21}|$, h of 1.41 cm is obviously chosen. When h is smaller, the $|S_{11}|$ is slightly lower, but the minimum $|S_{11}|$ is occurred at the higher frequency. The isolation of the smaller h is drastically lower. For h of larger than 1.41 cm, the reflection and isolation become worse.

The unidirectional beam is achieved by placing the circular ring above the square reflector. The square reflector size must be selected according to the compact size and good electrical characteristics. The $|S_{11}|$ and $|S_{21}|$ for various sizes of the square reflector is illustrated in Fig. 10. It is apparent that the reflection and isolation are not significantly sensitive with the size of the square reflector. To obtain the optimum $|S_{11}|$ and $|S_{21}|$, the square reflector size of 8 cm is chosen. Generally, the square reflector size has impacted on the radiation pattern especially the front-to-back (F/B) ratio. Fig. 11

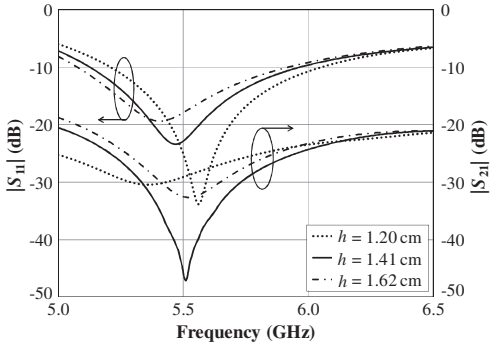

Figure 9. The $|S_{11}|$ and $|S_{21}|$ versus frequency for various spacing between probe and reflector h ($r_a = 2.18\,\text{cm}$, $l_f = 1.25\,\text{cm}$, $r_f = 0.75\,\text{mm}$, $r_p = 2.50\,\text{mm}$, $\alpha = 45^\circ$ and $l_p = 1.43\,\text{cm}$).

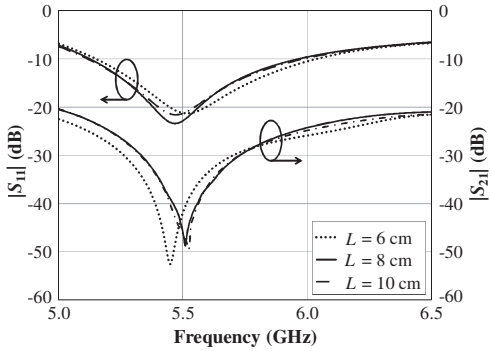

Figure 10. The $|S_{11}|$ and $|S_{21}|$ versus frequency for various square reflector size L ($r_a = 2.18\,\text{cm}$, $l_f = 1.25\,\text{cm}$, $r_f = 0.75\,\text{mm}$, $r_p = 2.50\,\text{mm}$, $\alpha = 45^\circ$ and $l_p = 1.43\,\text{cm}$).

shows the radiation pattern of the antenna in xy- and xz-plane for either Probe1 or Probe2 excitation. The unidirectional pattern with similar beamwidth is obtained with the square reflector size of 6 cm, 8 cm and 10 cm. As expected, the F/B ratio is lower when the square reflector size is smaller. To obtain the compact size with F/B ratio higher than 20 dB, the square reflector size L of 8 cm is accordingly chosen.

Based on the parametric study results, the design parameters of the proposed antenna are tabulated in Table 1.

The radiation pattern of the antenna in two principal planes for excitation of Probe1 and Probe2 is illustrated in Figs. 12(a)

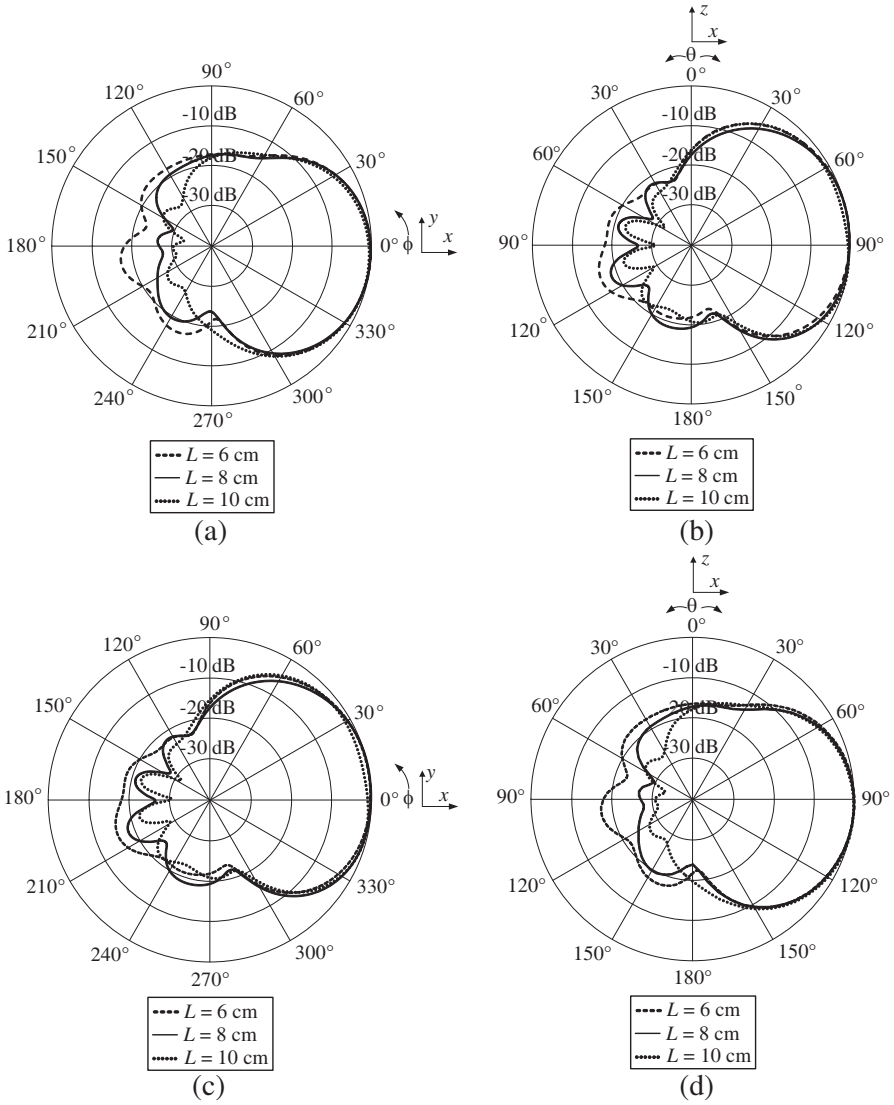

Figure 11. The radiation pattern at 5.5 GHz for various L (r_a = 2.18 cm, l_f = 1.25 cm, r_f = 0.75 mm, l_p = 1.43 cm, r_p = 2.50 mm and $\alpha = 45°$). (a) Probe1 excitation in xy plane. (b) Probe1 excitation in xz plane. (c) Probe2 excitation in xy plane. (d) Probe2 excitation in xz plane.

Table 1. The design parameters.

Parameter	Electrical size	Physical size line at 5.5 GHz
L	1.466λ	8.000 cm
r_a	0.400λ	2.181 cm
d	0.280λ	1.527 cm
t	0.055λ	3.000 mm
h	0.260λ	1.418 cm
l_f	0.229λ	1.250 cm
r_f	0.013λ	0.750 mm
l_p	0.262λ	1.430 cm
r_p	0.045λ	2.500 mm
α	45°	

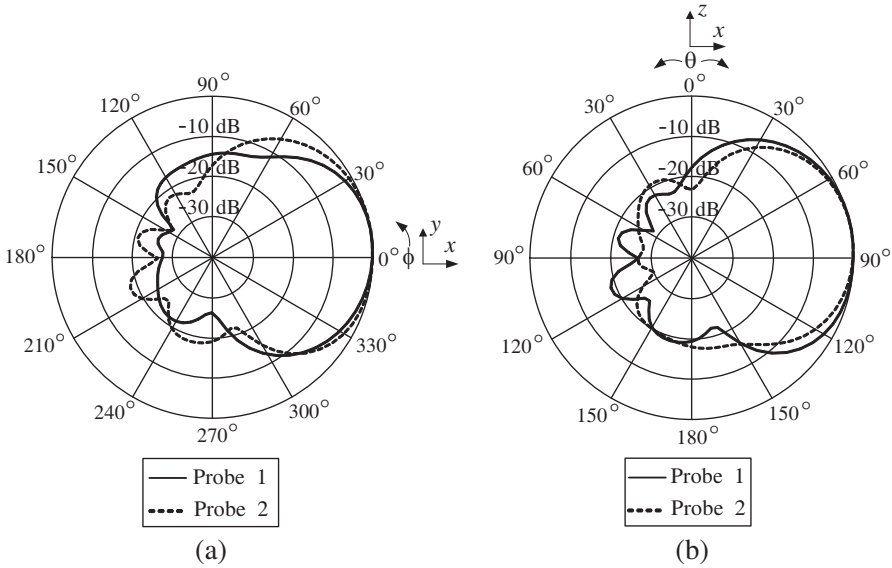

Figure 12. The radiation pattern at 5.5 GHz ($r_a = 2.18$ cm, $l_f = 1.25$ cm, $r_f = 0.75$ mm, $l_p = 1.43$ cm, $r_p = 2.50$ mm and $\alpha = 45°$). (a) xy plane. (b) xz plane.

and 12(b) in which the radiation patterns in xy-plane and xz-plane are respectively shown. The solid line represents the excitation of Probe1 whereas the dashed line is for Probe2 excitation. The unidirectional pattern is achieved for either Probe1 or Probe2 excitation. It is noted that the pattern in xy-plane for Probe1 excitation is identical to that in

xz-plane for Probe2 excitation due to the symmetrical configuration in two principal planes. The half-power beamwidths (HPBW) in xy-plane for excitation of Probe1 and Probe2 are 60 degrees and 80 degrees, respectively. The F/B ratio in both planes is 26 dB.

4. MEASURED RESULTS

To verify the antenna principle, the prototype antenna with the design parameters tabulated in Table 1 was fabricated as depicted in Fig. 13.

The reflection (in terms of $|S_{11}|$) and isolation (in terms of $|S_{21}|$) were measured using an HP872C Network Analyzer. It is noted that $|S_{11}|$ was measured at input port of Probe1 while Probe2 was terminated with matched load. Fig. 14 illustrates $|S_{11}|$ and $|S_{21}|$ compared between the simulated and measured results. The solid and dashed lines represent the simulated and measured results, respectively. The simulated and measured results are in reasonable agreement. At the center frequency, the simulated and measured $|S_{11}|$ are respectively -22.79 dB and -23.09 dB, whereas the simulated and measured $|S_{21}|$ are -46.54 dB and -33.99 dB, respectively. The impedance bandwidth ($|S_{11}| < -10$ dB) from the simulation is 15.16% (5.12–5.96 GHz), and that from the measurement is 23.64% (5.11–6.48 GHz). The obtained bandwidth can cover the requirement of WLAN system according to the IEEE802.11a standard. In addition, the isolation is relatively high. It thus can be concluded that the proposed antenna can be efficiently

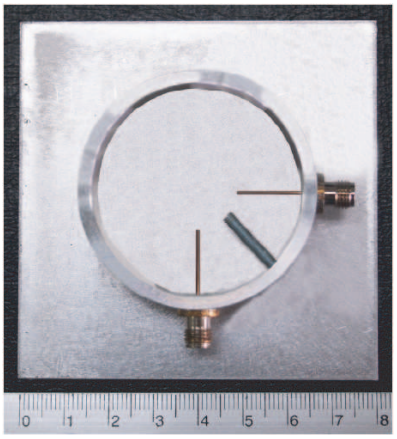

Figure 13. Photograph of the prototype antenna.

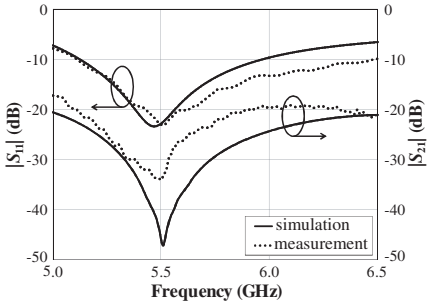

Figure 14. The comparison of $|S_{11}|$ and $|S_{21}|$ between simulation and measurement.

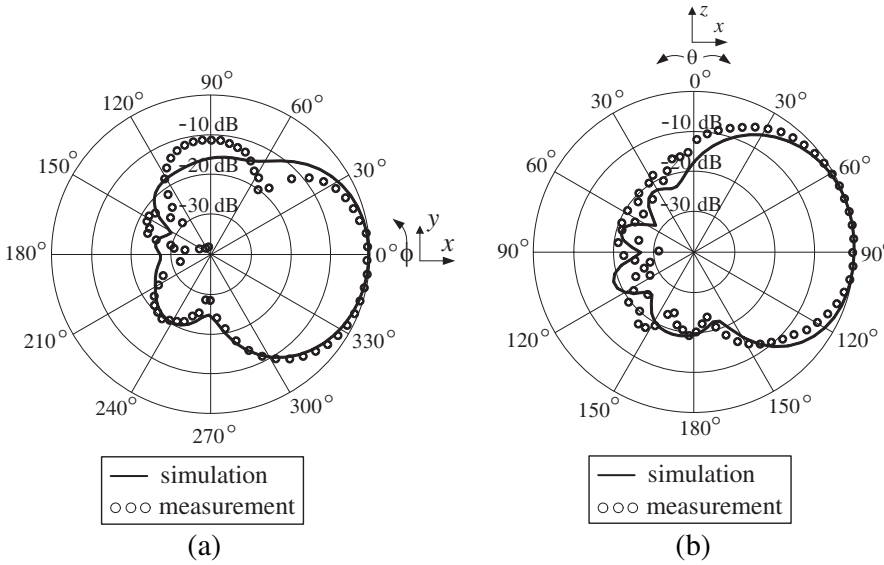

Figure 15. Simulated and measured radiation patterns with Probe1 excitation. (a) xy-plane. (b) xz-plane.

applied to polarization diversity reception.

The radiation patterns of the antenna were also measured. The measurement was carried out in two cases. The first case is performed for Probe1 excitation while Probe2 is terminated with a matched load. The measured results in xy-plane and xz-plane are superimposed with the simulated results as shown in Fig. 15. The second case is similar except that the antenna is excited at Probe2 while Probe1 is terminated with a matched load. The results are illustrated in Fig. 16. The solid and dashed lines represent the simulated and measured results, respectively. For both cases, the unidirectional pattern is achieved. From the symmetrical structure, the pattern with Probe1 excitation in xy-plane coincides with the excitation by Probe2 in xz-plane. The good agreement between the simulation and measurement is achieved. The simulated HPBW for Probe1 excitation in xy-plane and xz-plane are 60 and 80 degrees, respectively. For the measured results the HPBW are 65 and 75 degrees, respectively. The simulated and measured F/B are 26 dB and 31 dB, respectively. From the obtained results, it is apparent that this antenna possesses the good radiation pattern for polarization diversity of point-to-point communication.

The antenna gain was measured and compared with the simulated results as shown in Fig. 17. Both results display an identical trend with less than 2 dB difference. This discrepancy is due to the imperfect fabrication compared with the ideal simulation. For example, the loss

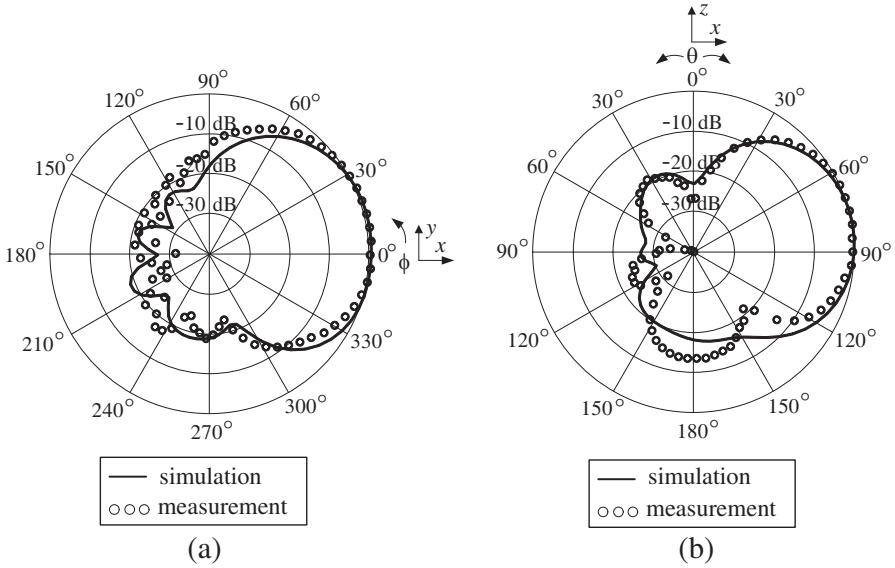

Figure 16. Simulated and measured radiation patterns with Probe2 excitation. (a) xy-plane. (b) xz-plane.

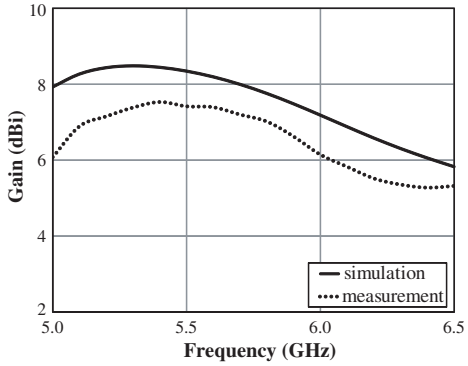

Figure 17. The simulated and measured gains.

tangent from the plastic rod that is used as the dielectic supporter between the circular ring and the square reflector was not taken into account in the simulation. It is obvious that the simulated (solid line) and measured (dashed line) gains at the center frequency are 8.35 dBi and 7.42 dBi, respectively. The variation of the gain along the bandwidth of 5.150–5.825 GHz is around 1 dB. This antenna thus has sufficient gain for point-to-point communication of WLAN system.

5. CONCLUSIONS

A unidirectional antenna for polarization diversity of WLAN system is achieved by using the circular ring excited by two perpendicular probes above the square reflector. The isolation is improved by adding a linear isolator at an angle of 45 degrees between two probes. The antenna principle is uncomplicated and the design straightforward. In addition, the prototype antenna is readily fabricated and conveniently produced on a mass scale. At the center frequency, the HPBW in two principal planes are 65 and 75 degrees, and the F/B is 31 dB. The obtained gain is 7.42 dBi. The antenna provides good radiation characteristics suitable for the point-to-point communication. $|S_{11}|$ and $|S_{21}|$ are -23.09 dB and -33.99 dB, respectively. The bandwidth can cover 5.11–6.48 GHz. It can be concluded that this antenna is appropriate for polarization diversity of WLAN system according to the IEEE802.11a standard. Furthermore, based on the antenna principle and design, the antenna parameters can be varied to realize the polarization diversity antenna of point-to-point communication in other wireless communication systems.

ACKNOWLEDGMENT

This work is financially supported by AUN/Seed-Net Program.

REFERENCES

1. IEEE Std. 802.11, Part 11, *Wireless LAN Medium Access Control (MAC) and Physical Layer (PHY) Specifications*, 1997.
2. IEEE Std. 802.11a, Supplement to Part 11, *Wireless LAN Medium Access Control (MAC) and Physical Layer (PHY) Specifications: Higher-Speed Physical Layer Extension in the 5 GHz Band*, 1999.
3. Chreim, H., E. Pointereau, B. Jecko, and P. Dufrane, "Omnidirectional electromagnetic band gap antenna for base station applications," *IEEE Antennas and Wireless Propagation Letters*, Vol. 6, 499–502, 2007.
4. Freytag, L., E. Pointereau, and B. Jecko, "Omnidirectional dielectric electromagnetic band gap antenna for base station of wireless network," *Proceedings of IEEE Antennas and Propagation Society International Symposium*, Vol. 1, 815–818, 2004.
5. Tsai, C.-L., "A coplanar-strip dipole antenna for broadband circular polarization operation," *Progress In Electromagnetics Research*, Vol. 121, 141–157, 2011.

6. Wounchoum, P., D. Worasawate, C. Phongcharoenpanich, and M. Krairiksh, "A switched-beam antenna using circumferential-slots on a concentric sectoral cylindrical cavity excited by coupling slots," *Progress In Electromagnetics Research*, Vol. 120, 127–141, 2011.
7. Eom, S.-Y., Y.-B. Jung, S. A. Ganin, and A. V. Shishlov, "A cylindrical shaped-reflector antenna with a linear feed array for shaping complex beam patterns," *Progress In Electromagnetics Research*, Vol. 119, 477-495, 2011.
8. Quan, X. L., R. L. Li, J. Y. Wang, and Y. H. Cui, "Development of a broadband horizontally polarized omnidirectional planar antenna and its array for base stations," *Progress In Electromagnetics Research*, Vol. 128, 441–456, 2012.
9. Wei, K. P., Z. J. Zhang, and Z. H. Feng, "Design of a dualband omnidirectional planar microstrip antenna array," *Progress In Electromagnetics Research*, Vol. 126, 101–120, 2012.
10. Li, R. L., T. Wu, and M. M. Tentzeris, "A triple-band unidirectional coplanar antenna for 2.4/3.5/5-GHz WLAN/WiMax applications," *Proceedings of IEEE Antennas and Propagation Society International Symposium*, 1–4, 2009.
11. Sze, J.-Y. and S.-P. Pan, "Design of broadband circularly polarized square slot antenna with a compact size," *Progress In Electromagnetics Research*, Vol. 120, 513–533, 2011.
12. Wang, X., M. Zhang, and S.-J. Wang, "Practicability analysis and application of PBG structures on cylindrical conformal microstrip antenna and array," *Progress In Electromagnetics Research*, Vol. 115, 495–507, 2011.
13. Fuschini, F., H. El-Sallabi, V. Degli-Esposti, L. Vuokko, D. Guiducci, and P. Vainikainen, "Analysis of multipath propagation in urban environment through multidimensional measurements and advanced ray tracing simulation," *IEEE Transactions on Antennas and Propagation*, Vol. 56, No. 3, 848–857, 2008.
14. Wang, X., Z. Du, and K. Gong, "A compact wideband planar diversity antenna covering UMTS and 2.4 GHz WLAN bands," *IEEE Antennas and Wireless Propagation Letters*, Vol. 7, 588–591, 2008.
15. Peng, H.-L., W.-Y. Yin, J.-F. Mao, D. Huo, X. Hang, and L. Zhou, "A compact dual-polarized broadband antenna with hybrid beam-forming capabilities," *Progress In Electromagnetics Research*, Vol. 118, 253–271, 2011.
16. Ding, Y., Z. Du, K. Gong, and Z. Feng, "A novel dual-

band printed diversity antenna for mobile terminals," *IEEE Transactions on Antennas and Propagation*, Vol. 55, No. 7, 2088–2096, 2007.

17. Toh, W., Z. Chen, X. Qing, and T. See, "A planar UWB diversity antenna," *IEEE Transactions on Antennas and Propagation*, Vol. 57, No. 11, 3467–3473, 2009.
18. Perini, P. L. and C. L. Holloway, "Angle and space diversity comparisons in different mobile radio environments," *IEEE Transactions on Antennas and Propagation*, Vol. 46, No. 6, 764–775, 1998.
19. Laneman, J. N., G. W. Wornell, and D. N. C. Tse, "An efficient protocol for realizing cooperative diversity in wireless networks," *Proceedings of IEEE Information Symposium on Information Theory*, 294, 2001.
20. Brown, T. W. C., R. Saunders, S. Stavrou, and M. Fiacco, "Characterization of polarization diversity at the mobile," *IEEE Transactions on Vehicular Technology*, Vol. 56, No. 5, 2440–2447, 2007.
21. Li, X., X. Huang, Z. Nie, and Y. Zhang, "Equivalent relations between interchannel coupling and antenna polarization coupling in polarization diversity systems," *IEEE Transactions on Antennas and Propagation*, Vol. 55, No. 6, 1709–1715, 2007.
22. Krairiksh, M., P. Keowsawat, C. Phongcharoenpanich, and S. Kosulvit, "Two-probe excited circular ring antenna for MIMO application," *Progress In Electromagnetics Research*, Vol. 97, 417–431, 2009.
23. Xie, J.-J., Y.-Z. Yin, J. Ren, and T. Wang, "A wideband dual-polarized patch antenna with electric probe and magnetic loop feeds," *Progress In Electromagnetics Research*, Vol. 132, 499–515, 2012.
24. Su, D., J. J. Qian, H. Yang, and D. Fu, "A novel broadband polarization diversity antenna using a cross-pair of folded dipoles," *IEEE Antennas and Wireless Propagation Letters*, Vol. 4, 433–435, 2005.
25. Eggers, P. C. F., J. Toftgard, and A. M. Oprea, "Antenna systems for base station diversity in urban small and micro cells," *IEEE Journal on Selected Areas in Communications*, Vol. 11, No. 7, 1046–1057, 1993.
26. Lee, B., S. Kwon, and J. Choi, "Polarization diversity microstrip base station antenna at 2 GHz using T-shaped aperture-coupled feeds," *Proceedings of IEE Microwave, Antennas and Propagation*, Vol. 148, No. 5, 334–338, 2001.

27. Dietrich, C. B., W. L. Stutzman, Jr., B. Kim, and K. Dietze, "Smart antennas in wireless communications: Base-station diversity and handset beamforming," *IEEE Antennas and Propagation Magazine*, Vol. 42, No. 5, 142–151, 2000.
28. Ou Yang, J., S. Bo, J. Zhang, and Y. Feng, "A low-profile unidirectional cavity-backed log-periodic slot antenna," *Progress In Electromagnetics Research*, Vol. 119, 423–433, 2011.
29. Xie, J.-J., Y.-Z. Yin, C. W. Zhang, and B. Li, "A novel trapezoidal slot patch antenna with a beveled ground plane for WLAN/WIMAX applications," *Progress In Electromagnetics Research Letters*, Vol. 27, 53–62, 2011.
30. Cai, D. S., Z.-Y. Lei, H. Chen, G.-L. Ning, and R. B. Wang, "Crossed oval-ring slot antenna with triple-band operation for WLAN/WIMAX applications," *Progress In Electromagnetics Research Letters*, Vol. 27, 141–150, 2011.
31. Liu, W.-C. and Y. Dai, "Dual-broadband twin-pair inverted-L shaped strip antenna for WLAN/WIMAX applications," *Progress In Electromagnetics Research Letters*, Vol. 27, 63–73, 2011.
32. Wang, X.-M., Z.-B. Weng, Y.-C. Jiao, Z. Zhang, and F.-S. Zhang, "Dual-polarized dielectric resonator antenna with high isolation using hybrid feeding mechanism for WLAN applications," *Progress In Electromagnetics Research Letters*, Vol. 18, 195–203, 2010.
33. Rezaeieh, S. A. and M. Kartal, "A new triple band circularly polarized square slot antenna design with crooked T and F-shape strips for wireless applications," *Progress In Electromagnetics Research*, Vol. 121, 1–18, 2011.
34. Panda, J. R. and R. S. Kshetrimayum, "A printed 2.4 GHz/5.8 GHz dual-band monopole antenna with a protruding stub in the ground plane for WLAN and RFID applications," *Progress In Electromagnetics Research*, Vol. 117, 425–434, 2011.
35. Weng, W.-C. and C.-L. Hung, "Design and optimization of a logo-type antenna for multiband applications," *Progress In Electromagnetics Research*, Vol. 123, 159–174, 2012.
36. CST-Microwave Studio, User's Manual, 2006.
37. Kosulvit, S., M. Krairiksh, C. Phongcharoenpanich, and T. Wakabayashi, "A simple and cost-effective bidirectional antenna using a probe excited circular ring," *IEICE Trans. Electronics*, Vol. E84-C, No. 4, 443–450, 2001.

Hindawi Publishing Corporation
International Journal of Antennas and Propagation
Volume 2014, Article ID 769816, 7 pages
http://dx.doi.org/10.1155/2014/769816

Research Article

Rectangular Ring Antenna Excited by Circular Disc Monopole for WiMAX System

Souphanna Vongsack,[1] Chuwong Phongcharoenpanich,[1] Sompol Kosulvit,[1] Kazuhiko Hamamoto,[2] and Toshio Wakabayashi[3]

[1] *Faculty of Engineering, King Mongkut's Institute of Technology Ladkrabang, Bangkok 10520, Thailand*
[2] *School of Information and Telecommunication Engineering, Tokai University, Kanagawa 259-1292, Japan*
[3] *Malaysia-Japan International Institute of Technology (MJIIT), Universiti Teknologi Malaysia, Kuala Lumpur 54100, Malaysia*

Correspondence should be addressed to Chuwong Phongcharoenpanich; pchuwong@gmail.com

Received 13 July 2014; Accepted 29 October 2014; Published 13 November 2014

Academic Editor: Giampiero Lovat

This research presents a rectangular ring antenna excited by a circular disc monopole (CDM) mounted in front of a square reflector. The proposed antenna is designed to cover a frequency range of 2.300–5.825 GHz and thereby is suitable for WiMAX applications. Multiple parametric studies were carried out using the CST Microwave Studio simulation program. A prototype antenna was fabricated and experimented. The measurements were taken and compared with the simulation results, which indicates good agreement between both results. The prototype antenna produces an impedance bandwidth ($|S_{11}| < -10$ dB) that covers the WiMAX frequency range and a constant unidirectional radiation pattern ($\theta = 0^{\circ}$ and $\emptyset = 90^{\circ}$). The minimum and maximum gains are 3.7 and 8.7 dBi, respectively. The proposed antenna is of compact size and has good unidirectional radiation performance. Thus, it is very suitable for a multitude of WiMAX applications.

1. Introduction

Besides an integral part of wireless communications, a wideband antenna is a crucial technology in the short-range, high-speed, and indoor wireless communications. According to [1–4], the WiMAX frequency bands are classified into three frequency bands of 2.500–2.690 GHz, 3.400–3.690 GHz, and 5.250–5.850 GHz (2.5/3.5/5.5 GHz). Over the past decades, a greater number of countries have utilized cellular base stations for installation of WiMAX antennas. Moreover, advances in mobile communications technology and rapid urbanization help promote the growth of indoor base stations, for example, in buildings, underground train systems, and tunnels. One distinct characteristic of indoor base stations is their omnidirectional radiation pattern, which is however their main drawback since an omnidirectional antenna can cover a limited circular area. This renders the omnidirectional antenna unsuitable for applications in the environment characterized by long and confined spaces in which a unidirectional antenna is more appropriate. In addition, unidirectional antennas are applicable to point-to-point communications. In these environments, for example, streets, highways, tunnels, and corridors, a unidirectional or bidirectional antenna performs better than an omnidirectional antenna [5–11]. To generate a unidirectional beam, a planar reflector [12, 13], corner reflector [14, 15], parabolic reflector [16], or conical reflector [17] was used with an omnidirectional monopole antenna. The unidirectional bandwidth is narrow and could be enhanced by replacing the linear monopole with a surface monopole, for example, circular, triangular, square, or rectangular monopole [18–22].

To achieve the unidirectional pattern along the WiMAX frequency range of 2.300–5.825 GHz, this research proposes a rectangular ring antenna excited by a CDM mounted in

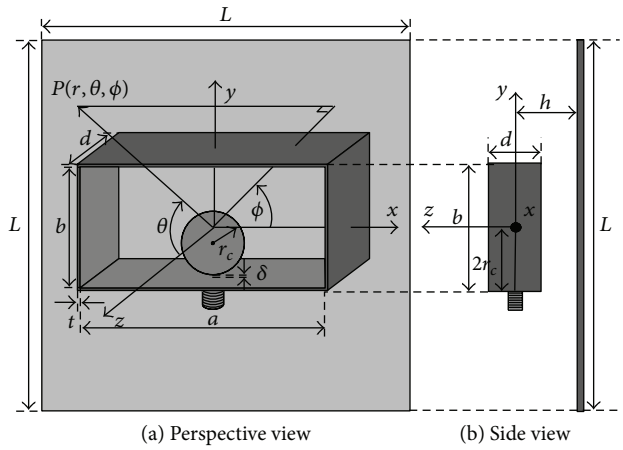

Figure 1: The structure of the proposed antenna with CDM.

front of a square reflector. The simulations and experiments were carried out along the WiMAX frequency band. The proposed antenna's $|S_{11}|$, radiation pattern, and gain along the WiMAX frequency were simulated using the CST Microwave Studio [23]. Based on the simulation results, the optimal rectangular ring dimensions and CDM radius are a = 7.20 cm, $b = a/2$, d = 2.60 cm, and r_c = 1.10 cm, respectively, as $|S_{11}| < -10$ dB along the WiMAX band. It is however found that the beam direction beyond a higher frequency of 5.5 GHz tilts upward as a result of the asymmetrical areas between the upper and lower portions of the rectangular ring chamber.

The organization of this paper is as follows. Section 1 is the introduction. Section 2 details the structure and parameters of the proposed antenna. Section 3 presents the design principle and the parametric study, while Section 4 compares the simulation and measured results. The concluding remarks are provided in Section 5.

2. Geometry of the Proposed Antenna

Figure 1(a) illustrates the structure of the proposed antenna, which consists of a CDM and a rectangular ring with width a, height b, length d, and thickness t. The rectangular ring center is at the yz-plane origin. The ring is excited by the CDM on the y-axis via a 50 Ω SMA connector to generate vertical polarization. The CDM radius r_c and the delta gap δ are 1.10 cm and 1.00 mm, respectively. The structure is mounted in front of an $L \times L$ square reflector. The space between the rectangular ring and the reflector is denoted by h, as illustrated in Figure 1(b). The antenna radiation pattern is unidirectional with the beam peak pointing in the z direction.

3. Design Principle and Parametric Study

The antenna is designed to operate in the WiMAX frequency range of 2.300–5.825 GHz. The design principle starts with exciting the rectangular ring with a circular-disc monopole (CDM), as shown in Figure 1. The initial ring width a of the 2.3 GHz frequency is slightly greater than $\lambda/2$ (i.e., 6.60 cm). The ring height b is proportional to the ring width a; that is, $b = a/2$. The ring length d and thickness t are 3.25 cm ($\lambda/4$) and 2.00 mm, respectively. The rectangular ring is excited by a circular-disc monopole with an r_c radius 1.3 cm (0.1λ). The selected square reflector is 16×16 cm ($L \times L$) in dimension with the space (h) between the rectangular ring and the reflector of 3.90 cm (0.3λ). Both the rectangular ring and the reflector are made of aluminum. Ideally, the width a and height b of a rectangular ring should be minimal to obtain an antenna of a size as compact as possible.

The width a of the proposed rectangular ring follows the following rule, where λ (i.e., 13.00 cm) is the wavelength at the 2.3 GHz frequency:

$$0.5\lambda < a < \lambda. \tag{1}$$

To enhance the bandwidth, the rectangular ring is thus excited by a *circular-disc* monopole with an r_c radius. The initial circular monopole radius (r_c) is determined by (2) with the predetermined feed gap (δ) of 1.00 mm and 0.21λ being referenced from [15]:

$$r_c = \frac{(0.21\lambda - \delta)}{2}. \tag{2}$$

Parametric studies were carried out to determine the optimal ring dimensions that produce an optimal combination of resonant frequency, radiation pattern, and gain and also are of compact size. Figure 2 illustrates the fractional bandwidths of resonant frequency (closest to the 2.3 GHz frequency) by varying a and d of the rectangular ring antenna which is excited by a CDM. Both the ring antenna and the CDM are together mounted in front of the square reflector. As shown in Figure 2, the fractional bandwidth of resonant frequencies at 2.3 GHz is achieved with a of 7.20 cm (0.553λ), b of 3.60 cm, and d of 2.60 cm, which are selected as the design parameters. It is noted that the ring width a of 7.20 cm (0.553λ) is selected because of the wide bandwidth, compact antenna size, and available material in the market suitable for the mass production.

To determine an optimal matching condition with a wide bandwidth, the space between the CDM and the square reflector h is varied from 1.65 (0.21λ) to 3.90 cm (0.30λ). The simulated unidirectional beam is achieved at h of 0.10λ–0.30λ and of 0.60λ-0.70λ, while that with the widest bandwidth is achieved at $h < 0.30\lambda$. The beam splits occur when h is between 0.30λ and 0.60λ. According to [13], the unidirectional beam can also be realized when h is ≥0.70λ. It is found that the radiation pattern becomes split for h between 0.30λ and 0.60λ. The simulation results are shown for h of 1.65–2.90 cm because while h is >2.90 cm the $|S_{11}|$ cannot cover the frequency bandwidth (e.g., h = 3.15 cm, the $|S_{11}| > -10$ dB from 4.92 to 5.91 GHz). Based on the simulation results (Figure 3), h of 2.40 cm (0.184λ) is selected as it produces a unidirectional beam with wide bandwidth.

Figures 4(a) and 4(b) show, respectively, the minimum and maximum frequencies ($|S_{11}| < -10$ dB) of resonance at 2.3 GHz as a function of b/a by varying r_c, where b/a is

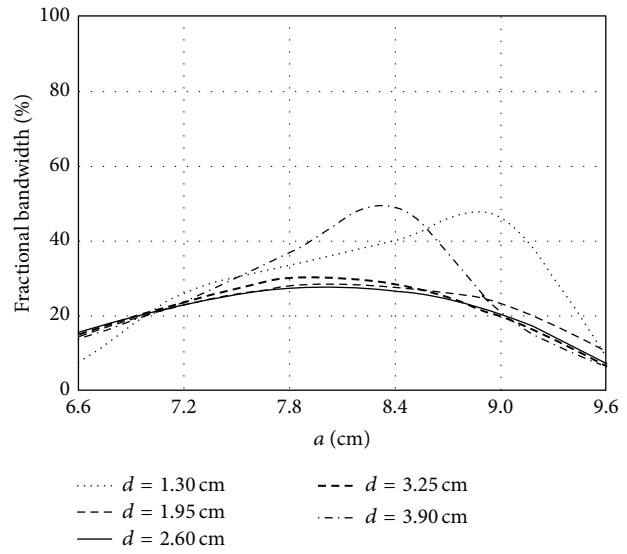

Figure 2: Fractional bandwidths of the resonant frequency at 2.3 GHz versus a as a function of d (r_c = 1.30 cm and h = 3.90 cm).

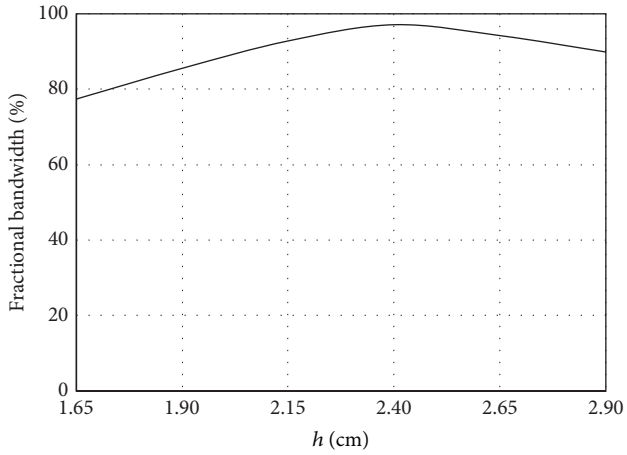

Figure 3: Fractional bandwidth of the resonant frequency at 2.3 GHz as a function of h (a = 7.20 cm, b = 3.60 cm, d = 2.60 cm, and r_c = 1.30 cm).

the ring height. The radius of CDM (r_c) is varied between 1.00 and 1.40 cm to determine a ring height (b/a) that gives good resonance at the 2.3 GHz frequency. To produce the rectangular ring of a size as compact as possible, r_c = 1.10 cm for $b = 0.48a$ or 3.40 cm is selected.

Figure 5 illustrates the impedance bandwidth $|S_{11}|$ of the resonant frequency closest to 2.3 GHz as a function of b/a of the rectangular ring antenna, assuming a constant r_c of 1.10 cm. To achieve the goal of a compact ring antenna with the widest bandwidth, the ring width (a) and ring height (b) of 7.20 and 3.40 cm are chosen for experiment.

Table 1: The optimal parametric values of the proposed antenna.

Parameters	Physical size	Electrical size (λ)
L	16.0 cm	1.2307
a	7.2 cm	0.5538
b	3.4 cm	0.2615
d	2.6 cm	0.2000
h	2.4 cm	0.1846
r_c	1.1 cm	0.0846
t	2.0 mm	0.0153
δ	1.0 mm	

The inclusion of the CDM into the rectangular ring antenna is to increase the antenna's frequency bandwidth to cover the WiMAX band of 2.300–5.825 GHz. Figure 6 illustrates the frequency response curves as a function of $|S_{11}|$ and the frequency for the CDM radii of 1.00 to 1.40 cm and constant feed gap (δ) of 1.00 mm. Even though the $|S_{11}|$ curves for five CDM radii follow a similar pattern, an r_c of 1.10 cm is selected as it gives the highest overall efficiency in terms of impedance bandwidth, radiation pattern, and gain.

In addition, the effect of the feeding gap (δ) is examined and the results are depicted in Figure 7. It is found that varying the feeding gap (δ) impacts the impedance bandwidth. That is, a reduction in δ from 1.50 mm to 0.50 mm causes the impedance bandwidth to become narrower and thereby fails to cover the entire WiMAX frequency band. Based on Figure 7, the feeding gap (δ) of 1.00 mm is chosen for the widest impedance bandwidth which covers the entire WiMAX band. Table 1 presents the optimal parametric values from the simulation of the proposed antenna.

4. Measured Results

To validate the simulation results, a prototype antenna was fabricated based on the optimal parameters in Table 1. Figure 8 is a photograph image of the prototype antenna.

4.1. Impedance Bandwidth. The measurements of impedance bandwidth, radiation pattern, and gain were taken using an HP8720C Network Analyzer. A comparison of the simulated and measured $|S_{11}|$, represented, respectively, by a solid line and a dashed line, is presented in Figure 9. The simulated impedance bandwidth ($|S_{11}| < -10$ dB) of 88% was achieved in a frequency range of 2.28–5.91 GHz (central frequency of 4.095 GHz), while that of the prototype antenna of 93% was in a frequency of 2.16–5.96 GHz (central frequency of 4.06 GHz). It is found that the simulation and measured results are in reasonable agreement. In addition, the frequency ranges of both simulation and experiment satisfy the WiMAX requirement.

Figure 10 illustrates a comparison of the gain along the 2.300–5.825 GHz frequency range of the prototype antenna and that of the simulation, in which the former is represented by a solid line and the latter by a dashed line. The minimum

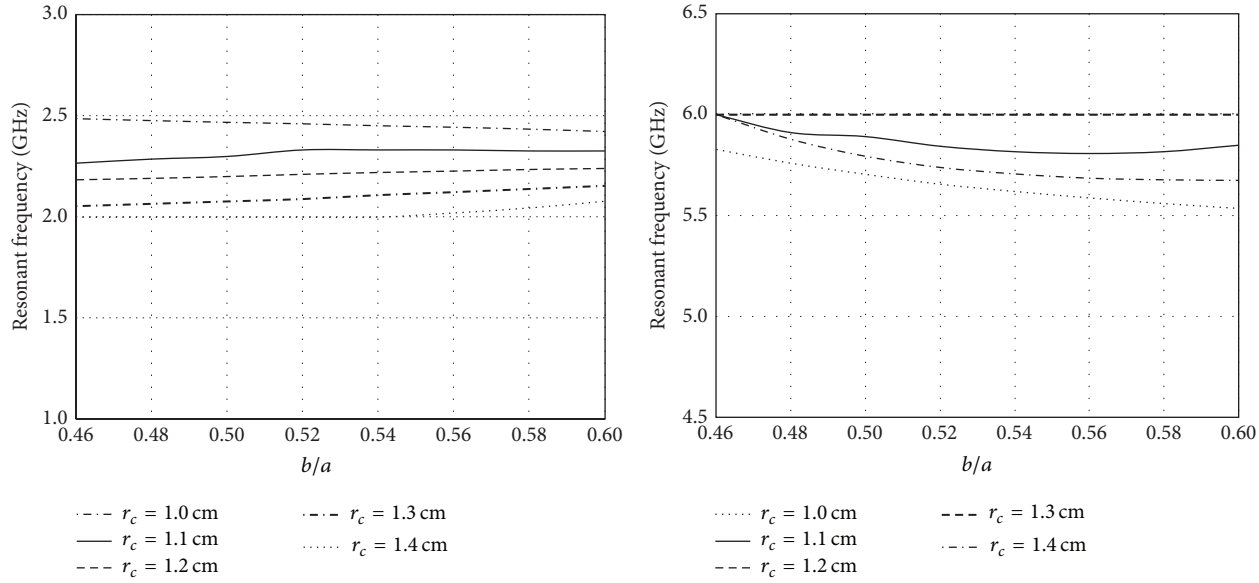

(a) The minimum frequency of resonance at 2.3 GHz by varying r_c

(b) The maximum frequency of resonance at 2.3 GHz by varying r_c

Figure 4: The resonant frequency relative to b/a for various r_c (a = 7.20 cm, d = 2.60 cm, and h = 2.40 cm).

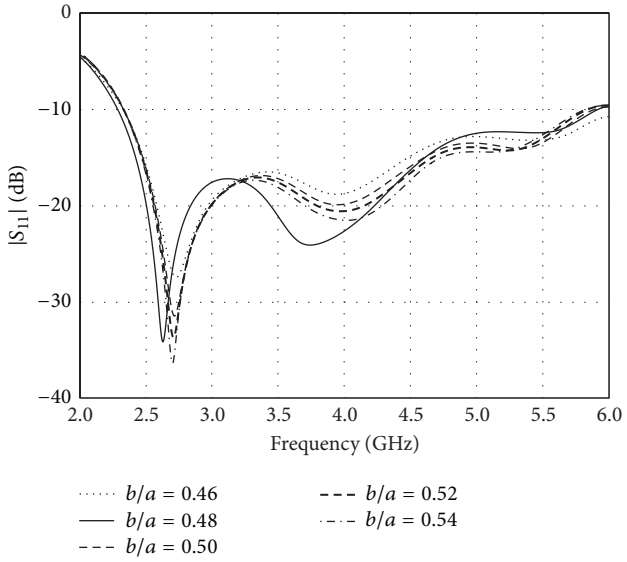

Figure 5: $|S_{11}|$ versus frequency as a function of b/a (a = 7.20 cm, d = 2.60 cm, h = 2.40 cm, and r_c = 1.10 cm).

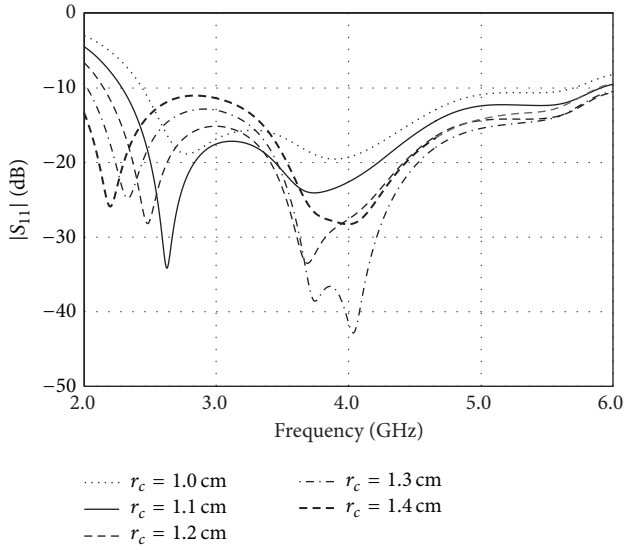

Figure 6: $|S_{11}|$ relative to frequency as a function of r_c (δ = 1.00 mm).

and maximum gains are 3.4 and 9.3 dBi for the simulation and 3.7 and 8.7 dBi for the prototype antenna.

4.2. Radiation Pattern. Figures 11 and 12 illustrate the simulation and measured radiation patterns in the yz- and xz-planes, respectively, at 2.5, 3.5, and 5.5 GHz. In Figure 11, the beam peaks direct in the 3 +z direction. The radiation pattern in the yz-plane at 5.5 GHz slightly tilts upward from the z-axis as a result of the CDM installation on the rectangular ring base. The CDM contributes to the asymmetrical areas between the upper and lower portions of the ring chamber. However, the radiation pattern in the xz-plane is symmetrical because of the symmetrical areas between the left and right portions of the ring chamber. The simulation and measured radiation patterns show good agreement. At 2.5 GHz, the

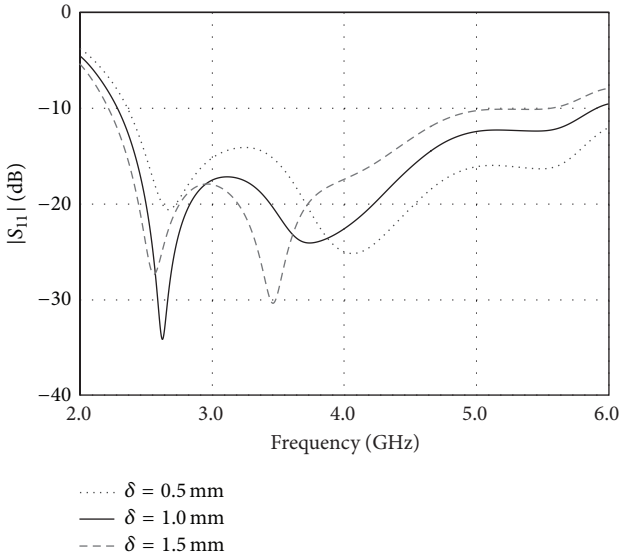

FIGURE 7: $|S_{11}|$ relative to frequency as a function of δ.

FIGURE 8: Photograph image of the prototype antenna.

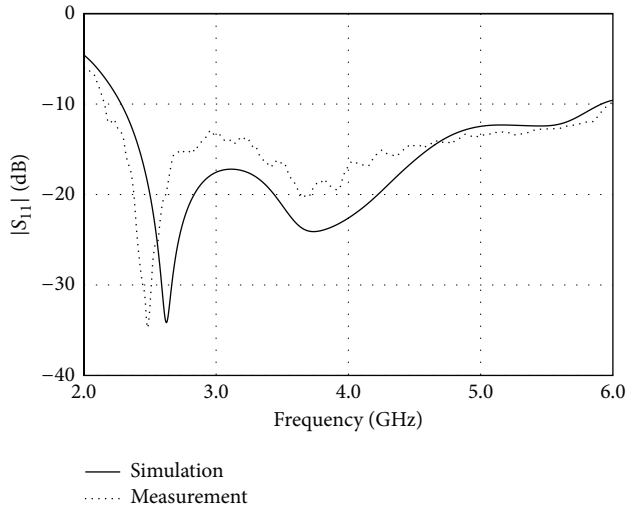

FIGURE 9: The comparison of the simulation and measured $|S_{11}|$ relative to frequency.

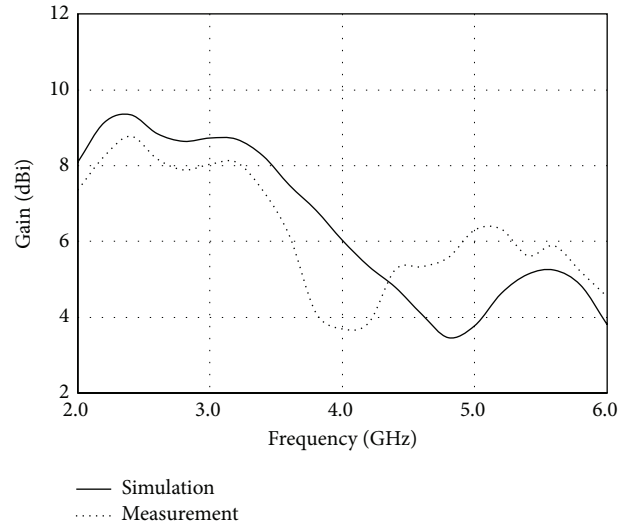

FIGURE 10: The simulated and measured gains relative to frequency.

measured half-power beamwidth (HPBW) in the yz- and xz-planes is 73 and 62 degrees. At 3.5 GHz, the measured HPBWs in the yz- and xz-planes are identical at 80 degrees, while those at 5.5 GHz are 28 and 40 degrees, respectively. The measured front-to-back ratio (F/B) in both yz- and xz-planes is greater than 20 dB. Thus, the proposed antenna produces a good radiation pattern and is a very good unidirectional antenna.

5. Conclusions

The unidirectional antenna suitable for WiMAX is developed using the CDM-excited rectangular ring mounted in front of the square reflector. The design principle is simple and straightforward. In addition, the antenna can be fabricated and manufactured on a large scale. At 2.5 GHz, the measured HPBWs in the yz- and xz-planes are 72 and 62 degrees, respectively. At 3.5 GHz, the measured HPBWs in both planes are identical at 80 degrees, while those at 5.5 GHz are 28 and 40 degrees, respectively. The measured F/B in both yz- and xz-planes are greater than 20 dB. The antenna has a good radiation pattern suitable for the point-to-point communications and can achieve the impedance bandwidth ($|S_{11}| < -10$ dB) of 93%, covering the frequency range of 2.16–5.96 GHz. Its compact size and good radiation performance render the proposed antenna suitable for the WiMAX applications.

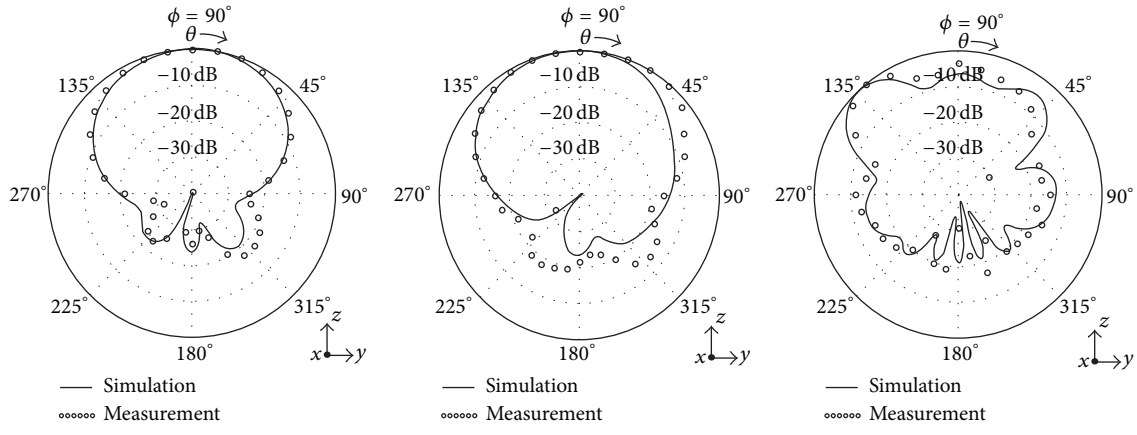

(a) 2.5 GHz (b) 3.5 GHz (c) 5.5 GHz

Figure 11: The comparison between the simulated and measured radiation patterns in the yz-plane.

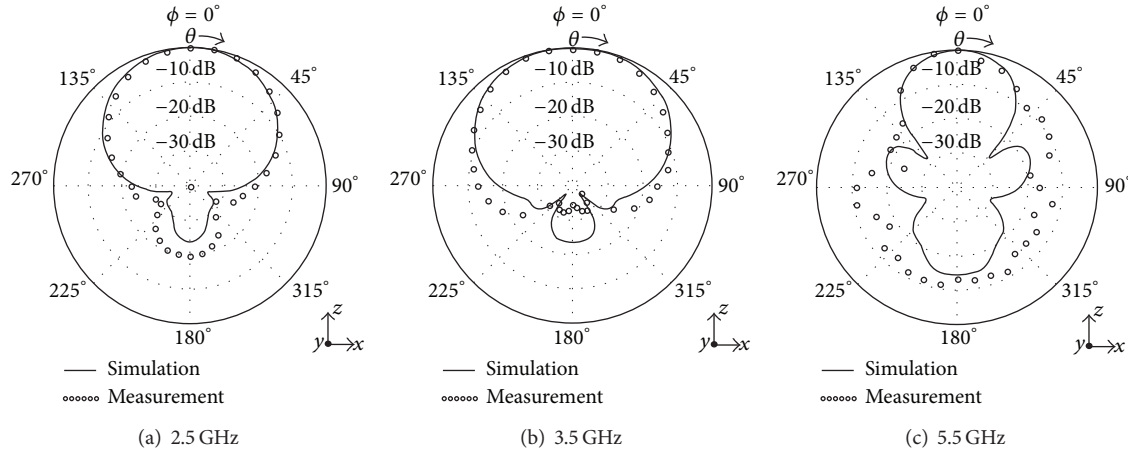

(a) 2.5 GHz (b) 3.5 GHz (c) 5.5 GHz

Figure 12: The comparison between the simulated and measured radiation patterns in the xz-plane.

Conflict of Interests

This paper is part of the lead author's Ph.D. degree dissertation. The authors ascertain that the use of CST Microwave Studio in this research paper presents no conflict of interests.

Acknowledgments

This research work is fully sponsored by the AUN/Seed-Net Program. The comments from anonymous reviewers to improve this paper are greatly appreciated.

References

[1] IEEE Std 802.16a-2003, "IEEE Standard for Local and Metropolitan Area Networks—Part 16: Air Interface for Fixed Broadband Wireless Access Systems—Amendment 2: Medium Access Control Modifications and Additional Physical Layer Specifications for 2–11 GHz," 2003.

[2] IEEE, "IEEE standard for local and metropolitan area networks part 16: air interface for fixed broadband wireless access systems," IEEE Std 802.16-2004, 2004, (Revision of IEEE Std 802.16-2001).

[3] F. Ohrtman, *WiMAX Handbook Building 802.16 Wireless Networks*, McGraw-Hill Communications, 2005.

[4] C.-Y. Pan, T.-S. Horng, W.-S. Chen, and C.-H. Huang, "Dual wideband printed monopole antenna for WLAN/WiMAX applications," *IEEE Antennas and Wireless Propagation Letters*, vol. 6, pp. 149–151, 2007.

[5] J. Wu, Z. Zhao, Z. Nie, and Q. H. Liu, "A broadband unidirectional antenna based on closely spaced loading method," *IEEE Transactions on Antennas and Propagation*, vol. 61, no. 1, pp. 109–116, 2013.

[6] S. Kosulvit, M. Krairiksh, C. Phongcharoenpanich, and T. Wakabayashi, "A simple and cost-effective bidirectional antenna using a probe excited circular ring," *IEICE Transactions on Electronics*, vol. E84-C, no. 4, pp. 443–450, 2001.

[7] F. Elek, R. Abhari, and G. V. Eleftheriades, "A uni-directional ring-slot antenna achieved by using an electromagnetic band-gap surface," *IEEE Transactions on Antennas and Propagation*, vol. 53, no. 1, pp. 181–190, 2005.

[8] K. Agarwal, Nasimuddin, and A. Alphones, "Unidirectional wideband circularly polarised aperture antennas backed

with artificial magnetic conductor reflectors," *IET Journal Microwave, Antennas & Propagation*, vol. 7, no. 5, pp. 338–346, 2013.

[9] Z. Y. Zhang, G. Fu, S. L. Zuo, and S. X. Gong, "Wideband unidirectional patch antenna with Γ-shaped strip feed," *Electronics Letters*, vol. 46, no. 1, pp. 24–26, 2010.

[10] G. M. Zhang, J. S. Hong, B. Z. Wang, G. Song, and P. Zhang, "Compact wideband unidirectional antenna with a reflector connected to the ground using a stub," *IEEE Antennas and Wireless Propagation Letters*, vol. 10, pp. 1186–1189, 2011.

[11] Y. Zhao, K. Wei, Z. Zhang, and Z. Feng, "A waveguide antenna with bidirectional circular polarizations of the same sense," *IEEE Antennas and Wireless Propagation Letters*, vol. 12, pp. 559–562, 2013.

[12] W. Li, J. Qiu, and Y. Suo, "Design and simulation of novel ultra wideband planar reflector antenna," in *Proceedings of the International Conference on Microwave and Millimeter Wave Technology (ICMMT '07)*, pp. 1–4, April 2007.

[13] C. Phongcharoenpanich, S. Lamultree, S. Kosulvit, and M. Krairiksh, "A unidirectional beam antenna using a probe excited rectangular ring near the reflector," in *Proceedings of the 3rd International Conference on Microwave and Millimeter Wave Technology (ICMMT '02)*, pp. 389–392, August 2002.

[14] C. Phongcharoenpanich, S. Lamultree, S. Kosulvit, M. Krairiksh, and J. Takada, "Analysis of a dihedral corner reflector antenna excited by a probe inside rectangular ring," in *Proceedings of the International Symposium on Antennas and Propagation*, pp. 225–228, 2004.

[15] J. D. Kraus, "The corner-reflector antenna," *The Proceedings of the IRE*, vol. 28, pp. 513–519, 1940.

[16] P. Lam, S.-W. Lee, K. Lang, and D. Chang, "Sidelobe reduction of a parabolic reflector with auxiliary reflectors," *IEEE Transactions on Antennas and Propagation*, vol. 35, no. 12, pp. 1367–1374, 1987.

[17] G. Ketwan, C. Phongcharoenpanich, and S. Kosulvit, "A wideband unidirectional antenna using conical reflector fed by circular ring," in *Proceedings of the Asia-Pacific Microwave Conference (APMC '05)*, vol. 5, pp. 2939–2942, 2005.

[18] M. J. Ammann and Z. N. Chen, "Wideband monopole antennas for multi-band wireless systems," *IEEE Antennas and Propagation Magazine*, vol. 45, no. 2, pp. 146–150, 2003.

[19] J. Liang, L. Guo, C. C. Chiau, X. Chen, and C. G. Parini, "Study of CPW-fed circular disc monopole antenna for ultra wideband applications," *IEE Proceedings-Microwave and Antennas Propagation*, vol. 152, pp. 505–508, 2005.

[20] N. P. Agrawall, G. Kumar, and K. P. Ray, "Wide-band planar monopole antennas," *IEEE Transactions on Antennas and Propagation*, vol. 46, no. 2, pp. 294–295, 1998.

[21] Z. N. Chen, M. J. Ammann, M. Y. W. Chia, and T. S. P. See, "Annular planar monopole antennas," *IEE Proceedings: Microwaves, Antennas and Propagation*, vol. 149, no. 4, pp. 200–203, 2002.

[22] M. Hammoud, P. Poey, and F. Colombel, "Matching the input impedance of a broadband disc monopole," *Electronics Letters*, vol. 29, no. 4, pp. 406–407, 1993.

[23] CST-Microwave Studio, User's Manual, 2006.

AUTHOR BIOGRAPHY

Souphanna Vongsack was born in Louangprabang Province, North of Laos. She received B. Eng in Electronic and Telecommunication Engineering from National University of Laos in 2004 and M. Eng. degrees in Telecommunication Engineering from King Mongkut's Insititute of Technology Ladkrabang (KMITL), Thailand, in 2008, respectively.

From 2006 to 2008, and 2009 to 2013, she was a Master and Ph.D. student supported by a scholarship from the ASEAN University Network Southeast Asia Engineering Education Development Network (AUN/SEED-Net) Project.

June 2010, while she studying Ph.D she was a visiting scholar in Tokai University Kanagawa, Japan. And during the time period from January to August, 2011 she was a visiting scholar for short term study in the Tokai University, Kanagawa, Japan. Her research interests are in the areas of antenna engineering, wireless communication and microwave engineering.